DOKUZ EYLÜL UNIVERSITY

GRADUATE SCHOOL OF NATURAL AND APPLIED SCIENCES

SIMULATION OF THE HYDRODYNAMICS IN WASTEWATER TREATMENT PLANTS USING COMPUTATIONAL FLUID DYNAMICS (CFD) TOOLS

by

Emre KÖKEN

March, 2023

İZMİR

SIMULATION OF THE HYDRODYNAMICS IN WASTEWATER TREATMENT PLANTS USING COMPUTATIONAL FLUID DYNAMICS (CFD) TOOLS

A Thesis Submitted to the
Graduate School of Natural and Applied Sciences of Dokuz Eylül University
In Partial Fulfillment of the Requirements for the Degree of Doctor of Philosophy in Environmental Engineering

by
Emre KÖKEN

March, 2023
İZMİR

Ph.D. THESIS EXAMINATION RESULT FORM

We have read the thesis entitled **"SIMULATION OF THE HYDRODYNAMICS IN WASTEWATER TREATMENT PLANTS USING COMPUTATIONAL FLUID DYNAMICS (CFD) TOOLS"** completed by **EMRE KÖKEN** under supervision of **PROF. DR. NURDAN BÜYÜKKAMACI** and we certify that in our opinion it is fully adequate, in scope and in quality, as a thesis for the degree of Doctor of Philosophy.

.....

Prof. Dr. Nurdan BÜYÜKKAMACI

Supervisor

.....	.....
Prof. Dr. Ayşe FİLİBELİ	Prof. Dr. Okan FISTIKOĞLU
Thesis Committee Member	Thesis Committee Member
.....	.....
Prof. Dr. Sinan UYANIK	Prof. Dr. Mehmet SORGUN
Examining Committee Member	Examining Committee Member

Prof. Dr. Okan FISTIKOĞLU

Director

Graduate School of Natural and Applied Sciences

ACKNOWLEDGEMENTS

First and foremost, I would like to express my sincere gratitude to my advisor, Prof. Dr. Nurdan BÜYÜKKAMACI, whose contribution was of immense importance in the preparation and completion of this thesis. I am grateful for her wonderful guidance, support, and mentorship throughout my academic journey. Her commitment to my success has been a driving force in the completion of this thesis, including three patentable inventions. She is the greatest mentor in my life and her impact on me will always be remembered.

My deep appreciation is also due to Prof. Dr. Ayşe FİLİBELİ and Prof. Dr. Okan FISTIKOĞLU for their constructive discussions and valuable suggestions during our progress meetings. I would also like to thank the examination committee members, Prof. Dr. Sinan UYANIK and Prof. Dr. Mehmet SORGUN, for providing insightful comments and suggestions.

I am grateful to acknowledge the funding received for my PhD from the Research Foundation of Dokuz Eylül University (Project No. 2021.KB.FEN.006).

I extend my heartfelt thanks to my colleagues, Mustafa Kemal TÜRKERİ and Emre SUCU, for their invaluable support and friendship during my research. Their expertise and willingness to help were instrumental in solving problems and overcoming obstacles in my thesis. Their insights, ideas, and collaboration made this process much smoother, and I am very grateful for their contributions. It was a pleasure to have worked with you both.

Words cannot express my gratitude to my parents, Ayşegül and Veli, the two most loving and supportive parents a person could ask for. Their unconditional love, affection, moral support, and encouragement have been the cornerstone of my life, and I am forever grateful for the person I am today because of you both. Their sacrifices and dedication have not gone unnoticed, and I am honored to have you as my parents. This thesis is a testament to their love and support.

I am deeply grateful to my uncle, Lütfü, who has been a true mentor and friend. His wisdom and advice have helped me navigate life's challenges and have given me the confidence to pursue my passions.

Last but not least, I would like to thank the two most important women in my life, my wife Burcu and my daughter Şimal, for their endless love, support, and encouragement. Their unwavering faith in me has given me the strength to chase my dreams and push through tough times. Their presence in my life has made it brighter and more meaningful, and I am eternally grateful to each of you. Their love and devotion are the foundation of our family, and I am blessed to have you by my side. May you always know how much you are loved and valued.

Emre KÖKEN

SIMULATION OF THE HYDRODYNAMICS IN WASTEWATER TREATMENT PLANTS USING COMPUTATIONAL FLUID DYNAMICS (CFD) TOOLS

ABSTRACT

Proper hydrodynamics is crucial in wastewater treatment systems for efficient pollutant removal and treatment process performance. Optimizing hydrodynamics has been a challenge in the past due to the lack of effective analysis tools, resulting in oversized treatment plants and poor energy efficiency. However, Computational Fluid Dynamics (CFD) tools have emerged as an effective solution to this challenge, enabling engineers to simulate and analyze fluid behavior and motion in treatment processes. Optimizing hydrodynamics can minimize energy input, reduce operating costs, and improve treatment performance, which is increasingly important as the world faces an energy crisis and growing demand for clean water and energy.

The dissertation investigates the benefits of using CFD to optimize hydrodynamics in wastewater treatment facilities, with a focus on the activated sludge system and secondary clarifiers. A pilot plant for wastewater treatment was used for the investigations. The study revealed that one of the aeration tanks and its clarifier could be left idle. CFD simulations were used to optimize mixer configurations in the aeration tanks, and it was found that reducing the mixer speed improves process efficiency and decreases energy consumption. Besides, CFD tools were used to diagnose and mitigate hydrodynamic problems, such as short-circuiting and sludge blanket deformation, in clarifiers. The dissertation resulted in three main inventions: snail- and spiral-shaped draw-off pipes and a novel deflector, which enhance hydrodynamic conditions and increase sludge discharge capacity. The proposed measures were found to reduce almost half of the energy and operational costs of biological processes while meeting discharge limits.

Keywords: CFD, Wastewater, Activated Sludge, Sedimentation, Clarifier, Energy Dissipating Inlet, Short-circuiting, Draw-Off Pipe

ATIKSU ARITMA TESİSLERİNDEKİ HİDRODİNAMİĞİN HESAPLAMALI AKIŞKANLAR DİNAMİĞİ (HAD) ARAÇLARI KULLANARAK SİMÜLASYONU

ÖZ

Atıksu arıtma sistemlerinde etkili kirletici giderimi ve arıtma süreci verimi için uygun hidrodinamik koşullar çok önemlidir. Ancak geçmişte hidrodinamiği optimize etmek etkili analiz araçlarının olmaması sebebiyle bu sorun görmezden gelindiğinden arıtma üniteleri daha büyük tasarlanıyor ve bu da düşük enerji verimliliğine neden oluyordu. Hesaplamalı Akışkanlar Dinamiği (HAD) araçları bu soruna etkili bir çözüm olarak ortaya çıkmış ve mühendislerin arıtma süreçlerindeki akışkan davranışını ve hareketini simüle ve analiz etmelerine imkan sağlamıştır. Hidrodinamiğin optimize edilmesi enerji ihtiyacı ve işletme maliyetlerinin azaltılmasının yanı sıra arıtma veriminin iyileştirilmesinde önemli rol üstlenmektedir; bu da dünyanın karşı karşıya olduğu enerji krizi ile birlikte artan temiz su ve enerji talebi sebebiyle giderek daha önemli hale gelmektedir.

Bu tez, aktif çamur sistemi ve son çökeltim havuzlarına odaklanarak atıksu arıtma tesislerinde hidrodinamiğin optimizasyonu için HAD araçları kullanmanın faydalarını araştırmaktadır. Araştırmalar için bir atıksu arıtma tesisi pilot olarak seçilmiştir. Çalışmada, tesisteki havalandırma havuzlarından birinin ve buna bağlı son çökeltim havuzunun kuruya alınabileceğini ortaya konmuştur. Havalandırma havuzundaki karıştırıcıları optimize etmek için yapılan HAD simülasyonları karıştırıcı hızının azaltılmasının proses verimliliğini artırdığı ve enerji tüketimini azalttığını ortaya koymuştur. Ayrıca, son çökeltim havuzundaki kısa devre ve çamur battaniyesinin deformasyonu gibi hidrodinamik sorunları teşhis etmek ve azaltmak için de CFD araçları kullanılmıştır. Tezde üç buluşa imza atılmıştır: Salyangoz ve spiral şekilli çekme boruları ile özgün tasarıma haiz deflektör. Bunlar hidrodinamik koşulları iyileştirirken ve çamur deşarj hızını arttırmaktadır. Tesis için önerilen tedbirler deşarj limitlerini sağlarken biyolojik prosesler için gerekli enerji ve işletme maliyetlerini neredeyse yarı yarıya azalttığı tespit edilmiştir.

Anahtar Kelimeler: HAD, Atıksu, Aktif Çamur, Sedimantasyon, Çökeltim Havuzu, Arıtıcı, Enerji Kırıcı Giriş, Kısa Devre, Çamur Tahliye Borusu

CONTENTS

Page

Ph.D. THESIS EXAMINATION RESULT FORM ii
ACKNOWLEDGEMENTS iii
ABSTRACT v
ÖZ vi
LIST OF FIGURES xi
LIST OF TABLES xvi
ABBREVIATIONS xvii
LIST OF SYMBOLS xviii

CHAPTER 1 – INTRODUCTION 1

1.1 Activated Sludge Process 3
1.1.1 Aeration Tanks 4
1.1.2 Clarifiers 7
1.1.2.1 Energy Dissipating Inlets (EDIs) 11
1.2 Defining the Problem 13
1.3 Research Objectives 14
1.4 Research Methodology 14

CHAPTER 2 – LITERATURE REVIEW 18

2.1 The Use of CFD Tools in Inlet and Outlet Design 23
2.2 The Use of CFD Tools in Baffle Design 24

CHAPTER 3 – COMPUTATIONAL FLUID DYNAMICS 28

3.1 Governing Equations 28
3.1.1 Conservation of Fluid Mass (Continuity Equation) 28
3.1.2 Conservation of Momentum (Momentum Equation) 29
3.1.3 Conservation of Energy 30
3.2 Turbulence Modeling 30
3.2.1 Direct Numerical Simulation (DNS) 31
3.2.2 Large Eddy Simulation (LES) 31

3.2.3 Reynolds Averaged Navier-Stokes (RANS) Models 32
3.3 Multiphase Models 35
3.3.1 Euler-Lagrange Model 35
3.3.2 Euler-Euler Models 37
3.3.2.1 Mixture Model 37
3.3.2.2 Volume of Fluid (VOF) 38
3.3.3 Single Phase Modeling 38

CHAPTER 4 – MATERIALS AND METHODS 40

4.1 Study Area 40
4.1.1 Aeration Tank 41
4.1.2 Clarifiers 42
4.2 CFD Modeling 43
4.2.1 Modeling Objective 43
4.2.2 Modeling Geometry 47
4.2.3 Discretization 52
4.2.4 Boundary Conditions 52
4.2.5 Solver Settings 52

CHAPTER 5 – RESULTS AND DISCUSSIONS 54

5.1 Investigation of Recorded Operational Data of the Scrutinized WWTP 54
5.2 Design Review of Biological Treatment Units 57
5.2.1 Comprehension of Investigation Results 59
5.3 Investigation of Hydrodynamics within the Aeration Tank 60
5.3.1 Velocity Flow Field 61
5.3.2 Streamlines 62
5.3.3 Aeration 63
5.3.4 Comprehension of Investigation Results 65
5.4 Investigation of Hydrodynamics within the Conventional Clarifier 65
5.4.1 Velocity Flow Field 66
5.4.1.1 Horizontal Cross-Section of the Velocity Flow Field 66
5.4.1.2 Vertical Cross-Section of the Velocity Flow Field 67
5.4.2 Solids Settling Velocity 68

5.4.3 Solids Concentration....69
5.4.4 Streamlines....70
5.4.5 Comprehension of Investigation Results....71
5.5 Retrofitting Conventional Central-Feed Circular Secondary Clarifiers with Opposing-Jet Type EDIs....72
5.5.1 LA-EDI Type-I....73
5.5.1.1 Velocity Flow Field....73
5.5.1.2 Solids Settling Velocity....75
5.5.1.3 Solids Concentration....76
5.5.1.4 Streamlines....78
5.5.2 LA-EDI Type-II....79
5.5.2.1 Velocity Flow Field....80
5.5.2.2 Solids Settling Velocity....82
5.5.2.3 Solids Concentration....83
5.5.2.4 Streamlines....85
5.5.3 Comprehension of Results....85
5.6 Two Novel Sludge Draw-Off Pipe Designs for Central-Feed Circular Secondary Clarifiers Retrofitted with Different Types of EDIs....87
5.6.1 Velocity Flow Field....88
5.6.1.1 Horizontal Cross-Section of the Velocity Flow Field....88
5.6.1.2 Vertical Cross-Section of the Velocity Flow Field....91
5.6.2 Solids Settling Velocity....93
5.6.3 Solids Concentration....96
5.6.4 Streamlines....98
5.6.5 Comprehension of Results....99
5.7 A Novel Deflector Design in Central-Feed Circular Secondary Clarifiers Equipped with Opposing-Jet Type EDIs....100
5.7.1 Velocity Flow Field....101
5.7.1.1 Horizontal Cross-Section of the Velocity Flow Field....101
5.7.1.2 Vertical Cross-Section of the Velocity Flow Field....102
5.7.2 Solids Settling Velocity....105
5.7.3 Solids Concentration....106

5.7.4 Streamlines 107
5.7.5 Comprehension of Results 107

CHAPTER 6 – CONCLUSIONS AND RECOMMENDATIONS 109

6.1 Future Works 111

REFERENCES 112

LIST OF FIGURES

Page

Figure 1.1 The cross-section of a clarifier that is equipped with an LA-EDI (Type-I on the left and Type-II on the right) 12
Figure 1.2 The influent well and opposing-jet nozzles in LA-EDI 12
Figure 1.3 The multiple baffles stacked on top of each other in MEDIC 13
Figure 4.1 The aerial view of the investigated WWTP 40
Figure 4.2 The nitrification and denitrification volumes in the aeration tank of the investigated WWTP 41
Figure 4.3 The general view of the clarifier, including the influent well and scrapers, in the investigated WWTP 42
Figure 4.4 The cross-section of the original clarifier 47
Figure 4.5 The cross-section of the clarifier equipped with only a LA-EDI 47
Figure 4.6 The cross-section of the clarifier equipped with a LA-EDI and a spiral-shaped draw-off pipe 48
Figure 4.7 The cross-section of the clarifier equipped with a LA-EDI and a snail-shaped draw-off pipe 48
Figure 4.8 The cross-section of the clarifier equipped with a MEDIC and a snail-shaped draw-off pipe 49
Figure 4.9 The cross-section of the clarifier equipped with a LA-EDI, a snail-shaped draw-off pipe and the novel deflector 49
Figure 4.10 The 3D geometry of the snail-shaped draw-off pipe 50
Figure 4.11 The 3D geometry of the spiral-shaped draw-off pipe 51
Figure 4.12 The 3D geometry of the novel deflector 51
Figure 5.1 The illustration of the key design parameters assumed in the design of the Aeration Tank of the investigated WWTP 54
Figure 5.2 The illustration of the key parameters recorded in the Aeration Tank of the investigated WWTP 57
Figure 5.3 Flow Velocity Vectors in the Aeration Tank 62
Figure 5.4 Streamlines and eddies in the Aeration Tank 63
Figure 5.5 Air Volume Fraction right after onset of the operation (t=5sec) 64

Figure 5.6 Air Volume Fraction after a course of the operation (t=60sec).....64
Figure 5.7 The flow velocity contours at the elevation of orifices in the original conventional clarifier and simulated under existing conditions.....67
Figure 5.8 Flow velocity vectors in the original conventional clarifier and simulated under existing conditions.....68
Figure 5.9 Solids settling velocity contours (m/s) in the original conventional clarifier and simulated under existing conditions.....68
Figure 5.10 Solids concentration contours (kg/m³) in the original conventional clarifier and simulated under existing conditions.....69
Figure 5.11 The change of solids concentration drawn-off from the original conventional clarifier.....70
Figure 5.12 Streamlines simulated in the original clarifier during sludge withdrawal under existing inflow conditions.....71
Figure 5.13 The flow velocity contours at the elevation of orifices in the clarifier equipped with only an Standard Type-1 LA-EDI and simulated under existing conditions.....74
Figure 5.14 The flow velocity contours at the elevation of orifices at which represent the formation of opposing jets in the case where the existing influent well was replaced with an LA-EDI Type-1.....74
Figure 5.15 Flow velocity vectors in the clarifier equipped with only a Standard Type-1 LA-EDI and simulated under existing conditions.....75
Figure 5.16 Solids settling velocity contours (m/s) in the clarifier equipped with only a Standard Type-1 LA-EDI and simulated under existing conditions.....76
Figure 5.17 Solids concentration contours (kg/m³) in the clarifier equipped with only a Standard Type-1 LA-EDI and simulated under existing conditions.....77
Figure 5.18 The change of solids concentration drawn-off from the clarifier equipped with a Standard Type-1 LA-EDI.....78
Figure 5.19 Streamlines simulated in the clarifier equipped with only a Standard Type-1 LA-EDI and simulated under existing conditions.....79
Figure 5.20 The flow velocity contours at the elevation of orifices in the clarifier equipped with only an Standard Type-2 LA-EDI and simulated under existing conditions.....81

Figure 5.21 The flow velocity contours at the elevation of orifices at which represent the formation of opposing jets in the case where the existing influent well was replaced with an LA-EDI Type-2 81
Figure 5.22 Flow velocity contours in the clarifier equipped with only a Standard Type-2 LA-EDI and simulated under existing conditions 82
Figure 5.23 Solids settling velocity contours (m/s) in the clarifier equipped with only a Standard Type-2 LA-EDI and simulated under existing conditions 83
Figure 5.24 Solids concentration contours in the clarifier equipped with only a Standard Type-2 LA-EDI and simulated under existing conditions 84
Figure 5.25 The change of solids concentration drawn-off from the clarifier equipped with a Standard Type-2 LA-EDI 84
Figure 5.26 Streamlines simulated in the clarifier equipped with only a Standard Type-2 LA-EDI and simulated under existing conditions 85
Figure 5.27 The flow velocity contours at the elevation of orifices in the clarifier equipped with an LA-EDI, and a spiral-shaped draw-off pipe and simulated for doubled inflow conditions. 89
Figure 5.28 The flow velocity contours at the elevation of orifices in the clarifier equipped with an LA-EDI, and a snail-shaped draw-off pipe and simulated under doubled inflow conditions. 89
Figure 5.29 The flow velocity contours at the elevation of orifices in the clarifier equipped with a MEDIC, and a snail-shaped draw-off pipe and simulated under doubled inflow conditions. 90
Figure 5.30 Flow velocity vectors in the clarifier equipped with an LA-EDI, and a spiral-shaped draw-off pipe and simulated for doubled inflow conditions 91
Figure 5.31 Flow velocity vectors in the clarifier equipped with an LA-EDI, and a snail-shaped draw-off pipe and simulated for doubled inflow conditions 91
Figure 5.32 Flow velocity vectors in the clarifier equipped with a MEDIC, and a snail-shaped draw-off pipe and simulated under doubled inflow conditions ... 92

Figure 5.33 Solids settling velocity contours (m/s) in the clarifier equipped with an LA-EDI, and a spiral-shaped draw-off pipe and simulated for doubled inflow conditions. 94
Figure 5.34 Solids settling velocity contours (m/s) in the clarifier equipped with an LA-EDI, and a snail-shaped draw-off pipe and simulated for doubled inflow conditions. 95
Figure 5.35 Solids settling velocity contours (m/s) in the clarifier equipped with a MEDIC, and a snail-shaped draw-off pipe, and simulated under doubled inflow conditions. 95
Figure 5.36 Solids concentration contours in the clarifier equipped with an LA-EDI, and a spiral-shaped draw-off pipe and simulated for doubled inflow conditions. 96
Figure 5.37 Solids concentration contours in the clarifier equipped with an LA-EDI, and a snail-shaped draw-off pipe and simulated for doubled inflow conditions. 97
Figure 5.38 Solids concentration contours in the clarifier equipped with a MEDIC, and a snail-shaped draw-off pipe and simulated under doubled inflow conditions. 97
Figure 5.39 Streamlines simulated during sludge withdrawal in the clarifier equipped with an LA-EDI, and a spiral-shaped draw-off pipe and simulated for doubled inflow conditions. 98
Figure 5.40 Streamlines simulated during sludge withdrawal in the clarifier equipped with a MEDIC, and a spiral-shaped draw-off pipe and simulated for doubled inflow conditions. 99
Figure 5.41 The flow velocity contours at the elevation of orifices in the clarifier equipped with an LA-EDI, a spiral-shaped draw-off pipe, and a novel deflector and simulated for doubled inflow conditions. 101
Figure 5.42 Flow velocity vectors in the clarifier equipped with an LA-EDI, a spiral-shaped draw-off pipe, and a deflector and simulated for doubled inflow conditions 102

Figure 5.43 Solids settling velocity contours (m/s) in the clarifier equipped LA-EDI, a spiral-shaped draw-off pipe, and a deflector and simulated for doubled inflow conditions. 105
Figure 5.44 Solids concentration contours in the clarifier equipped with an LA-EDI, a spiral-shaped draw-off pipe, and a novel deflector and simulated for doubled inflow conditions. 106
Figure 5.45 Streamlines simulated during sludge withdrawal in the clarifier equipped with an LA-EDI, a spiral-shaped draw-off pipe, and a novel deflector and simulated for doubled inflow conditions. 107

LIST OF TABLES

Page

Table 5.1 Descriptive Statistics of the Operational Data Recorded in the Investigated WWTP 55

Table 5.2 The comparison of the design parameters between the previous design and the current design check.....58

ABBREVIATIONS

2D	:	Two Dimensional
3D	:	Three Dimensional
A^2O	:	Anaerobic–Anoxic–Oxic Configuration in BNR
BNR	:	Biological Nutrient Removal
BOD	:	Biological Oxygen Demand
CFD	:	Computational Fluid Dynamics
DPM	:	Discrete Phase Modeling
DNS	:	Direct Numerical Simulation
EDI	:	Energy Dissipating Inlet
EVM	:	Eddy Viscosity Model
F	:	Flux Term
HRT	:	Hydraulic Residence Time
LA-EDI	:	The Los Angeles Energy Dissipating Inlet
LES	:	Large Eddy Simulation
MEDIC	:	Multilayer Energy Dissipating Inlet Column
MLSS	:	Mixed Liquor Suspended Solids
NSE	:	Navier-Stokes Equations
RANS	:	Reynolds Averaged Navier Stokes
RNG	:	Renormalized Group
RSM	:	Reynolds Stress Model
S	:	Source Term
SGS	:	Sub Grid Scale
SVI	:	Sludge Volume Index
SOR	:	Surface Overflow Rate
SLR	:	Sludge Loading Rate
SRT	:	Sludge Retention Time
SST	:	Shear Stress Transport
UDF	:	User Defined Function
URANS	:	Unsteady Reynolds Averaged Navier Stokes
VOF	:	Volume of Fluid
WWTP	:	Wastewater Treatment Plant

LIST OF SYMBOLS

C_ε	:	Model constant
C_μ	:	Model constant
ε	:	The rate of dissipation of turbulent kinetic energy
F_g	:	Body forces
g	:	Gravitational force
G_b	:	Turbulence generation due to buoyancy
G_k	:	Turbulence generation due to the mean velocity gradient
k	:	Turbulent kinetic energy
μ_t	:	Turbulent viscosity
p	:	Pressure
r_h	:	A constant in Takacs settling function
r_p	:	A constant in Takacs settling function
ρ	:	Density
S	:	Filtered rate of strain tensor
SS	:	Specific density of activated sludge
σ_ε	:	Model constant
σ_k	:	Model constant
t	:	Time
$\bar{\tau}$	:	Stress tensor
$\vec{v}$	:	Velocity vector
V_S	:	Solids settling velocity
V_{s0}	:	Reference solids settling velocity
X	:	Local solids concentration
X_{ns}	:	Non-settleable solid concentration

CHAPTER 1
INTRODUCTION

Wastewater treatment is the process of removing pollutants from wastewater before it is released into the receiving environment. The goal of wastewater treatment is to reduce the environmental impact of the pollutants and to make the treated wastewater safe for discharge. Wastewater treatment is a critical process that plays a key role in protecting the environment and public health.

There are several types of wastewater treatment processes, each with its own specific goal and methods:

- The primary treatment process is to remove large solids such as debris and sediment that are present in the wastewater. Common treatment technologies include physical processes such as screening, sedimentation, filtration, and flotation.

- Secondary treatment process is to remove dissolved pollutants and organic matter from the wastewater. Common treatment technologies include biological processes such as activated sludge, trickling filters, and rotating biological contactors; and chemical processes such as coagulation and flocculation.

- Tertiary treatment process is to remove nutrients and remaining pollutants and to disinfect the wastewater. Some of the advanced treatment technologies include membrane filtration, electrochemical and advanced oxidation processes, selective ion exchange, activated carbon absorption, electrocoagulation, ozonation, etc.

Wastewater treatment plants are complex systems that require careful design to ensure their efficient and effective operation. The design process involves the selection and integration of various treatment technologies, as well as the optimization of the flow and mixing of fluids in the system:

- The first step in the design process is the characterization of the wastewater to be treated. This includes the determination of the type and concentration of pollutants in the wastewater, as well as the flow rate and volume of the wastewater.

- The next step is the selection and integration of treatment technologies. This includes the selection of primary, secondary, and tertiary treatment processes, as well as the selection of any additional treatment processes, such as sludge treatment and disposal. The treatment technologies are integrated in such a way that they work together to effectively remove pollutants from the wastewater.

- The final step in the design process is the optimization of the flow, the movement of fluids, and the mixing of fluids in the system. This includes the optimization of the design of mixing devices, such as aerators and diffusers, as well as the optimization of the layout of tanks and other components in the treatment system. Proper hydrodynamics ensures that microorganisms, chemicals, and other materials are mixed and distributed evenly, which allows for the efficient removal of pollutants and improves the performance of treatment processes.

Computational Fluid Dynamics (CFD) tools have been used to optimize the design of treatment systems, to predict the performance of different treatment options, and to identify the most effective ways to remove pollutants from wastewater. Simulation of hydrodynamics in wastewater treatment plants using CFD tools has been an active area of research in recent years.

The use of CFD tools is an advantage in addressing common design problems in wastewater treatment plants, such as: insufficient treatment capacity, inadequate mixing and flow, poor sludge management, lack of flexibility, insufficient monitoring and control, and energy inefficiency. Addressing common design problems can help to improve the performance of treatment systems, reduce maintenance costs, and minimize negative environmental and public health impacts. In other words, addressing common design problems plays a key role in achieving the desired environmental and economic outcomes.

Intensive use of CFD tools in wastewater treatment and accumulation of knowledge will enable to perform better design and operational models. These models will help to facilitate process yield (such as enhancing pollutant removal by smart mixing methods) and minimize energy consumption (such as rearranging the configuration of mixers, aerators and control instruments or making smart changes in operation order).

Applications of CFD tools in wastewater treatment engineering for researching novel processes and innovations, improving design methods of available processes, dimensioning plants, operating plants and troubleshooting are not prevailing. Therefore, there is a need for doing research and accumulation of knowledge using these tools for wastewater treatment.

In the scope of this dissertation, CFD simulations were performed to examine and optimize the hydrodynamic processes of the activated sludge system (aeration tank and clarifier units) in an urban wastewater treatment plant. The flow and mixing behavior in the aeration tanks and short-circuiting problems and sludge blanket deformation in clarifiers were evaluated using CFD tools.

1.1 Activated Sludge Process

The activated sludge process is one of the most widely used biological treatment systems in wastewater treatment. It is an eminent treatment technology that has been implemented for over a century for domestic, municipal, and industrial wastewaters.

The process yields favorable living conditions for a culture of microorganisms that utilize the organic matter and nutrients available in the wastewater as a substrate, consequently treating the wastewater. The process takes place in multiple reactors; among them, usually clarifiers (as known as secondary or final sedimentation tanks or settling tanks) are the final step, where the activated sludge is isolated and well-clarified treated effluent is yielded (Ekama, et al., 1997); (Tchobanoglous, Burton, & Stensel, 2003).

1.1.1 Aeration Tanks

Aeration tanks are an essential component of the activated sludge process. They are large tanks, filled with wastewater, and aerated to create favorable living conditions for a culture of microorganisms to consume the organic matter and nutrients available in the wastewater as a source of food and convert it into biomass. Eventually, the microorganisms grow and reproduce themselves in aeration tanks.

The activated sludge process has multiple modifications particularly for Biological Nutrient Removal (BNR). Among those Modified Ludzack-Ettinger, A^2O, and Modified Bardenpho are the most known ones. Nitrogen and phosphorus removal is provided as well as carbon removal by forming aerobic, anoxic and anaerobic environments in different sequences in one or more regions of the aeration tank in these modifications.

The growth and reproduction of microorganisms in aeration tanks are constrained by adjusting several parameters in the activated sludge process. Among those the F/M ratio is kept low at high sludge age thus the microorganisms consume their own cytoplasm by internal respiration and eventually minimize sludge production; due to the fact that treatment, handling, and removal of excess sludge are expensive. However, hydraulic retention of sludge in the aeration tanks for a long time also increases the need for oxygen.

Aeration is the focal point of the activated sludge system. The effluent water quality is provided by adjusting the air flow rate as per the discharge limits of the receiving environment. In other words, increasing the airflow often leads to better effluent water quality. It also has many advantages, such as inhibition of filamentous bacteria growth with high dissolved oxygen, higher biomass supply in the aeration tank, better sludge generation, less sludge production, higher oxygen transfer efficiency, and more stable operation (Liu, 2003).

The required air can be supplied by different mechanical aerators in activated sludge systems. There are diverse options for mechanical aerators in the market. Among those, diffuser aeration systems and surface aerators are the most used mechanical aerators. Each aeration system has benefits and drawbacks compared with its competitors. The efficiency is low in both diffuser aeration systems and surface aeration systems.

Increasing the airflow causes electrical energy consumption to increase exponentially. Electrical energy consumption is the most important expense item of WWTPs. In a WWTP with activated sludge, the aeration process accounts for more than 50% of the total energy requirement. Therefore, reducing the airflow as much as possible provided that the effluent water quality is maintained at a sufficient level will significantly reduce the energy consumption of the plant. While reducing the airflow, the power given should be sufficient to keep all microorganisms suspended and to survive. It should not be overlooked that if the oxygen level limits the growth of microorganisms, sludge may lose its deposition property.

The design of the biological treatment process is usually based on the empirical formulas given in the design guides. The average flow rate is used in the design of biological treatment units (activated sludge system aeration tanks and clarifiers) (Tchobanoglous, Burton, & Stensel, 2003). Details other than the basic variables (volumes, air demand, mixing requirement) that affect the nitrification and denitrification process can be assessed by performing laboratory experiments on physical models.

The aerobic and anoxic zone volumes required for nitrification and denitrification can be determined by biokinetic models. However, under hydrodynamic and meteorological conditions, the process which is attempted to be constructed in dimensioning without knowing the efficiency of the aerating equipment and apparatus cannot be dimensioned correctly.

Although the design guide gives empirical formulas about the volumes (nitrification and denitrification) required for the removal of fundamental pollutants (carbon and nitrogen), there are no answers to the following questions: How the geometry of the tank should be, do the anoxic and aerobic conditions prevail as designed, how the wastewater should enter and exit from the tank, where the mixers should be located, how to install mechanical systems to maintain internal recycle in the tank; the impact of hydrogeometric design on the track that active sludge suspension follows and validating that solid and liquid phases are homogenous.

Once the required airflow is calculated in the design of the activated sludge process, no detailed design can be made for the application of the selection of the aeration equipment and the arrangement of the device. The design suggests a layout based on the information supplied by the aeration equipment supplier. In practice, although the proposed layout is considered, it can also be formed in a different order by applying engineering experience. Since there is no valid calculation method for the selection of the aeration equipment and the arrangement of the device, the method of oversizing is used in the aeration process. A larger blower is selected; diffusers are placed to ignore unwanted and unexpected situations. In this way, targeted discharge limits are satisfied. Operating costs are increased due to excessive or inefficient aeration. For this purpose, the design of the aeration process in activated sludge systems should be improved, and a system to ensure energy efficiency should be established.

1.1.2 Clarifiers

The clarification (or sedimentation) is the process of isolation of activated sludge that is heavier than water through settling by gravity. The favorable conditions in the clarifier enhance the suspension to segregate into two phases, and while the solid phase inside the suspension submerges to the bottom, the fluid phase glides to the surface. In the meantime, the solids adhere to each other, and the size of the flocs gradually increases during the sedimentation process. Consequent to the agglomeration of flocs, the heavy ones settle faster, while the light ones settle slower -or may never have a chance to reach the bottom, they may escape from the weirs and drain with the treated effluent-. The flocs that are deposited on the bottom of the tank compress the previously deposited ones and form a sludge layer, which is called a sludge blanket (Ekama, et al., 1997); (Tchobanoglous, Burton, & Stensel, 2003).

The depth of the sludge blanket increases with the accumulation of solids in the clarifier. It is not favorable to operate the clarifier with a deep sludge blanket, since it facilitates solids to escape over the weirs and increases organic load (BOD) in the effluent (Tchobanoglous, Burton, & Stensel, 2003). Moreover, the sludge blanket may even fill the clarifier and overflow the weirs at transient peak flows, since the depth of the sludge blanket is affected by flow rate and solids loadings variations. Furthermore, it is required to maintain the target MLSS (Mixed Liquor Suspended Solids) concentration in the aeration tanks for the sake of the activated sludge process, with this respect, the settled sludge must be pumped back into the aeration tanks. Therefore, the depth of the sludge blanket is kept at an optimum level by withdrawing settled solids from the clarifier (Ekama, et al., 1997); (Tchobanoglous, Burton, & Stensel, 2003).

The settling behavior of the solids in the wastewater is usually grouped into four classes: Non-flocculent, discrete-flocculent, hindered, and compressive settling. Among those settling behaviors, the sedimentation of activated sludge is characterized as hindered settling since the terminal settling velocity of a floc is influenced by the neighboring flocs and the sludge concentration. Although the sludge concentration

depends on the specific gravity, size, and shape of flocs, the volumetric concentration of suspended solids is the sufficient parameter that discloses whether hindered settling will occur or not in the clarifier.

The settling behavior can be easily detected by measuring the Sludge Volume Index (SVI). In practice, it is also a process control parameter for a treatment plant operator to decide and adjust the amount of return activated sludge -to keep the sludge blanket level in the clarifier- and the waste activated sludge -to keep the sludge retention time (SRT) at the desired level-.

The settling behavior of the MLSS is the essential parameter in the design of the clarifier. However, sludge behavior is rarely known in the design phase. Therefore, it is usually assumed as per designers' experience from previous projects. In this context, the design is performed for either the peak flowrate or the escalated design flowrate with a safety factor. Oversizing the treatment units is a conventional method practiced to overcome the shortcomings of the design, due to the fact that steady-state conditions do not usually prevail in the wastewater treatment plant. This augmentation pledges to ensure enough volume for the clarification of the effluent and the thickening of the sludges, by capacitating the clarifier to serve a wide range of SVI and compensate for high fluctuations in flowrates.

The conventional design of the clarifiers is based on the surface overflow rates (SOR) and the solids loading rates. Although typical surface overflow rates usually ranges between 24-32 $m^3/m^2.d$ and solids loading rates (SLR) usually ranges between 4-6 $kg/m^2.h$, there are clarifiers that satisfy effluent quality with surface overflow rates as much as 65-73 $m^3/m^2.d$, and provide efficient sludge settling with solids loading rates as much as 10-16 $kg/m^2.h$ (Tchobanoglous, Burton, & Stensel, 2003). Moreover, among those two key design parameters, the solids loading rate is more dominant on the effluent quality than the surface overflow rate (Tchobanoglous, Burton, & Stensel, 2003). The effluent quality will deteriorate if the solids loading is increased beyond the design value, even if there is enough surface area to provide the required surface

overflow rates. Therefore, peak flowrates should be assumed to govern to prevent the solids from overflowing the tank.

The auxiliary factors that impact the design and performance of clarifiers include tank geometry, sidewater depth, inlet design, flow distribution and energy dissipation, weir placement, weir loading rates, sludge removal mechanisms (through scrapers –or rakes– or sludge suction) and scum removal.

The preferred tank geometry is usually circular rather than rectangular. Aside from the advantages of a smaller footprint and better structural integrity, circular clarifiers are favored in clarifier design due to improved hydraulic conditions. The circular tanks allow for a more uniform flow of water through the clarifier, promoting better solids separation and improved clarification. Besides, circular clarifiers have fewer dead zones compared to rectangular clarifiers. Therefore, circular geometry provides improved performance and greater efficiency in clarification.

Circular clarifiers can be designed as center-fed or peripheral-fed. The center-fed design provides more uniform flow and reduced turbulence, while peripheral-fed clarifiers have a larger surface area, leading to increased capacity compared to center-fed clarifiers of similar size, and improved solids retention for better clarification.

The depth of liquid in a clarifier is usually measured at the sidewall in circular tanks. This depth is a crucial aspect in the efficiency of removing suspended solids and determining the concentration of return sludge. Currently, a minimum side-water depth of 3.5 meters is preferred, while depths up to 6 meters have been utilized in some cases (Tchobanoglous, Burton, & Stensel, 2003). Deeper tanks offer more operational flexibility and a wider margin of safety in case of any changes in the activated sludge system (Tchobanoglous, Burton, & Stensel, 2003).

Poor distribution or jetting of influent entering the tank can cause density currents and scouring of settled sludge, leading to inadequate tank performance. To address this, tank inlets should be designed to dissipate influent energy, distribute the flow

evenly in both horizontal and vertical directions, mitigate density currents, maintain sludge blanket performance, and enhance flocculation. In circular center-feed tanks, cylindrical baffles with solid skirts are often used to dissipate the influent energy and distribute flow. However, studies show that these baffles can create a density current waterfall, causing poor vertical flow distribution. To overcome this, using a large center diffusion well with a minimum diameter of 25% of the tank diameter can provide a greater area for energy dissipation and flow distribution. The bottom of the feed well should be positioned well above the sludge blanket interface to reduce turbulence and minimize solids resuspension. Flocculating center-feed clarifiers can have an energy-dissipating inlet and mechanisms to promote flocculation in the center feed well. The typical diameter of flocculation feed wells is 30-35% of the tank diameter.

The clarifier bottom is usually shaped to facilitate the gathering of the solids at the lower center of the clarifier. The clarifier floor is usually radially sloped (1:12) towards the center of the clarifier. Besides, an inverted cone-shaped small volume, the so-called sludge hopper, is usually formed at the lower center of the clarifier. The solids thickened on the clarifier floor are usually swept by a rotating scraper towards the center of the clarifier. The solids gathered at the sludge hopper are then rather conveyed to a sump pit, where the pumps exist, with a draw-off pipe, or directly pumped back into the aeration tank. Besides, a negligible volume compared to the return activated sludge is pumped from the sump pit or directly from the sludge hopper to the sludge handling units for disposal (Tchobanoglous, Burton, & Stensel, 2003). In addition to the described conventional sludge collection and withdrawal procedure above, there are a few patented inventions for the collection and withdrawal of solids from the clarifier (US Patent No. 5,340,485, 1994); (Wright, 2004); (US Patent No. 9,339,743 B2, 2016).

1.1.2.1 Energy Dissipating Inlets (EDIs). The EDIs are usually types of equipment that are mounted at the inlet of the clarifier and enhance the diffusion of the influent into the clarifier without disturbance and facilitate the formation of density currents in a horizontal direction. The early examples of EDIs are Stengel, Geiger and Stuttgarter.

Plenty of EDIs has been invented in the last few decades, which are either patented or patent-pending. The EDIs can be classified as (Esler J. K., 2022): (i) gated-opening, (ii) scooped-opening (or tangential port opening), (iii) multiple plate, and (iv) opposing-jet type inlets.

The opposing-jet nozzle type EDIs, particularly the LA-EDI, was reported to be one of the most superior among their alternatives in the literature. There are two configurations of the LA-EDI (Figure 1.1):

- In the LA-EDI Type I, the multiple wing-type outlet nozzles are mounted below the periphery of the influent-well, and a feed-well is created on the periphery of the influent-well (Figure 1.2).

- In the LA-EDI Type II, instead of forming a feed-well on the periphery of the influent well, the multiple wing-type outlet nozzles are placed not on the periphery, but closer to the center of the influent well; besides, the periphery of the influent well is lowered to a distance to form a buffer wall like a skirt to mimic a feed-well.

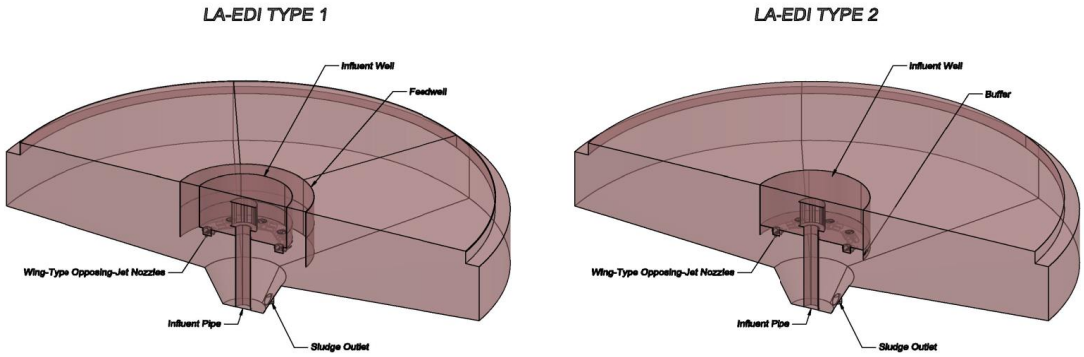


Figure 1.1 The cross-section of a clarifier that is equipped with an LA-EDI (Type-I on the left and Type-II on the right)



Figure 1.2 The influent well and opposing-jet nozzles in LA-EDI (CPE Services Inc., 2022).

The multilayer-type EDI, particularly the MEDIC, is another good option instead of an opposing-jet nozzle type EDIs. The MEDIC consists of multiple perforated plates or baffles stacked on top of each other in a vertical column, as depicted in Figure 1.3 (Hydrosims, 2022). As the wastewater flows into the column, it encounters the baffles, which cause the flow to change direction and velocity. This change in flow direction and velocity dissipates the energy of the incoming wastewater and reduces turbulence, allowing the solids to settle more easily.



Figure 1.3 The multiple baffles stacked on top of each other in MEDIC (Hydrosims, 2022).

EDIs are designed to effectively dissipate the influent's kinetic energy, diffuse it uniformly in both directions, promote flocculation, and mitigate density currents. This results in improved hydrodynamics inside the clarifier and allows for an increased capacity compared to conventional clarifiers.

1.2 Defining the Problem

Proper hydrodynamics refers to optimal fluid behavior and motion in wastewater treatment systems, and it is crucial for efficient pollutant removal and treatment process performance. However, the optimization of hydrodynamics was a challenge in the past due to the lack of effective analysis tools. As a result, wastewater treatment plants were often oversized to compensate for inadequate design, leading to poor energy efficiency and high energy input requirements. This paradoxical situation arises because while wastewater presents a potential source of energy, the treatment process demands a significant amount of energy input.

Fortunately, computational fluid dynamics (CFD) tools have emerged as an effective solution to this challenge, enabling engineers to simulate and analyze fluid behavior and motion in treatment processes. With the advancements in computer technology and the accumulation of knowledge, CFD tools have become essential in wastewater engineering to optimize hydrodynamics.

The current global energy crisis requires diversifying energy sources and improving energy efficiency, making it increasingly necessary to optimize hydrodynamics in wastewater treatment. Through optimizing hydrodynamics, it is possible to minimize energy input, reduce operating costs, and improve treatment performance. Additionally, as sustainability becomes increasingly important, wastewater treatment systems that optimize hydrodynamics will be critical in meeting the growing demand for clean water and energy.

Aeration, pumping, and mixing are the most energy-demanding operations in wastewater treatment. Proper hydrodynamics have a significant positive impact on decreasing energy requirements in these operations. From the perspective of improving energy efficiency in biological treatment units whilst sustaining efficient pollutant removal and treatment process performance the hydrodynamics in biological treatment units must be investigated, and efficient measures should be developed.

1.3 Research Objectives

The main objective of this dissertation is to research methods to enhance wastewater treatment processes and exploring smart methods to minimize energy consumption by investigating the hydrodynamic conditions in wastewater treatment plants through the use of CFD tools.

1.4 Research Methodology

This dissertation hypothesizes that optimizing hydrodynamics in wastewater treatment plants can minimize energy input, reduce operating costs, and improve treatment performance. To test this hypothesis, this research focuses on examining and optimizing the hydrodynamic processes of the activated sludge system. In this context, CFD simulations will be utilized to investigate the flow and mixing behavior in the aeration tanks and the sedimentation process in the secondary clarifiers. Necessary modifications and optimizations will be made to enhance the treatment process based on the results of these simulations.

An urban wastewater treatment plant has been chosen as a pilot plant to conduct hydrodynamic investigations and optimization studies. To begin with, a design review of the treatment plant will be carried out based on operational records, aiming to identify any inefficiencies or excesses that may exist in the current system.

CFD tools will be employed to model the flow and mixing behavior in the aeration tanks, which will allow for the optimization of mixer placement. This will involve evaluating the current mixer configurations to ensure they are situated in the most energy-efficient position to enhance the treatment process. The CFD simulations will help identify any flow patterns that are not optimal, and necessary adjustments will be made to the design and placement of mixers to address these issues. The evaluation of different mixer configurations using CFD simulations will provide insight into the mixing intensity, flow field, and energy consumption in aeration tanks. This information will be used to guide the design of mixer placement and enhance the energy efficiency of the wastewater treatment process. Ultimately, this investigation will provide a comprehensive understanding of the hydrodynamics inside the aeration tank and enable the selection of the best possible mixer configuration to optimize the treatment process.

CFD simulations will be utilized to provide a comprehensive understanding of the sedimentation process and to identify and address hydrodynamic issues such as short-circuiting and sludge blanket deformation. Moreover, the simulations will help diagnose the conditions that limit the further capacity increase in the clarifier. Although conventional clarifiers do not typically feature an EDI, prolonged operational and capacity issues may necessitate retrofitting clarifiers with an EDI. In this context, the clarifier of the pilot plant is planned to undergo a capacity increase by retrofitting either a multilayer- or opposing jet-type EDI. The insights gained from the CFD simulations will inform the selection of the most suitable EDI configuration for maximizing the efficiency and capacity of the clarifier.

Although there are two routes of short-circuiting in clarifiers, up-flow (or effluent) short-circuiting comes first to mind. While up-flow short-circuiting is the escape of

solids by overflowing the weirs, underflow short-circuiting is the discharge of the supernatant along with the thickened sludge from the draw-off pipe (Mendis & Benedek, 1980; Wright, 2004; Frost, Halliday, & Dee, 1993; Krebs, 1995).

The underflow short-circuiting is an important phenomenon in clarifiers equipped with an EDI (Esler J. K., 2022). Many studies in the literature demonstrated that on the one hand, EDIs well-dissipate the influent kinetic energy, diffuse the influent uniformly in both directions, promote flocculation, and mitigate density currents, on the other hand, EDIs facilitate scouring the sludge blanket and discharge of the supernatant along with the thickened sludge from the draw-off pipe (Grau & Aquanova, 2022); (Esler J. K., 2022). From this point of view, the obstacle in enhancing the clarifier performance to a better level is assumed to be not due to the geometry of an EDI, but the geometry of the draw-off pipe.

It is conceptualized that having multiple draw-off pipes would decrease the underflow capacity. To that end, the advantages of CFD tools will be taken in this study first to improve the design of the draw-off pipes to decrease underflow short-circuiting. Furthermore, the potential for further capacity increase will be assessed by retrofitting the clarifier of the pilot plant with an EDI and a novel design draw-off pipe, using CFD simulations.

To compare and contrast the advantages and drawbacks of retrofitting, various retrofit options will be simulated. These retrofit options include coupling a multilayer- or an opposing jet-type EDI with novel design draw-off pipes, in addition to the existing conventional clarifier. CFD tools will be employed to analyze the performance of each retrofit option, assessing the potential for minimizing energy consumption, decreasing operational costs, enhancing treatment capacity, improving treatment performance, and meeting discharge limits. After evaluating the results, the best retrofit option will be selected for the studied pilot plant.

Validation is a critical step in the research process to ensure the accuracy and reliability of simulation results. Initially, field experiments were planned to verify the

CFD simulations. However, due to unforeseen constructional issues with the pilot plant, the units were emptied for an extended period to fix the problems, which resulted in the exclusion of field experiments from the dissertation's scope.

The findings of this research are expected to provide valuable insights into the optimization of hydrodynamic conditions in urban wastewater treatment plants, which can lead to more sustainable and efficient wastewater treatment processes.

CHAPTER 2
LITERATURE REVIEW

CFD is a powerful technique used to investigate and comprehend fluid flow in complex geometries and boundary conditions. CFD utilizes numerical methods to solve the differential equations governing fluid flow, heat transfer, and associated phenomena such as chemical reactions through computer-based simulation (Dadvand & Motlagh, 2022). Engineers and scientists can analyze and predict the velocity and pressure fields, and other focused characteristics of fluid flow using CFD.

CFD is an interdisciplinary topic that bridges the gap between physics, applied mathematics, and computer science (Dadvand & Motlagh, 2022). The versatility of CFD makes it applicable to a broad range of problems from various fields, such as mechanical engineering, chemical engineering, aeronautical engineering, and naval architecture.

The earliest CFD modeling study in the field of wastewater treatment was carried out by Larsen in 1977 (Larsen, 1977). In the past, CFD tools were not very much preferred by wastewater engineers because of the long computational time required. However, in recent years, CFD tools have gained more popularity as commercial software has become more accessible, open-source software has developed more quickly than commercial software, the graphical user interfaces of the software have become more user-friendly, and high-performance computers have become more affordable due to advancements in computer science (Wicklein, et al., 2016). Consequently, the interest in using CFD tools have been increased, and CFD tools have been practiced in solving a broad range of wastewater engineering problems, from simple to complex (Patziger, 2021; Samstag, et al., 2016).

The number of research articles on the application of CFD in wastewater engineering has approached almost 2000 by early 2023. The majority of these articles concentrate on improving the understanding of processes undergoing in the treatment units, the application of mathematical models, and designing mechanical equipment.

There is a growing interest in the use of CFD tools to gain a deeper understanding of activated sludge processes in the last decade. Researchers from various fields have dedicated extensive efforts to modeling mechanisms undergo in the activated sludge processes. Despite these efforts, some mechanisms remain poorly modeled, besides, specialists were still unable to reach a consensus on how to model some mechanisms (Karpinska & Bridgeman, 2015).

An early, significant study in the field of using CFD tools to model activated sludge processes involved simulating a cross-flow gas-liquid flow in aeration tanks. This research aimed to understand the effect of cross-flow on flow field and the residence time in the aeration tanks (Le Moullec, Potier, Gentric, & Leclerc, 2008). The study was then advanced by incorporating mass transport and biological reactions into the simulation, all while maintaining the same hydrodynamic conditions (Le Moullec, Gentric, Potier, & Leclerc, 2010).

The aggregation and breakup mechanism of microbial flocs, which play a crucial role in removing carbonaceous and nitrogenous pollutants in activated sludge processes, were also modeled using CFD tools, considering the hydrodynamic conditions (Sobremisana, Ducoste, & de los Reyes III, 2011).

Karpinska and Bridgeman (2015) reviewed CFD studies performed for activated sludge systems. They thoroughly described the single- and multiphase approaches commonly used in CFD studies of aeration tank operation and identified and discussed the limitations of the modeling assumptions made to assess mixing and mass transfer. They also evaluated the examples and methods of combining CFD with biokinetics, taking into account the actual flow field and its impact on oxygen mass transfer and the yield of biological processes in the aeration tanks. Additionally, the authors highlighted the unaddressed modeling issues, such as coupling the aeration tank with the secondary clarifier and the use of population balance models to simulate bubbly flow or flocculation of the activated sludge and discussed their significance.

There has been an ongoing effort by many researchers to integrate IWA activated sludge models with CFD tools, however, there is still a lack of agreement among specialists regarding the modeling of activated sludge models using CFD. Rehman et al. (2014) attempted to address this by combining these models and conducting a case study. The study assumed that the reactor was under aerobic conditions and completely mixed, but it was later discovered that some regions were mixed poorly, leading to the accumulation of oxygen and ammonium nitrogen in different regions of the reactor.

The influence of mixing on the activated sludge process has also been studied using CFD tools. Samstag et al. (2012) has shown that the failure of nitrogen removal was due to inadequate mixing when aeration was turned off in a sequential batch reactor. They conducted studies to identify the optimal mixing speed to maintain nitrogen removal.

Modern clarifiers serve dual purposes: Clarification of suspended solids and thickening sludge for recirculating or wasting (Kleine & Reddy, 2005). The efficiency of these processes is impacted by several interrelated factors, including hydrodynamics, sludge rheology, sludge settling, flocculation, turbulence, heat transfer, and temperature changes (McCorquodale, La Motta, Griborio, Homes, & Georgiou, 2004). Besides, buoyancy plays a significant role in the flow field, as clarifiers detain solids with varying concentrations and particle sizes, leading to the flocculation of particles (Kleine & Reddy, 2005).

Despite the intricacy of the processes occurring in clarifiers, the underlying theory behind conventional clarifier design has been in existence for over a century. Hazen (1904) was the first to propose the horizontal flow model and introduced empirical formulas of surface overflow rate (SOR) and hydraulic retention time (HRT). However, this approach oversimplifies the design by ignoring turbulence, assuming a uniform horizontal flow, and neglecting the relationship between solid concentration and settling velocity (Stypka, 1998). This leads to the use of large safety factors in the design, resulting in either an unnecessarily large clarifiers or, even worse, a poorly performing one (DeVantier & Larock, 1987).

The ineffectiveness of clarifiers in clarification and thickening can often be attributed to the failure to account for the intricate interrelated processes in the design. A thorough understanding of these processes is crucial for the effective design of a clarifier. The conventional design approach, known as a black box model, lacks transparency in its functioning. CFD, on the other hand, is a cutting-edge modeling technique that provides an in-depth view of the processes occurring inside the clarifier like never before and is therefore referred to as a glass box model (Hirom & Devi, 2022).

Gao and Stenstrom (2020) classified the conducted CFD studies of clarifiers into three groups: (i) the era of CFD models run under neutral density conditions in the 1980s, (ii) the era of CFD models run for density-driven flows between the late 1980s and early 1990s, and (iii) the era of CFD models run to investigate interrelated processes and hydrogeometric design of the reactor after the mid-1990s.

CFD models had to be developed in two-dimensional (2D) prior to the early 2000s due to the lack of computational power (Gao & Stenstrom, 2020; Hirom & Devi, 2022). Quasi-3D model has become the most popular CFD tool for modeling clarifiers, due to their improved accuracy compared to 2D models, especially for symmetrical geometries (Gao & Stenstrom, 2020). Due to the substantial boost in computational power and late advances in both commercial and open-source software, CFD models have been developed in three-dimensional (3D) (Gao & Stenstrom, 2020), particularly for optimizing reactor geometry and improving process efficiency (Burt & Ganeshalingam, 2005; Patziger, 2016; Das, et al., 2016; Wicklein, Rauch-Williams, Luna, Samstag, & Michalski, 2018). The sedimentation mechanisms have been thoroughly studied and all aspects of it can be modeled with the use of CFD tools. Despite the significant increase in computational power over the past few decades, there is still a need for more computing power to model a full-scale, realistic simulation of a clarifier by incorporating sub-models for flocculation, sludge rheology, thermal and wind all at once (Hirom & Devi, 2022).

The CFD researches along with field- and lab-scale experiments on sediment- and thermal-driven density currents in clarifiers showed that density currents can either be beneficial or adverse depending on their origin, either from sediment or temperature differences (Zhou, McCorquodale, & Vitasovic, 1992; Samstag, et al., 1992; McCorquodale & Zhou, 1993; Gao & Stenstorm, 2017; DeVantier & Larock, 1987; Goula A. M., Kostoglou, Karapantsios, & Zouboulis, 2008). Research studies demonstrated that negative effects can be mitigated by implementing inlet baffles or hydrogeometric modifications (Krebs, 1991; 1995).

CFD tools were utilized to examine the detrimental effects of wind on the hydraulic and settling performance of sedimentation tanks. It was thoroughly demonstrated that wind resulted in large-scale circulations and short circuits, thus significantly impacting the hydraulic and settling performance (Gkesouli & & Stamou, 2018). The CFD research studies assisted demonstrating that although the mild co-current winds may have a slightly positive impact, for most wind speeds and directions, it has a negative effect on both rectangular and circular clarifiers (Larsen, 1977; Sivakumar & Lowe, 1990; Gao & Stenstrom, 2019a; Gao & Stenstrom, 2019b). The potential measures for combating the impact of wind on clarifiers should be covering the clarifiers in windy areas or using in-tank baffles can be used.

CFD tools were extensively used to investigate the optimal inlet-outlet configuration, improve the hydrogeometric design of the clarifier and find the optimal location, size, and number of baffles to resolve performance problems (Hirom & Devi, 2022). Besides, there is a growing interest in the use of perforated baffles, which are found to be more effective in solid settling (Hirom & Devi, 2022). A thorough review of CFD studies on the inlet-outlet configuration and baffles for circular clarifiers can be found in the next subheading.

CFD has also been applied to various treatment units, such as physical treatment units (Şahin & Şibil, 2023), membrane treatment (Vlaev, Dzhonova-Atanasova, & Tsibranska, 2020), disinfection (Gun, Chatterjee, & Hens, 2022), anaerobic processes (Saini, Paritosh, Singh, & Vivekanand, 2021), and flotation processes (Yang, et al.,

2021) in wastewater treatment plants, but not all were reviewed in the scope of this dissertation.

2.1 The Use of CFD Tools in Inlet and Outlet Design

The design of the inlet and outlet has a significant impact on the flow field in a clarifier, beyond just fluid factors such as temperature, mass flow rate, and particle concentration (Bajcar, Gosar, Širok, Steinman, & Rak, 2010; Bajcar, Steinman, Širok, & Prešeren, 2011). The design of the inlet affects the potential energy, which is generally higher than kinetic energy. To reduce the potential energy and make energy dissipation easier, inlets are usually placed near the bottom of the tank and designed to dissipate as much energy from the influent as possible, promoting flocculation and reducing short-circuiting, density currents, and scouring (Patziger, Kainz, Hunze, & Józsa, 2012). A well-placed, energy-dissipating inlet with in-tank baffles can lead to re-flocculation and a uniform flow distribution (Xanthos, et al., 2011).

The most popular type of inlet-outlet configuration for circular clarifiers is centrally fed and peripheral draw-off (De Clercq, Computational fluid dynamics of settling tanks, 2003). Other configurations include (Hirom & Devi, 2022): Hoppered spiral-flow (Phiri, Saito, Ishak, Harada, & Nakajima, 1996), peripherally fed and central draw-off (Bajcar, Steinman, Širok, & Prešeren, 2011), and transversely operated (Lengricht, Graw, & Schulz, 2000). Several studies have been done on the effects of different inlet configurations Deinger (1994) and Deinger et al. (1998) with some showing that centrally fed and peripheral draw-off performed better than peripherally fed and central draw-off (Bajcar, Steinman, Širok, & Prešeren, 2011). However, these studies have limitations as they only used single particle diameters and densities; and further research is needed to compare different types of feed and draw-off configurations with a range of particle diameters and densities (Hirom & Devi, 2022).

Two types of launder systems are used in rectangular clarifiers. Older studies recommended the transverse-type launder over the finger-type due to observed upward flow around the longer finger-type launder (Kawamura & Lang, 1986). Recent studies,

however, through CFD simulations and laboratory experiments, have shown that the finger-type launder outlet is generally considered to be the most effective configuration, compared to the transverse-type launder (Kriš & Hadi, 2007; Ghawi & Kriš, 2008; 2012; Hadi & Kriš, 2009).

Studies have also been done on inlet design. Jayanti and Narayanan (2004) investigated the flow fields produced by three different inlet designs; and found that the tulip type inlet with the conical deflector was the most efficient, producing a relatively calm flow, despite the presence of large recirculation regions in all three cases. Das et al. (2016) studied the improved performance of a clarifier retrofitted with the energy dissipating inlet designed by Esler et al. (US Patent No. 6,276,537 B1, 2001); the inlet was fitted with a submerged skirt and an inward baffle and multiple inlets were positioned so that the inflows from them were directed in opposite directions, thus increasing the dissipation of energy (Hirom & Devi, 2022).

2.2 The Use of CFD Tools in Baffle Design

A number of studies have investigated the impact of baffles on the performance of clarifiers, both circular and rectangular, in wastewater treatment plants (Hirom & Devi, 2022).

On one hand, baffles are practical solutions that are installed to enhance the hydrodynamics of the tank, eliminate the dead zones/recirculation zones, mitigate short-circuiting, re-suspension of settled particles, wind effects and density currents, and thus improve sedimentation efficiency of clarifiers (Tamayol, Firoozabadi, & Ahmadi, 2008; Tamayol, Firoozabadi, & Ashjari, 2010). However, improper positioning of baffles can harm the sedimentation efficiency. There have been several studies investigating the optimum number, position and size of baffles for clarifiers.

The use of flocculation wells in circular clarifiers has also been studied (Hirom & Devi, 2022). Alonso and Alex (2006) noted that the diameter of flocculation wells should be between 20-35% of the clarifier diameter for maximum efficiency.

Brouckaert and Buckley (1999) demonstrated that the presence of baffles near the inlet of a clarifier effectively reduces the occurrence of upflow vortices and recirculating currents, which are commonly observed near outlet weirs. It was previously demonstrated by Crosby (1984) that the addition of a mid-radius, mid-depth baffle in a clarifier was found to result in a 38% reduction in the concentration of suspended solids.

Fan et al. (2007) proved that the solid concentration near the baffle was not significantly different from that of a non-baffled tank, but there was a sharp increase in the outer region of the baffle, demonstrating its effectiveness in congregating solids and improving clarification performance.

Goula et al. (2008) showed a substantial improvement in efficiency and a reduction in settleable solids concentration of up to 85% through the installation of a vertical baffle at the inlet region.

Yang and Wen (2019) studied the flocculation and sedimentation behavior of a clarifier and proposed the addition of a grid flocculation well (perforated McKinney baffle) to reduce settleable solids concentration. This modification resulted in better flocculation conditions due to improved energy dissipation and homogenized flow.

Gao and Stenstrom (2019a) conducted a thorough study of the McKinney baffle and found that it significantly improved the performance of the clarifier, with a 1.4 to 2 times improvement in limiting flux. In a follow-up study it was found that appropriate baffling could effectively dissipate the impact of buoyancy on turbulence (Gao & Stenstrom, 2019b).

Ekama and Marais (2004) examined the effect of the installing Stamford baffle below the effluent weirs on the limiting flux of circular clarifiers and found that while it had a negligible effect on the flux rating, it had a significant impact on the concentration of settleable solids in the tank when it was underloaded.

There is less attention given to researching the use of baffles in circular clarifiers in comparison to rectangular clarifiers.

In rectangular clarifiers, installing a baffle between the inlet and 5% of the tank length, with a height of 67% of the tank's depth maximized the solid removal efficiency Ahmed et al. (1996). Likewise, Mostafa et al. (2005) found that the best horizontal position is at 3% of the tank's length from the inlet, and the best vertical position is when 33% of the tank depth is left at the bottom.

Tamayol et al. (2010) concluded that upper-mounted baffles are more effective in primary sedimentation tanks where buoyancy forces and density currents are negligible, while lower-mounted baffles are more effective in clarifiers that are dominated by these forces. Tamayol et al. (2010) also found that the optimum baffle position should have the ratio of horizontal distance from the inlet to the length of the tank between 0.15 and 0.4.

Xanthos et al. (2011; 2012) developed a complex 3D CFD model that showed significant improvements in the performance of a rectangular clarifier with the addition of a slotted inlet baffle and a slotted in-tank baffle placed 10 meters from the inlet.

Al-Sammarraee and Chan (2009) found that the overall performance of a rectangular sedimentation tank increased with the number of vertical upper-mounted baffles, and Asgharzadeh et al. (2011) studied the effects of different bottom-mounted vertical baffles and found that the optimum position was in the middle of the recirculation region in the original non-baffled tank.

Park et al. (2006; 2014) observed an improvement in turbidity removal of up to 38% after adding a longitudinal baffle to the central plane of a rectangular clarifier.

Al-Mafraji and Al-Mussawy (2021) found that the use of both upper-mounted and bottom-mounted baffles increased turbidity removal by up to 25%; besides the

proposed baffle arrangement also lengthened the flow path and increased detention time from 1.33 to 4 hours.

Overall, the reviewed literature demonstrated that the optimal positioning and size of baffles in clarifiers is an important area of study, as their proper placement and design can significantly improve the efficiency and effectiveness of the clarifiers.

CHAPTER 3
COMPUTATIONAL FLUID DYNAMICS

CFD models utilize numerical methods to solve the conservation equations of mass, energy, momentum, heat, and species in their partial differential equation form, which governs fluid motion, the so-called Navier-Stokes Equations, by using iteration techniques in computers (ANSYS, Inc., 2019). These equations describe the relationship between fluid velocity, pressure, temperature, and density in motion (NASA Glenn Research Center, 2022).

In this chapter, a brief explanation is given of the governing equations, basic numerical solution procedure, and some key concepts utilized in commercial CFD software such as pressure-velocity coupling, residual, convergence criteria, and under-relaxation factor, which will be utilized in the upcoming chapters.

3.1 Governing Equations

CFD is based on three fundamental governing equations of fluid dynamics, which are: the continuity equation, the momentum equation (also known as the Navier-Stokes equation), and the energy equation.

The fluid flow characteristics in a wastewater treatment plant are unsteady and incompressible, therefore turbulent flow can be described using the following governing equations.

3.1.1 Conservation of Fluid Mass (Continuity Equation)

The flow domain is divided into infinitesimal control volumes. The total amount of mass within a control volume remains constant, meaning that the mass flowing into the control volume must equal the mass flowing out of it, based on the principle of the conservation of mass.

The amount of mass within the control volume is dependent to the source (S) and the flux (F) terms, keeping in mind that the mass density is constant. The source term is the total mass within the control volume, and the flux term is the flow of mass through the boundary surface of the control volume. The instantaneous rate of change in the source term with respect to time equals to the flux term. The Equation 3.1 was arrived upon performing the requisite mathematical manipulations:

$$\frac{\partial p}{\partial t} + \nabla \cdot (\rho \vec{v}) = 0 \tag{3.1}$$

where t is the time, p is the static pressure, $\vec{v}$ is the velocity vector, ρ is the density.

3.1.2 Conservation of Momentum (Momentum Equation)

The momentum equation is derived from Newton's second law, which states that the forces acting on a control volume must equal the rate of change of momentum within that control volume.

The forces on a control volume can be divided into two categories: body forces and surface forces. Body forces are forces that act throughout the control volume, such as gravitational and electromagnetic forces, while surface forces are forces exerted on the surface of the control volume, such as pressure and viscous forces.

The Equation 3.2 describes the preservation of momentum in a reference frame that is not accelerating (ANSYS, Inc., 2019).

$$\frac{\partial}{\partial t}(\rho \vec{v}) + \nabla \cdot (\rho \overrightarrow{vv}) = -\nabla p + \nabla \cdot \bar{\tau} + \rho \vec{g} + F_g \tag{3.2}$$

where t is the time, p is the static pressure, $\vec{v}$ is the velocity vector, ρ is the density, $\bar{\tau}$ is the stress tensor, $\rho \vec{g}$ is the gravitational body force and $\vec{F}$ is the body source term.

The body source term also includes other model-specific source terms, such as those associated with porous media and user-defined sources (ANSYS, Inc., 2019). The body source term in the case of a sedimentation problem is given in the Equation 3.3 (Xanthos, et al., 2011):

$$F_g = g\left(1 - \frac{1}{SS}\right)X \tag{3.3}$$

where, SS is the specific density of the dry particles and X is the local sludge concentration.

3.1.3 Conservation of Energy

The energy equation (Equation 3.4) outlines how the energy of a fluid changes over time, taking into account the total heat input and the work done on a fluid particle. It represents another form of the first law of thermodynamics.

$$\frac{\partial}{\partial t}(\rho E) + \nabla \cdot \left(\vec{v}(\rho E + p)\right) = -\nabla\left(\sum_j h_j J_j\right) + S_h \tag{3.4}$$

3.2 Turbulence Modeling

The majority of fluid flow in nature and engineered systems –such as wastewater treatment units– is characterized as turbulent flow. Turbulent flow is recognized as chaotic and unsteady patterns of swirling, eddying, and flow instabilities, and causes small-scale fluctuations in flow variables such as velocity, pressure, and temperature (Raeesh, Devi, & Hirom, 2023). It is important to incorporate the right turbulence model in CFD simulations, since it impacts the accuracy of the results, particularly in areas of high turbulence like the inlet (Gao & Stenstrom, 2018).

The simulation of turbulent flow in CFD codes can be accomplished through different methods, which are Direct Numerical Simulation (DNS), Large Eddy Simulation (LES) and Reynolds-averaged Navier-Stokes (RANS).

3.2.1 Direct Numerical Simulation (DNS)

The DNS approach provides an exact solution for all scales of turbulence, including the Kolmogorov scales and larger motions that carry most of the kinetic energy within the flow domain (Karpinska & Bridgeman, 2015). However, the computational demand for the DNS approach is extremely high, making CFD unfeasible for most industrial applications and use for general-purpose design tools (Karpinska & Bridgeman, 2015). The simulation of wastewater treatment units in CFD models must use methods that are more computationally efficient.

3.2.2 Large Eddy Simulation (LES)

The LES approach utilizes the spatial filtering technique to distinguish between large and small eddies, and while the large eddies –which are important in transporting mass, momentum, and energy– are calculated directly, the smaller eddies are calculated using the sub-grid scale (SGS) model, which reduces computational cost compared to DNS (Karpinska & Bridgeman, 2015; Raeesh, Devi, & Hirom, 2023).

The LES approach has been applied successfully in modeling complex flows, high Reynolds numbers, and severe shear. It is a suitable model for more accurate representation of mixing, short-circuiting, and recirculating characteristics (Goodarzi, Lari, & Alighardashi, 2018).

The LES approach appears to be the most appropriate numerical method for accurately simulating turbulent flows until the DNS approach can be practiced for engineering purposes (Hirom & Devi, 2022).

There is a growing interest in using the LES approach to accurately predict turbulent flow. A few research studies have already been published, in which the LES turbulence models were utilized in investigating the sedimentation process (Al-Sammarraee & Chan, 2009; Goodarzi, Lari, & Alighardashi, 2018).

Although researchers have made great advancements in using the LES approach for the simulation of complex turbulent flows since the 1960s and have found it to be a more accurate method compared to Reynolds Averaged Navier-Stokes (RANS), the utilization of LES approach is limited by its high computational cost and mesh requirements (Raeesh, Devi, & Hirom, 2023). However, it is expected to see a significant increase in number of research articles investigating wastewater treatment processes utilizing the LES approach in the near future.

3.2.3 Reynolds Averaged Navier-Stokes (RANS) Models

The RANS and unsteady RANS (URANS) models employ the Reynolds decomposition method to differentiate the velocity, pressure, and temperature variables of the Navier-Stokes Equation into mean and fluctuating components (Karpinska & Bridgeman, 2015; Raeesh, Devi, & Hirom, 2023). This method is broadly practiced in engineering applications, including wastewater treatment, due to its reduced computational demands.

To describe the fluctuations in fluid flow, a correlation between the fluctuating values and the mean flow variables must be established. Unlike LES, which uses spatial filtering to distinguish between large and small eddies, RANS uses time-averaging the Navier-Stokes Equation. This results in the creation of numerous turbulence models (Karpinska & Bridgeman, 2015; Raeesh, Devi, & Hirom, 2023). These models can be broadly divided into two categories: first-order models, including the zero-equation, one-equation, and two-equation models, and second-order models, such as the algebraic stress model and the Reynolds Stress Model.

A relationship between the fluctuating values and the mean flow variables must be established to describe these fluctuations, and this is achieved by averaging the Navier-Stokes equation over time, leading to the development of many turbulence models. These models can be broadly categorized into two groups (Karpinska & Bridgeman, 2015; Raeesh, Devi, & Hirom, 2023): First-order models (such as the zero-equation or Mixing Length Model, the one-equation or the Spalart-Allmaras Model, and two-

equation models like k-ε and k-ω) and second-order models (such as the Algebraic Stress Model and the Reynolds Stress Model). The first order models, also known as Eddy Viscosity Models (EVM), are based on the Boussinesq hypothesis, which assumes that turbulence is proportional to the mean deformation rate and Reynolds stresses can be linked to mean velocity gradients (Karpinska & Bridgeman, 2015; Raeesh, Devi, & Hirom, 2023). EVMs are also based on the assumption that turbulence is locally isotropic (Karpinska & Bridgeman, 2015).

The popular commercial CFD software that is used to account for Reynolds stresses closure includes several turbulence models, which are (Zhang, 2014): the standard, the renormalized group (RNG) and the realizable k-ε models, the standard and the shear stress transport (SST) k-ω models, and the Reynolds Stress Model (RSM). These turbulence models are included in the CFD software to help calculate the Reynolds stresses and provide a more accurate simulation of the flow. The choice of the turbulence model depends on the complexity of the flow, the desired level of accuracy, and computational resources available.

Karpinska and Bridgeman (2015) can be referred to for more in-depth information on the turbulence models used in wastewater engineering, in which, the two-equation turbulence models were compared and contrasted, and the advantages and limitations of each were outlined. The summary table on the comparison of turbulence models is incredibly valuable for wastewater engineers using CFD tools, as it enables them to choose the most appropriate turbulence model for their specific simulation scenario.

The k-ε turbulence model is one of the most commonly used models in CFD for wastewater engineering problems (Das, et al., 2016; Karpinska & Bridgeman, 2015). Therefore, the k-ε turbulence model was utilized in this study.

The transport equations for the turbulence kinetic energy (k) and its dissipation rate (ε) is modeled using the Equation 3.5 and 3.6 (ANSYS, Inc., 2019):

$$\frac{\partial}{\partial t}(\rho k) + \frac{\partial}{\partial x_i}(\rho k u_i) = \frac{\partial}{\partial x_j}\left[\left(\mu + \frac{\mu_t}{\sigma_k}\right)\frac{\partial k}{\partial x_j}\right] + G_k + G_b - \rho\varepsilon \qquad (3.5)$$

$$\frac{\partial}{\partial t}(\rho\varepsilon) + \frac{\partial}{\partial x_i}(\rho\varepsilon u_i) = \frac{\partial}{\partial x_j}\left[\left(\mu + \frac{\mu_t}{\sigma_\varepsilon}\right)\frac{\partial \varepsilon}{\partial x_j}\right] + C_{1\varepsilon}\frac{\varepsilon}{k}(G_k + C_{3\varepsilon}G_b) - C_{2\varepsilon}\rho\frac{\varepsilon^2}{k} \quad (3.6)$$

where, G_k and G_b are the generation of turbulence kinetic energy due to the mean velocity gradients and buoyancy, respectively. G_k is defined in Equation 3.7 using the exact equation for the transport of k:

$$G_k = -\rho\overline{u_i' u_j'}\frac{\partial u_j}{\partial x_i} \quad (3.7)$$

In order to evaluate G_k according to the Boussinesq hypothesis (Equation 3.8),

$$G_k = \mu_t S^2 \quad (3.8)$$

where S is the modulus of the mean rate-of-strain tensor (Equation 3.9), which is defined as:

$$S \equiv \sqrt{2S_{ij}S_{ij}} \quad (3.9)$$

G_b is calculated from the Equation 3.10:

$$G_b = g\frac{\mu_t}{\sigma_c}\frac{\partial c_s}{\partial y} \quad (3.10)$$

The turbulent Prandtl numbers for k and ε are represented as σ_k and σ_ε; and the other empirical constants have the following default values: $C_{1\varepsilon} = 1.44$, $C_{2\varepsilon} = 1.92$, $C_\mu = 0.09$, $\sigma_k = 1.0$, and $\sigma_\varepsilon = 1.3$ (ANSYS, Inc., 2019). The model constant $C_{3\varepsilon}$ determine the magnitude of the buoyancy's influence on ε; it ranges between 0.8 and 1.0 for stable stratification that prevails in clarifiers, and it goes toward zero for unstable stratification (Lakehal, Krebs, Krijgsman, & Rodi, 1999).

Although the effects of buoyancy on the generation of k are understandable, the impact on ε is less clear (Xanthos, et al., 2011).

G_b is mainly negative in the settling tank, due to the negative gradient in sludge concentration; besides, except for the inlet region, where turbulent mixing is prevailing and the solids distribution gradient is not always negative, G_b tends to stabilize the flow, and the unstable stratification could therefore increase the mixing in the inlet region (Xanthos, et al., 2011).

3.3 Multiphase Models

Multiphase models are sophisticated mathematical representations utilized to model and simulate the behavior of fluid systems containing multiple phases. The phases present in a fluid system are usually modeled as individual, clearly distinct entities that interact with each other through a range of physical processes.

The majority of challenges in wastewater treatment are related to multiphase problems. Therefore, accurate modeling of the transport mechanisms and the interactions between the phases is crucial to precisely simulating the sedimentation, flotation, aeration, and mixing processes. The multiphase models in commercial CFD software can be grouped into two categories: the Euler-Lagrange and the Euler-Euler approaches.

3.3.1 Euler-Lagrange Model

The Euler-Lagrange Model also known as the Lagrangian Model or Discrete Phase Model (DPM), is used to simulate fluid systems that include continuous (either a gas or liquid) and dispersed phases (particles, bubbles, or liquid drops) (Zhang, 2014). This model is often employed to study the behavior of discrete particles (Karpinska Portela, 2013).

The primary phase is treated as a continuum and its behavior is described through the solution of time-averaged Navier-Stokes equations in an Eulerian reference frame (Karpinska & Bridgeman, 2015; Zhang, 2014). Meanwhile, the behavior of the discrete phase, such as solids, is modeled by tracking a large number of individual particles through the flow field of the continuous phase using random-walk Lagrangian trajectory calculations (Karpinska & Bridgeman, 2015).

The Euler-Lagrange model is appropriate for use when the secondary phase (e.g. particles) occupy a relatively small volume fraction of the fluid system, as is the case in clarifiers (Hirom & Devi, 2022). However, as the volume fraction of the secondary phase increases beyond 10-12%, this model becomes less accurate and should not be used, according to various studies (De Clercq & Vanrollelghem, 2002). Therefore, although the Euler-Lagrange model is suitable to simulate gas-liquid flow, it is not suitable for modeling solid-liquid flow in the activated sludge systems with high particle volume fractions (Karpinska & Bridgeman, 2015).

At first glance, it appears that the Euler-Lagrange model could be useful for modeling of sedimentation processes. This statement is valid for sedimentation tanks in drinking water treatment plants (De Clercq, 2003). However, researchers argued that the Euler-Lagrange model ignores the aspects such as the effects of density currents, sludge flocculation, and hindered settling, which are the most critical factors in secondary clarifiers (De Clercq, 2003; Burt D. J., 2010). Also, the complexity of particle interactions in clarifiers requires a substantial amount of computational power to model accurately, making it challenging to apply the Euler-Lagrange approach (De Clercq, 2003). The Euler-Lagrange model has not yet been implemented for a comprehensive analysis of clarifiers (Karpinska & Bridgeman, 2015).

Among the multiphase modeling approaches, the Euler-Lagrange approach is the most demanding, requiring extensive computation times and a large number of central processing units, which limits its use in wastewater engineering problems (Karpinska & Bridgeman, 2015).

3.3.2 Euler-Euler Models

The Euler-Euler approach models multiple phases as an interpenetrating continuum, assuming that their volume fractions are continuous and add up to one (Karpinska & Bridgeman, 2015; Raeesh, Devi, & Hirom, 2023). There are three types of models that can be used with the Euler-Euler method: Volume of Fluid (VOF), Mixture, and Eulerian. While the Mixture and Eulerian models are more successful in simulation of dispersed flows, the VOF model is used for simulation of immiscible fluids, where the different phases do not mix with each other.

The Euler-Euler technique, a mathematical approach for modeling diffusion problems, does not account for individual particle motion in the flow field (Karpinska & Bridgeman, 2015). Despite this limitation, the method has been used to analyze sedimentation processes and aeration systems in wastewater treatment plants (WWTPs). However, the validity of the Euler-Euler model in predicting sludge concentration is yet to be verified (Karpinska & Bridgeman, 2015; Raeesh, Devi, & Hirom, 2023). Additionally, the significant computational demands of modeling the particle settling process in full-scale clarifiers limits the applicability of the Euler-Euler technique (Karpinska & Bridgeman, 2015).

3.3.2.1 Mixture Model

The mixture model is based on the assumption that a local equilibrium between the phases is reached over a short spatial length scale (Karpinska & Bridgeman, 2015). It can be used to model homogeneous multiphase flow when the phases move with the same velocity (Wicklein & Samstag, 2009). While the model relies on a single momentum equation for the mixture, the exclusion of interfacial interactions can lead to significant inaccuracies in the predictions made by the model (De Clercq, 2003). Thus, it is important to consider the potential limitations of the approach when using it for specific applications (Ratkovich, 2010).

The model has been effectively applied to analyze the turbulence in flows where both solid-liquid and liquid-gas phases are present, such as simulating sediment-induced density currents, solid-liquid mixing in activated sludge tanks, and turbulent transport of suspended solids in clarifiers (Wicklein & Samstag, 2009; Samstag, et al., 2016).

3.3.2.2 Volume of Fluid (VOF)

The VOF model is designed to simulate the behavior of two or more immiscible fluids, such as air and water, which do not mix with each other (Raeesh, Devi, & Hirom, 2023). The model provides a detailed representation of the fluid dynamics at the fluid interface by solving the momentum equations for the continuous phase and tracking the volume fraction of fluids in every computational cell (Karpinska & Bridgeman, 2015). It is commonly utilized for analyzing the free surface of water, such as open channel flows. The potential limitations in implementation of the model are the immiscible fluid assumption and the required computational resources for large-scale simulations.

3.3.3 Single Phase Modeling

Single-phase flow models were extensively used in wastewater engineering problems due to their affordability and accuracy (Raeesh, Devi, & Hirom, 2023). It is widely used to model both in sedimentation processes and oxygen mass transfer in aeration processes (Karpinska & Bridgeman, 2015). Wicklein and Samstag (2009) demonstrated that transport models based on empirical equations for solids settling velocity provide a more accurate estimate of the behavior of activated sludge in clarifiers than multiphase models. The transport model for solids settling is introduced using user-defined functions. Thus, the solids transport is calculated by solving a passive scalar equation, rather than the multiphase model. The fluid flow problem is simplified to a single-phase flow problem by coupling fluid dynamics and solids transport. The governing equations for fluid flow and solids settling are solved together in this approach.

The necessary user-defined functions (UDF) were compiled to simulate the solids settling and transport in the clarifier, along with the impact of density changes due to sludge concentration profile on fluid momentum was taken into consideration (Das, et al., 2016); (Xanthos, et al., 2011); (Samstag R. , et al., 2012); (Wicklein & Samstag, 2009); (De Clercq, Computational fluid dynamics of settling tanks, 2003); (Lakehal, Krebs, Krijgsman, & Rodi, 1999). The transport equation for the solids can be written as in Equation 3.11 (Das, et al., 2016):

$$\frac{\partial X}{\partial t} + \frac{\partial uX}{\partial x} + \frac{\partial vX}{\partial y} + \frac{\partial wX}{\partial z} = \frac{\partial}{\partial x}\left(v_{SX}\frac{\partial X}{\partial x}\right) + \frac{\partial}{\partial y}\left(v_{SY}\frac{\partial X}{\partial y}\right) + \frac{\partial}{\partial z}\left(v_{SZ}\frac{\partial X}{\partial z}\right) + \frac{\partial (V_S X)}{\partial z} \quad (3.11)$$

where v_{SX}, v_{SY}, and v_{SZ} are the eddy diffusivities of the suspended solids in the x, y, and z directions, and V_S is the solid settling velocity.

The sedimentation process of the activated sludge was modeled using the Equation 3.12 (Takács, Patry, & Nolasco, 1991), due to the fact that it well-describes the hindered settling of activated sludge flocs.

$$V_s = V_{s0} \times \left[-r_h(X - X_{ns}) - V_{s0} \times \exp\left[-r_p(X - X_{ns})\right]\right] \quad (3.12)$$

where V_{s0} is the reference settling velocity, r_h and r_p are the coefficients of the climbing and falling limbs of the velocity-concentration curve, respectively; X_{ns} is the non-settleable concentration (Lakehal, Krebs, Krijgsman, & Rodi, 1999).

The rheological properties of the fluid are not negligible since the studied fluid is activated sludge. Several models have been developed to simulate the rheology of activated sludge (Das, et al., 2016); among them, Bokil and Bewtra (1972) function (Equation 3.13) was used to account the effect of sludge concentration on the molecular viscosity of the fluid in the CFD simulations (Lakehal, Krebs, Krijgsman, & Rodi, 1999).

$$\mu_P = 0.00327 \times 10^{0.132C}\ [kg/(m \cdot s)] \quad (3.13)$$

CHAPTER 4
MATERIALS AND METHODS

In the scope of this chapter, the study area was introduced and the CFD modeling strategy and its implementation were explained.

4.1 Study Area

The simulations and relevant investigations in the scope of this thesis were carried out for the biological treatment units in an urban wastewater treatment plant. However, the name of the treatment facility was not written as per the confidentiality agreement with the relevant administration.

To give an idea to the reader about the investigated urban wastewater treatment plant, this urban area was grouped under the second-grade socioeconomically-developed urban areas among six classes in Turkey.



Figure 4.1 The aerial view of the investigated WWTP

The facility treats domestic, commercial, and industrial effluents generated in this urban area. The treatment plant was designed based on the Modified Ludzack-Ettinger process in two stages, where the first stage was projected to serve until 2025 and the second stage was projected to serve for 2040. The first stage was designed to serve 111.000 PE. The design flow was estimated as 13.762 m^3/d. The biological treatment units were designed as per the design manual ATV-DVWK-A 131E (2000).

4.1.1 Aeration Tank

There are two aeration tanks with a volume of 27208 m^3. The nitrification and denitrification volumes of the aeration tank are shown in Figure 4.2.

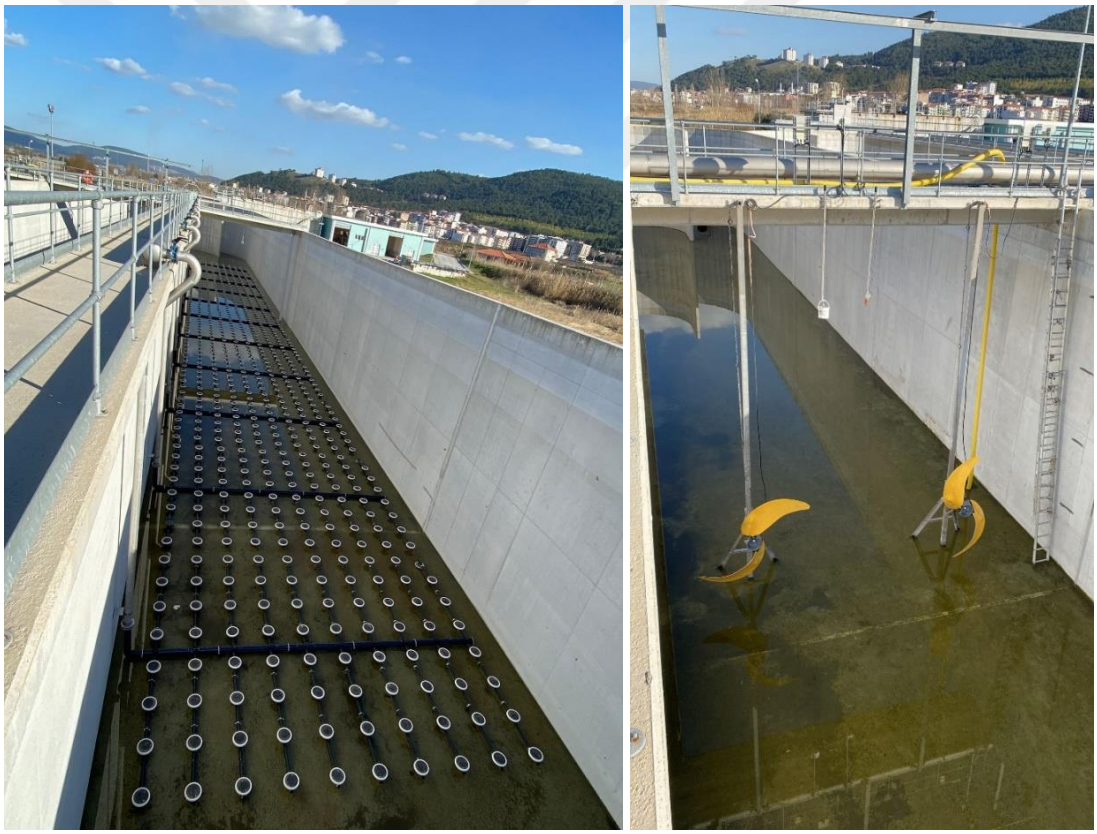


Figure 4.2 The nitrification and denitrification volumes in the aeration tank of the investigated WWTP

Each of the aeration tank is equipped with a blower (100+ KW) with a capacity of 4900 m^3/h and 1225 diffusers with a capacity of 5 m^3/h. In addition, 3 banana-type low

velocity mixers (6.3 KW) were formed per tank to ensure complete mixing in the basins. The detail design of the aeration device is not designed.

4.1.2 Clarifiers

The diameter of the existing clarifiers is 30 m. The existing clarifiers have a 27.4 $m^3/m^2/day$ overflow rate and a 6.8 $kg/m^2/h$ sludge loading rate. These values satisfy the limit values in the literature, which are between 24 and 32 $m^3/m^2/day$ for overflow rates and lower than 7 $kg/m^2/h$ for sludge loading rates (Tchobanoglous, Burton, & Stensel, 2003).

The current clarifier has an influent well, that has a diameter of 13% of the clarifier diameter, and each has 4 large openings to diffuse the influent into the clarification zone. The influent well was not equipped with energy dissipating baffles.



Figure 4.3 The general view of the clarifier, including the influent well and scrapers, in the investigated WWTP

4.2 CFD Modeling

The simulations were carried out in ANSYS Fluent 2020 R2, which was licensed to Dokuz Eylul University. The CFD modeling was performed as per the Good Modelling Practices in wastewater CFD applications (Wicklein, et al., 2016) determined by the International Water Association (IWA) working group on Computational Fluid Dynamics.

4.2.1 Modeling Objective

The main modeling objective is to investigate and optimize the hydrodynamic processes of the activated sludge system. CFD simulations would be utilized to investigate the flow and mixing behavior in the aeration tanks and the sedimentation process in the secondary clarifiers.

Locating mixers in aeration tanks is crucial for optimizing the efficiency of the wastewater treatment process. In this context, CFD tools would be first employed to model the flow and mixing behavior in the aeration tanks, which would allow for the optimization of mixer placement. This investigation would ensure that the mixers were situated in the most energy-saving and efficient position to enhance the treatment process. The CFD simulations would also identify any flow patterns that are not optimal, and necessary adjustments would be made to the design and placement of mixers to address these issues. The evaluation of different mixer configurations using CFD simulations would provide insight into the mixing intensity, flow field, and energy consumption in aeration tanks. This information would be used to guide the design of mixer placement, ultimately improving the energy efficiency of the wastewater treatment process.

The calm and uniform distribution of the flow in the sedimentation zone is the most important factor affecting the clarification process. For this purpose, Stengel, Geiger, Clifford, or Stuttgarter-type nozzles are usually mounted to the outlets of the influent well in conventional clarifiers. However, these nozzles are not very sufficient to

dissipate the energy of the inflow. They often cause operational problems as well. Although conventional clarifiers are not usually equipped with an EDI, prolonged operational and capacity problems might lead clarifiers to be retrofitted with an EDI. Plenty of EDIs have been invented in the last few decades to overcome the problems.

It has been known that EDIs are useful designs that facilitate the dissipation of energy, increase the treatment capacity and enable operating clarifiers with high overflow rates (Ghawi & Kris, 2011). It was previously uncovered that, on one hand, the EDIs prevent short-circuiting of overflow, on the other hand, they facilitate short-circuiting of underflow (Köken & Büyükkamacı, 2022). Since EDIs can well-dissipate the energy of larger inflowing volumes, clarifiers equipped with EDIs are usually operated at higher treatment capacities than conventional clarifiers. As the influent volume of a clarifier increase, the outflow volume increases accordingly, however, the capacity of a conventional draw-off pipe is limited and cannot convey the thickened sludge at high capacities; consequently, the sludge blanket is deformed, and solids are withdrawn from the draw-off pipe below the solicited concentration. Besides, although uniformity is being sought during inflow distribution and effluent laundering along the perimeter of the circular central-feed secondary clarifiers, this concept is neglected during sludge draw-off, since the sludge has to be discharged from a single point. Consequently, the flow velocity profile would be not symmetrical in the sludge hopper. However, the discharge from the draw-off pipe is usually two-to-three times more than the weirs. This could also be one of the facts that facilitate the rotational currents occurring in some clarifiers; however, this problem was not extensively researched in the scope of this dissertation.

CFD tools would be employed to diagnose the conditions limiting the further capacity increase in clarifiers equipped with an EDI, alternative options to retrofit the draw-off system would be developed, and CFD simulations would be carried out at doubled influent volume conditions to test the capability of enhancing the treatment capacity by two times.

At first, it was attempted to enlarge the draw-off pipe diameter for troubleshooting; however, further enlargement of the draw-off pipe diameter did not yield good results since it was already sizeable. The second attempt was to increase the number of draw-off pipes: a total number of eight identical draw-off pipes were radially arrayed at the bottom of the sludge hopper; the draw-off pipe diameter had enough cross-sectional area to keep discharge flow velocity below 0.9 m/s. This simulation yielded a very good flow velocity field, sludge sedimentation velocity field, and sludge sedimentation field in the clarifier. Although this attempt solved the problem within the clarifier, the problem was then turned into solving how the multiple draw-off pipes should be connected to the sump pit. It was difficult to connect each of the radially arrayed draw-off pipes to the sump pit. It required each draw-off pipe to be connected to the sump pit by following a different path. Besides the draw-off pipes had to be bent or twisted, and many fittings had to be used to form the paths. These would cause each draw-off pipe to have different friction and head losses; and once the hydraulic losses in each draw-off pipe are not identical then uniformity would be lost; consequently, the fields would be off the simulation. Perhaps the most primitive solution would be to build a sump pit at the end of each draw-off pipe along the perimeter of the clarifier. However, it was decided to implement an advanced engineering solution. Inspired by the spiral-casing in reaction-type turbines and distribution pipes in impulse-type turbines, which are customized penstocks that maintain even flow distribution in hydropower, but run in the opposite direction, were designed to draw off thickened sludge from the clarifier. Although the shape of the sludge hopper in the clarifier equipped with a snail-shaped draw-off pipe was kept as it was in the original clarifier, it was lowered in the clarifier equipped with a snail-shaped draw-off pipe -preserving the side slopes to mount the draw-off pipe.

The modeling objective is defined as retrofitting the conventional draw-off pipe with either a snail- or a spiral-shaped draw-off pipe to mitigate the underflow short-circuiting and enhance the treatment performance of clarifiers. The auxiliary modeling objective is determined as retrofitting the clarifier of an urban wastewater treatment plant with either a multilayer- or opposing jet-type EDI for a capacity increase.

The following simulation scenarios are developed by hybridizing the two modeling objectives:

- the clarifier equipped with an opposing-jet nozzle type EDI and assisted with a spiral-shaped draw-off pipe,
- the clarifier equipped with an opposing-jet nozzle-type EDI and assisted with a snail-shaped draw-off pipe,
- the clarifier equipped with a multilayer-type EDI and assisted with a snail-shaped draw-off pipe.

Moreover, the following scenarios would be simulated to create a basis for the comparison:

- the original clarifier and draw-off pipe under existing flow conditions, and
- the clarifier equipped with an opposing-jet nozzle type EDI, without any changes in the draw-off pipe.

It was also worth to note that although there were two types of opposing-jet nozzle type EDI, The Los Angeles Type-1 EDI was yielded better results than the Los Angeles Type-2 EDI in the preliminary studies (Köken & Büyükkamacı, 2022); therefore, only the Los Angeles Type-1 EDI was used in the scope of this dissertation.

At last, since the sludge blanket in the clarifier equipped with an LA-EDI was scoured by small eddies between the influent well and the sludge hopper, a novel deflector was designed to mitigate scouring of the sludge blanket by eddies. The mitigation of eddies that scour the sludge blanket and the uniform radial distribution of the influent across the diameter of the clarifier would be evaluated using CFD simulations.

4.2.2 Modeling Geometry

The geometries of the simulation scenarios were drafted in AutoCAD. The aeration tank geometry was not represented, as it was directly transferred from the as-built project without any modifications or adjustments. The problem geometries of the clarifier simulations were illustrated in the following figures.

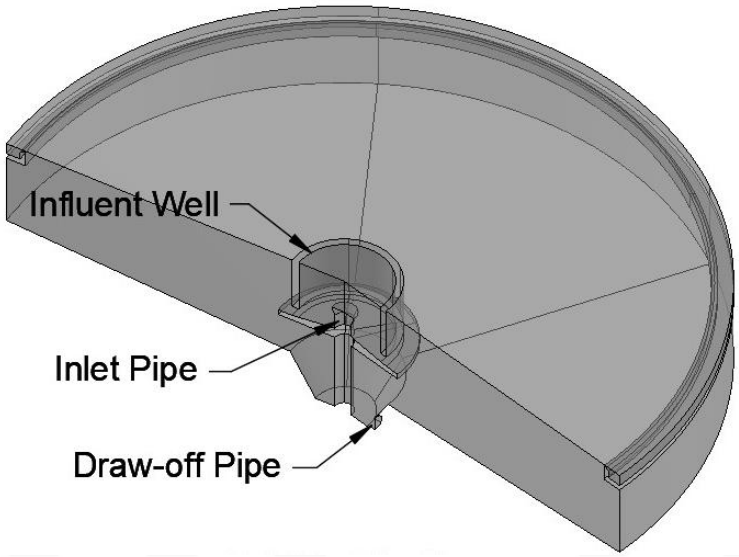


Figure 4.4 The cross-section of the original clarifier

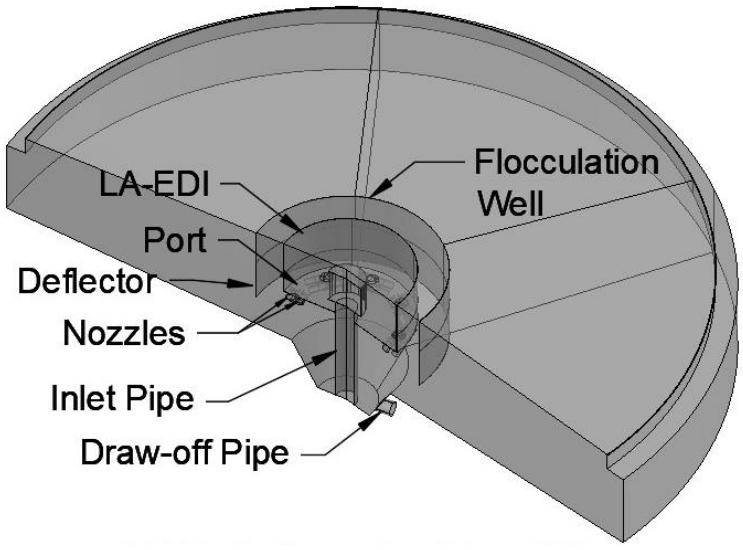


Figure 4.5 The cross-section of the clarifier equipped with only a LA-EDI

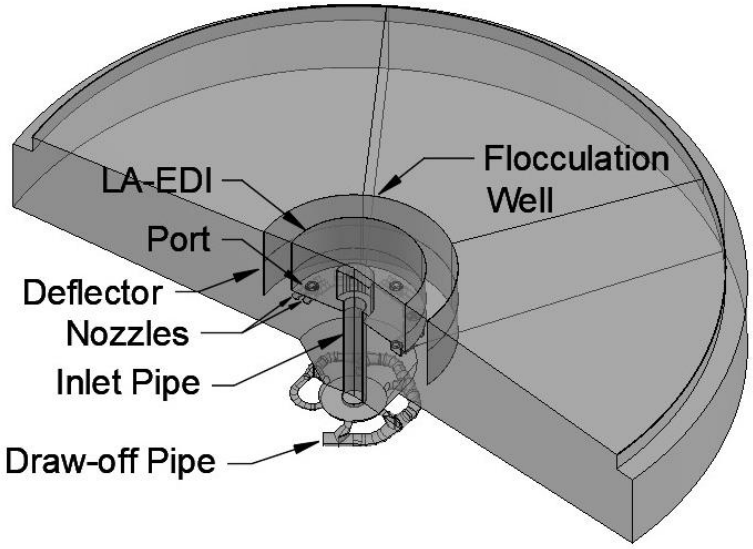


Figure 4.6 The cross-section of the clarifier equipped with a LA-EDI and a spiral-shaped draw-off pipe

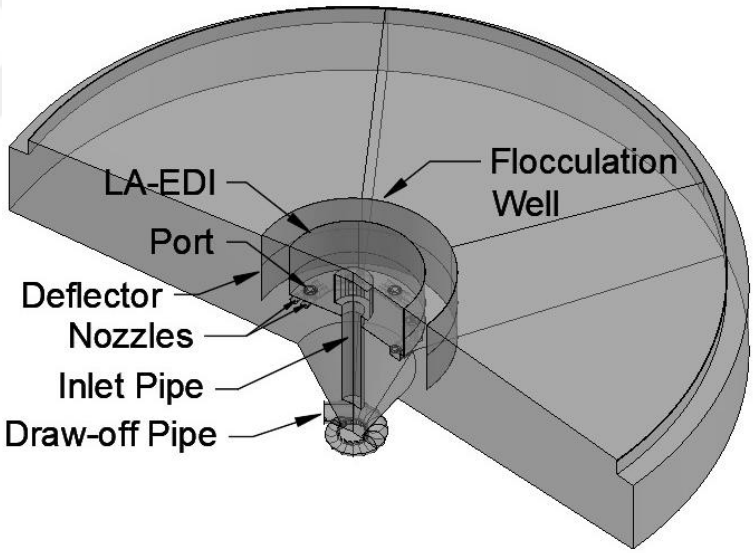


Figure 4.7 The cross-section of the clarifier equipped with a LA-EDI and a snail-shaped draw-off pipe

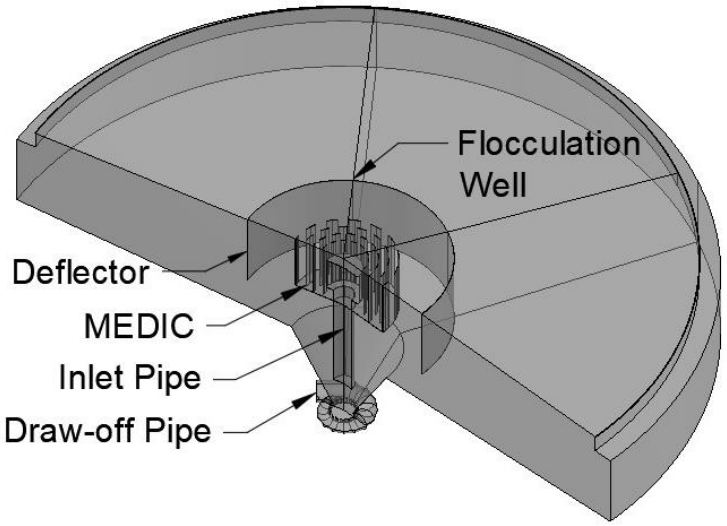


Figure 4.8 The cross-section of the clarifier equipped with a MEDIC and a snail-shaped draw-off pipe

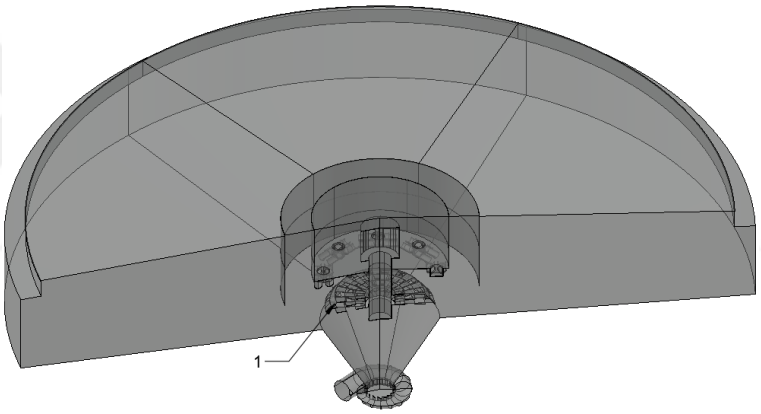


Figure 4.9 The cross-section of the clarifier equipped with a LA-EDI, a snail-shaped draw-off pipe and the novel deflector

The dimensions for the geometry of the opposing-jet nozzle type EDI (LA-EDI) and the multilayer type EDI (MEDIC) are drafted following the descriptions available in their patent documents (US Patent No. 6,276,537 B1, 2001, US Patent No. 7,378,027 B2, 2008).

The optimum geometry of the spiral casing of a reaction turbine has been investigated for decades and the main dimensions were determined as a function of inner diameter and specific speed (Kovalev, 1965). It is impossible to dimension a

snail-shaped draw-off pipe using the equations derived for a reaction turbine; because, the discharge velocity of the sludge withdrawal, which should be below 0.9 m/s (Tchobanoglous, Burton, & Stensel, 2003), is remarkably slower than the inflow velocity of a reaction turbine, and the dimensioning equations do not yield a valid design for small velocities. Therefore, the preliminary dimensions of the snail-shaped draw-off pipe were calculated, considering that the diameter of the outlet should maintain the discharge velocity below 0.9 m/s, and the inner diameter of the sludge hopper is usually 60 cm. The remaining parameters were determined by proportioning to the known dimensions. The optimum dimensions of the snail-shaped draw-off pipe were optimized by CFD simulations. The geometry of the snail-shaped draw-off pipe is illustrated in Figure 4.10.

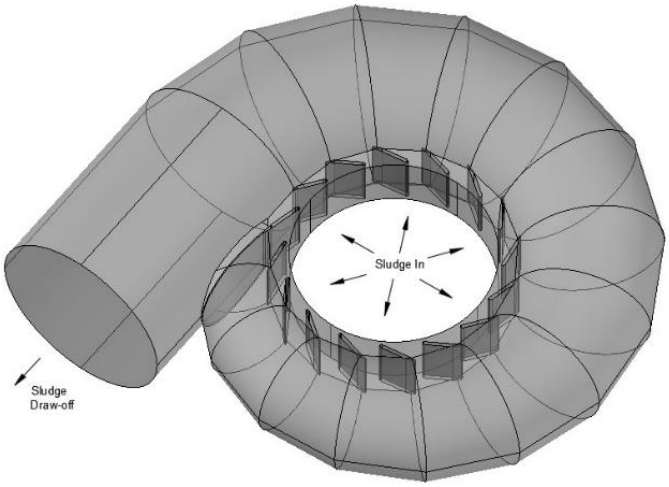


Figure 4.10 The 3D geometry of the snail-shaped draw-off pipe

The parameters such as the bending radius, the split angle, the length and the diameter of the distributor, and the joint of the distributor impact the flow conditions within the distributor of an impulse turbine. However, the optimum dimensions of those parameters are unknown. Therefore, the preliminary dimensions of the spiral-shaped draw-off pipe were estimated based on trial-and-error and optimized using CFD tools. The geometry of the spiral-shaped draw-off pipe is illustrated in Figure 4.11.

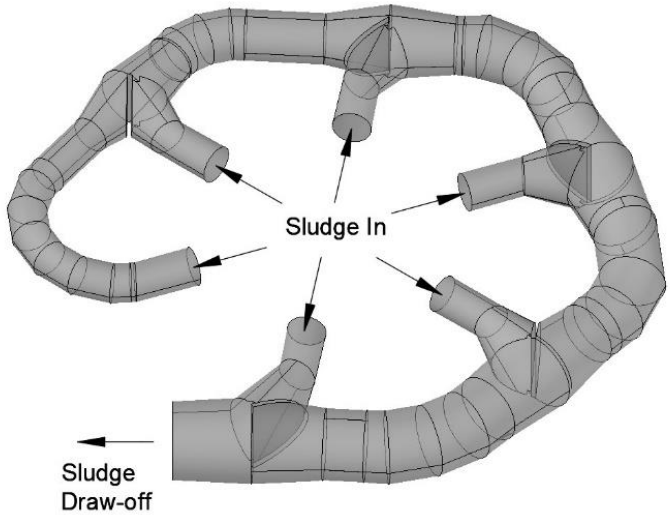


Figure 4.11 The 3D geometry of the spiral-shaped draw-off pipe

The shape of the sludge hopper in the clarifier equipped with a snail-shaped draw-off pipe was kept as it was in the original clarifier, but the sludge hopper was lowered in the clarifier equipped with a snail-shaped draw-off pipe -preserving the side slopes to mount the draw-off pipe.

The dimensions for the geometry of the novel deflector were determined through empirical analysis.

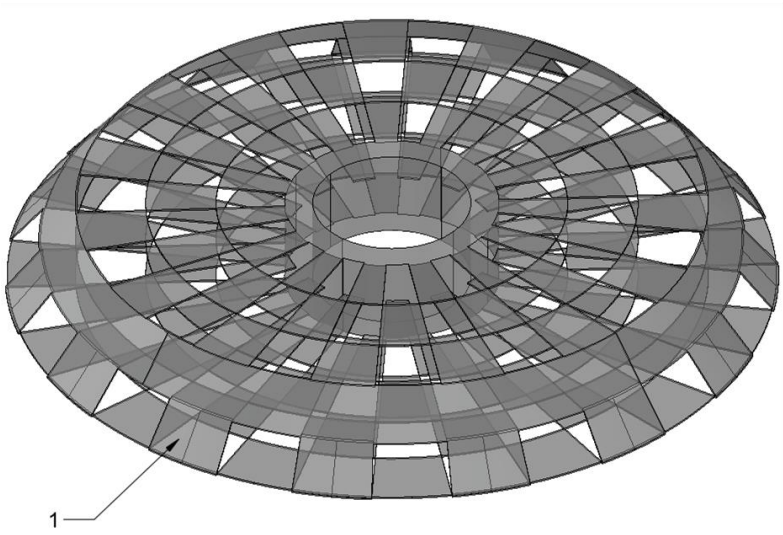


Figure 4.12 The 3D geometry of the novel deflector

The problems were decided to be solved in a 3D domain. Rigid-lid approximation was done considering that the fluctuations on the water surface of the clarifiers are negligible.

4.2.3 Discretization

The geometries were imported to ANSYS and discretized into computation cells using meshing methods. Since the geometries were very complex, the mesh generated by the software seemed acceptable. Over 4,5M triangular elements were used in meshing per clarifier. A grid dependency study was also performed to verify that simulation will be accurate, stable, and easily convergable with minimum computational time.

4.2.4 Boundary Conditions

The boundary conditions were inputted as followed: The inlet was defined as velocity inlet, the water outlet was defined as pressure outlet, the sludge outlet was defined as velocity inlet, the top was defined as symmetry, and other surfaces were defined as walls.

4.2.5 Solver Settings

The solver settings were inputted as followed: The fundamental governing equations (the continuity and momentum) were solved under transient conditions in a 3D domain using the Finite Volume Method. The double-precision pressure-based solver was selected with second-order implicit as its unsteady formulation to achieve a more accurate result. Semi-Implicit Method for Pressure-Linked Equations (SIMPLE) scheme was utilized for pressure-velocity coupling calculations. The k-ε turbulence model was utilized to involve mean flow components for turbulent flow conditions and close the set of equations. The standard discretization scheme was used for the pressure equation, but second-order upwind discretization was chosen for both

momentum and energy equations. The under-relaxation factors were used for numerical stability. The convergence criteria were set to be 10^{-6}.

The simulations were run and since they were found well-modeled, the post-processes were performed to illustrate the results.

CHAPTER 5
RESULTS AND DISCUSSIONS

In the scope of this chapter, the operational data recorded at the investigated WWTP was investigated, then a design review was performed based on the analysis of the operational records. The potential measures were sought and their CFD simulations were carried out to minimize energy consumption and decrease operational costs while enhancing the treatment capacity, facilitating treatment performance, and meeting the discharge limits in the treatment plant.

5.1 Investigation of Recorded Operational Data of the Scrutinized WWTP

The design of the biological treatment process of the investigated WWTP was based on the empirical formulas given in the design manual ATV-DVWK-A 131E (2000). Since the characteristics of the wastewater was unknown, the influent parameters were estimated as per literature and expert judgment. The important parameters used in the design were illustrated in Figure 5.1.

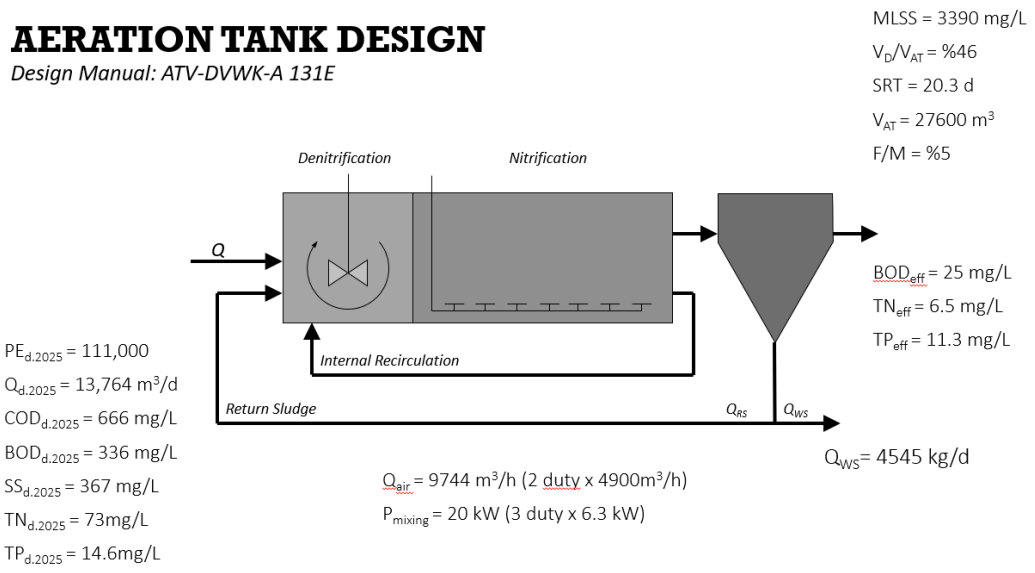


Figure 5.1 The illustration of the key design parameters assumed in the design of the Aeration Tank of the investigated WWTP

Although the average flowrate was used in the design of biological treatment units, the designer followed the approach of dimensioning units that can ignore unwanted and unexpected situations by oversizing the design, in other words masking the inadequate design.

The operational data of the investigated WWTP, recorded between 24.09.2018 and 31.12.2019, were investigated. The results were given in Table 5.1.

Table 5.1 Descriptive Statistics of the Operational Data Recorded in the Investigated WWTP

Operational Data	**Number of Data**	**Upper Quartile (Q3)**	**Median (Q2)**	**Lower Quartile (Q1)**	**Max**	**Mean**	**Min**
Daily Wastewater Volume @ Inlet (Q_{mean}=13762 m³/day)	465	15014	14342	13303	18459	14104	7521
Daily Wastewater Volume @ Outlet (Q_{mean}=13762 m³/day)	465	14648	13708	12671	18691	13585	2911
Daily Sludge Volume (m³)	465	321	241	196	598	250	0
Wasted Sludge Amount (kg)	392	16868	9550	8740	36990	12149	6650
Imhoff value @ AT-1 (mL)	445	730	620	540	910	621	220
Imhoff value @ AT-2 (mL)	449	730	620	530	920	624	220
Imhoff Value of RAS (mL)	458	900	860	810	990	847	250
SVI @ AT-1 (DV=120 mg/g)	272	169	152	135	242	154	68
SVI @ AT-2 (DV=120 mg/g)	276	169	151	134	244	153	65
Food (F = kg COD)	70	151	125	102	219	127	48
Mass (M = kg MLSS)	70	5240	4972	4044	5923	4673	2846
F/M (DV=0.052)	68	0.031	0.026	0.022	0.061	0.027	0.009
SRT (Sludge Age) (DV=25 days)	63	14.8	9.7	7.7	18.5	10.9	4.1
Excess Sludge (DV=17500 kg/day)	63	17285	9900	8565	32820	12800	7360
MLSS @ Aeration Tank-1 (DV =3390 mg/L)	277	4645	3957	3652	7985	4189	2645
MLSS @ Aeration Tank-2 (DV =3390 mg/L)	276	4590	3974	3646	8362	4202	2625
SS @ Inlet (DV=369mg/L)	278	211	163	121	560	174	33
SS @ Outlet (DL=35mg/L)	278	7	6	4	30	6	1
SS Removal Rate	278	96.7%	96.3%	96.7%	94.6%	96.6%	97.0%
COD @ Inlet (DV=669mg/L)	260	350	279	212	595	287	85
COD @ Outlet (DL=125mg/L)	256	17	14	12	54	16	3
COD Removal Rate	256	95.2%	95.1%	94.5%	90.9%	94.6%	96.9%

DL: Discharge Limit, DV: Design Value

Table 5.1 Descriptive Statistics of the Operational Data Recorded in the Investigated WWTP (continued)

Operational Data	Number of Data	Upper Quartile (Q3)	Median (Q2)	Lower Quartile (Q1)	Max	Mean	Min
BOD @ Inlet (DV=334mg/L)	130	156	125	85	256	124	19
BOD @ Outlet (DL=25mg/L)	128	2	1	1	18	2	1
BOD Removal Rate	128	98.7%	99.2%	98.8%	93.0%	98.4%	94.7%
COD/BOD Ratio @ Inlet	115	2.8	2.2	1.8	8.2	2.4	0.9
Equivalent BOD Load	256	21.3	16.2	10.3	43.0	15.9	1.3
NH4-N @ Inlet (mg/L)	176	20.8	17.0	13.8	35.0	16.9	0.3
NH4-N @ Outlet (mg/L)	180	0.8	0.3	0.1	12.4	0.9	0.0
NO3-N @ Inlet (mg/L)	179	1.3	0.7	0.6	3.2	1.0	0.3
NO3-N @ Outlet (mg/L)	181	0.7	0.5	0.4	4.2	0.6	0.2
TN @ Inlet (DV=74mg/L)	203	37.6	31.2	27.8	537.7	35.0	3.9
TN @ Outlet (DL=15mg/L)	203	2.3	1.7	1.3	13.7	2.2	0.7
TN Removal Rate	203	93.8%	94.6%	95.3%	97.5%	93.8%	81.5%
TP @ Inlet (DV=15mg/L)	206	4.7	4.1	3.4	14.5	4.2	1.4
TP @ Outlet (DL=2mg/L)	205	2.4	1.8	1.4	11.7	2.3	0.4
TP Removal Rate	205	48.4%	55.6%	57.8%	19.3%	46.4%	72.6%

DL: Discharge Limit, DV: Design Value

The 14-month recorded operational data after the commencement reflected that the real conditions did not align with the design (see Figure 5.2). The influent flow rate measured in the current year (2019) was almost 5% more than the estimated influent flow rate for 2025. The design must be rechecked using the influent flowrate of 15,000 m^3/day for the current status and 20,000 m^3/day for the 2025-forecast. Besides, although the influent wastewater characteristics were estimated to be 336 mg/L BOD, 73 mg/L TN, and 14.6 mg/L TP, the median of 14-months measured influent parameters were 156 mg/L BOD, 37.6 mg/L TN, and 4.7 mg/L TP. Since the measured parameters were way more divergent than the estimated design parameters, the design had to be reviewed to take necessary actions for the improvement and optimization of the treatment performance.

5.2 Design Review of Biological Treatment Units

A design review was done based on the operational records (median and third-quartile values) instead of assumed design values as per the empirical formulas given in the design manual. Figure 5.2 illustrates the differences between the previous design and the design-review based on the third quartile value of the 465-day operational records.

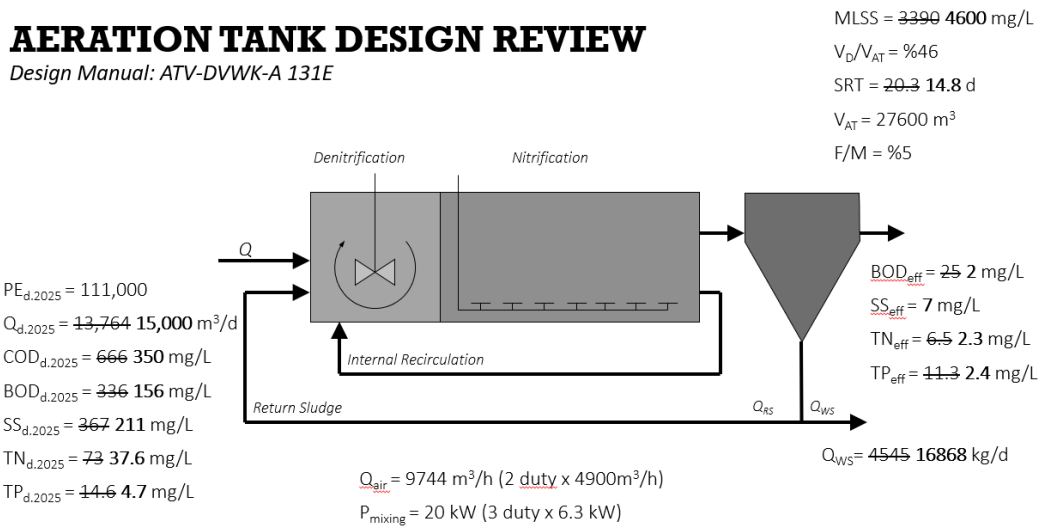


Figure 5.2 The illustration of the key parameters recorded in the Aeration Tank of the investigated WWTP

The design parameters were summarized in Table 5.2. The design parameters were summarized per different scenarios in Table 5.2. 2025 and 2040 scenarios are the design review for 2025 and 2040 according to the design report, respectively. The Q2 and Q3 scenarios are the design revision based on the median and the third (or upper) quartile value of the 465-day operational records, respectively.

Table 5.2 The comparison of the design parameters between the previous design and the current design check

Parameter	Unit	Scenarios			
		2040(1)	**2025(2)**	**Q2(3)**	**Q3(4)**
Inflow rate (Q)	m^3/d	17,824	12,966	14,300	15,000
Hourly peak flow during wet weather ($Q_{WW,h}$)	m^3/h	1,615	1,182	1,182	1,182
BOD ($C_{BOD,IAT}$)	mg/L	339	336	125	156
NH_4-N ($C_{N,IAT}$)	mg/L	73	73	17	21
Volume utilization ratio (V_D/V_{AT})	-	53%	53%	11%	16%
Sludge age for only Nit. & Denit. ($t_{SS,dim}$)	days	20.3	20.3	20.3	20.3
Daily BOD load ($B_{d,BOD}$)	kg/d	5,686	4,097	1,502	2,040
Total sludge production (SP_d)	kg/d	5,317	3,855	1,603	2,238
Mass of SS in reactor ($M_{SS.AT}$)	kg	107,895	78,255	32,547	45,423
MLSS concentration (SS_{AT})	kg/m^3	3.39	3.39	3.39	3.39
Volume of reactor (V_{AT})	m^3	31,799	23,063	9,592	13,387
Volume loading rate (B_R)	kg.BOD/ m^3.d	0.18	0.18	0.16	0.15
Sludge loading rate (B_{SS})	kg.BOD/ kg.SS.d	0.05	0.05	0.05	0.04
Volume of denitrification (V_D)	m^3	16,925	12,308	1,063	2,096
Volume of nitrification (V_N)	m^3	14,874	10,756	8,529	11,291
Recirculation ration (RC)	-	825%	825%	125%	125%
Retention time (t_R)	d	19.7	19.5	8.1	11.3

(1) The 2040 scenario is the design review for the year 2040 according to the design report.
(2) The 2025 scenario is the design review for the year 2025 according to the design report.
(3) The Q2 scenario is the design revision based on the median value of 465-day operational records.
(4) The Q3 scenario is the design revision based on the third quartile value of the 465-day operational records.

The key findings of the comparison were listed as:

- The denitrification volume was 3 times larger than the required volume;
- Sludge age in the operation was 10-15 days, although it should be 20 days as per design criteria.
- The wasted sludge (9.5-17 t/day) was 5-8 times larger than the required amount (2.24 t/day).
- The aeration tank volume (26,000 m^3) was 2 times larger than the required volume (13,387 m^3).
- The F/M ratio was in the order of 0.025-0.030, although it should be 0.05.
- Internal recycle was 6-7 times more than the required recycle.
- The supplied air flow was 2-3 times more than the required air volume.

The clarifier was also examined since clarifiers are part of the biological treatment system. The diameter of the existing clarifiers is 30 m. The existing clarifiers have a 27.4 $m^3/m^2/day$ overflow rate and a 6.8 $kg/m^2/h$ sludge loading rate. These values satisfy the limit values in the literature, which are between 24 and 32 $m^3/m^2/day$ for overflow rates and lower than 7 $kg/m^2/h$ for sludge loading rates (Tchobanoglous, Burton, & Stensel, 2003). Besides, the current clarifier has an influent well, that has a diameter of 13% of the clarifier diameter, and each has 4 large openings to diffuse the influent into the clarification zone. The influent well was not equipped with energy dissipating baffles.

5.2.1 Comprehension of Investigation Results

The findings indicated that the required volume for aeration could be maintained by only one of the two aeration tanks. Therefore, it was considered to idle one of the aeration tanks since the required volume was half of the available volume.

The findings also indicated that the available denitrification volume was almost three times less than the initial design. Therefore, once it was decided to idle one of the two aeration tanks, the aeration tank -that was supposed to operate alone should be equipped with more diffusers and aeration pipelines to provide the required nitrification volume.

In the case of idling one of the two aeration tanks, the aeration tank -that was supposed to be operated alone would be operated at high capacity. No answers are usually sought to many questions in the conventional design of the biological treatment process due to the fact that the design is usually oversized to bear unwanted and unexpected conditions. However, since the biological system would be more fragile to unexpected conditions during the operation since the aeration tank would be operated at high capacity, the hydrodynamic conditions in the aeration tank must be investigated in detail. Therefore, it would have to be verified that:

- The fluid flow pattern inside the reactor has behaved as it was designed. In other words, the hydraulic pattern of the activated sludge suspension inside

the aeration tank was traced as either completely mixed or plug flow or somewhere in between the two regimes, as it was designed. Besides, no inefficient (dead) volumes were formed. Homogeneous conditions have prevailed in the environment.

- The aerobic, anoxic, or anaerobic environments were formed in the aeration tank since the WWTP was designed as an Modified Ludzack-Ettinger process.
- The aeration equipment and its arrangement enabled the environment suitable for biological activity.
- The interaction between the solid (activated sludge, microorganism) and gas (oxygen) phases in the fluidized bed (wastewater) was suitable to enhance the biological process.

5.3 Investigation of Hydrodynamics within the Aeration Tank

The biological activity in the aeration tank depends on hydraulic conditions and also affects the treatment efficiency. The biological activity depends on whether the hydraulic pattern in the tank is either completely mixed or plug flow or somewhere in between the two regimes. Therefore, it was first investigated whether there were any hydrodynamic problems due to the geometry of the aeration tank. In this context, it was investigated whether any hydraulic problems occur while the influent entered, or the outflow exited from the aeration tank. It was investigated whether the hydraulic pattern of the activated sludge suspension inside the aeration tank behaved as it was designed, inefficient (dead) volumes were not formed, and homogeneous conditions prevailed in the aeration tank. It was also investigated whether the required aerobic, and anoxic environments were formed in the aeration basin as the biological system was designed based on the Modified Ludzack-Ettinger process. Moreover, the internal recirculation inside the aeration tank and whether mixers were located at the proper locations were investigated.

Aeration is the most critical point of the biological system. The required air volume is usually calculated by empirical formulas which is not a so precise calculation

method. Although it is usually neglected, the hydraulic losses in the aeration system should also be calculated, which is so cumbersome. Once the required airflow volume is calculated for the biological system, there are multiple options to supply the calculated air volume to the aeration tank. Usually, no detailed design is usually done for the selection and positioning of the aeration equipment; the equipment and its installation layout are usually decided either by the equipment supplier's recommendation or the engineer's experience. Therefore, it was investigated whether the diffusers were placed in the proper pattern, whether the created environment was suitable for the biological activity and whether the calculated amount of air could be supplied for nitrification purposes.

5.3.1 Velocity Flow Field

Although the flow velocity was investigated in 3D, cross-sections in 2D were taken for the sake of illustrating the outputs.

The velocity field in the aeration tank at the depth of the center of the mixers was depicted in Figure 5.3. The agitation provided by the mixers induced the fluid to flow at a very high velocity. It was observed that the flow velocity was higher than 4,0 m/s right after the mixers until the aeration zone. The asymmetric flow field due to the airflow induced by fine bubble diffusers decreased the velocity of the fluid flow. Although the mixers were selected to provide a recirculation ratio of 8 as per the previous design, this ratio was found to be decreased to 1,25 as per the design review. Therefore, the mixers were not required to be operated at nominal speed anymore.

It would not be feasible to idle one of the two mixers, even if the mixer that would be going to be operated alone would be repositioned as centered across the transverse of the tank. This is because a single mixer could not mix the whole cross-sectional area, and dead volumes would be left over at the cross-sectional area of the tank. Therefore, it is better to keep both of the mixers operational but operate them at minimum speed.

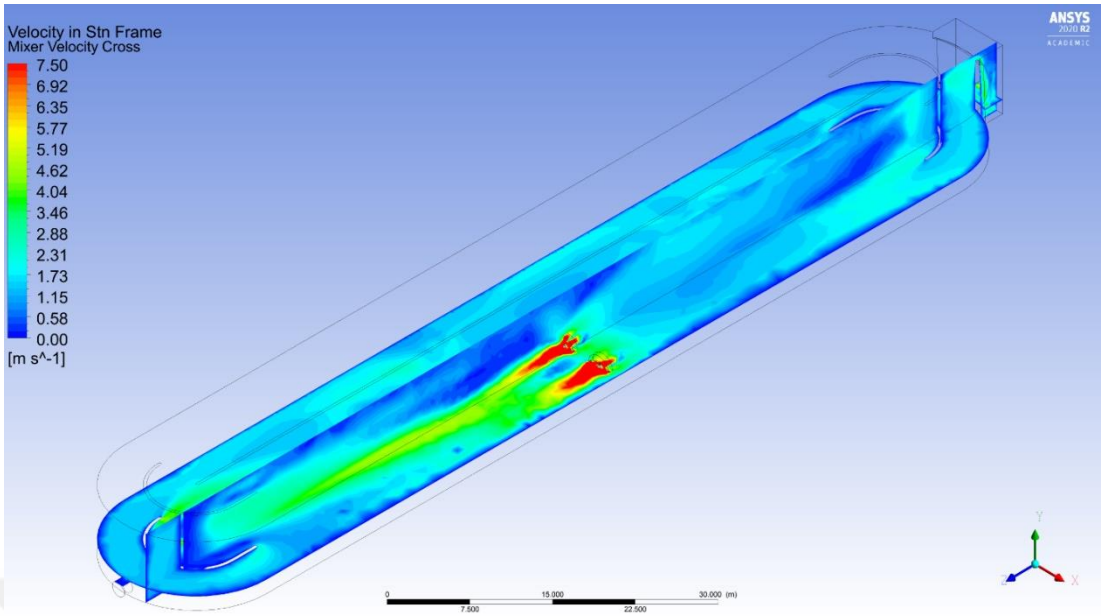


Figure 5.3 Flow Velocity Vectors in the Aeration Tank

Although the flow velocity is not as a limiting parameter as it is in clarifiers, it affects the residence time of the substrate in the nitrification and denitrification zones of the aeration tank. Since the flow velocity was found to be very high after the mixers, the residence time of the substrate at the denitrification zone was less than was calculated.

5.3.2 Streamlines

Figure 5.4 represents the streamlines that occurred during the fluid flow in the aeration tank. The streamlines indicated that the plug flow conditions prevail in the aeration tank; however, eddies were formed at the region where mixers were located, due to the fact that the mixers were operated at a high rate induced flow regime changes in this region.

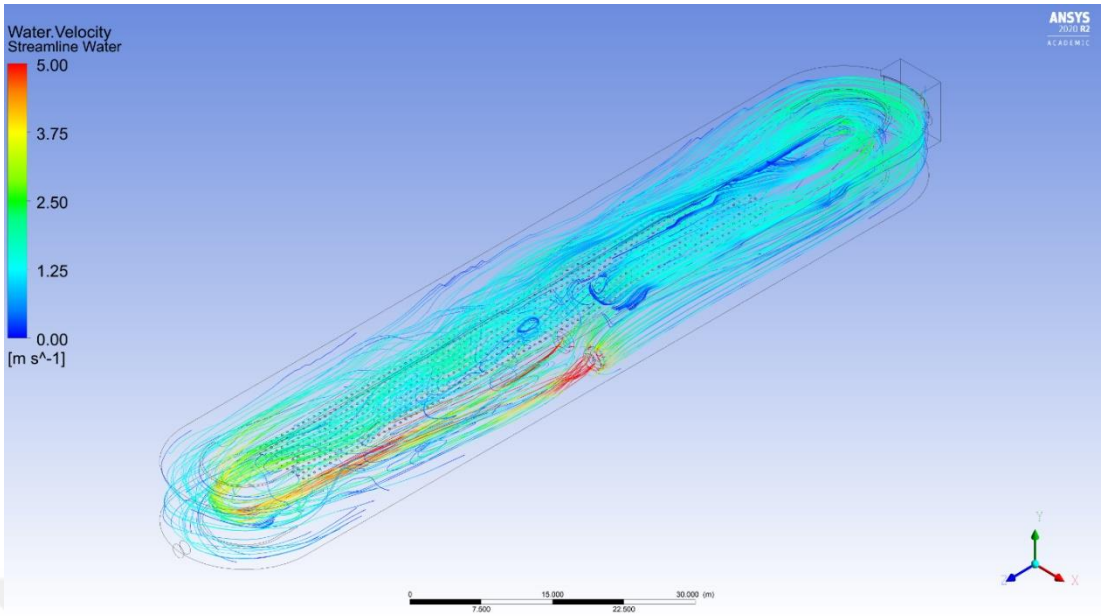


Figure 5.4 Streamlines and eddies in the Aeration Tank

No dead volumes were observed in the aeration tank; however, the denitrification volume could not be efficiently used due to the high flow velocity in this zone.

5.3.3 Aeration

Figure 5.5 and Figure 5.6 represent the volumetric fraction of air in the aeration tank, at 5 and 60 seconds of operation, respectively.

Although Figure 5.5 revealed that all fine bubble diffusers were operated simultaneously and the air volume fraction was simulated to be almost identical in the nitrification region, Figure 5.6 indicated that fluid flow shifted the nitrification and denitrification regions in the aeration tank. It could be said that nitrification did not occur at the first one-third distance of the nitrification region. The following one-third distance of the nitrification region could be entitled a transitional nitrification region where nitrification could partially occur. Finally, the last one-third distance of the nitrification region is the volume where nitrification could effectively occur.

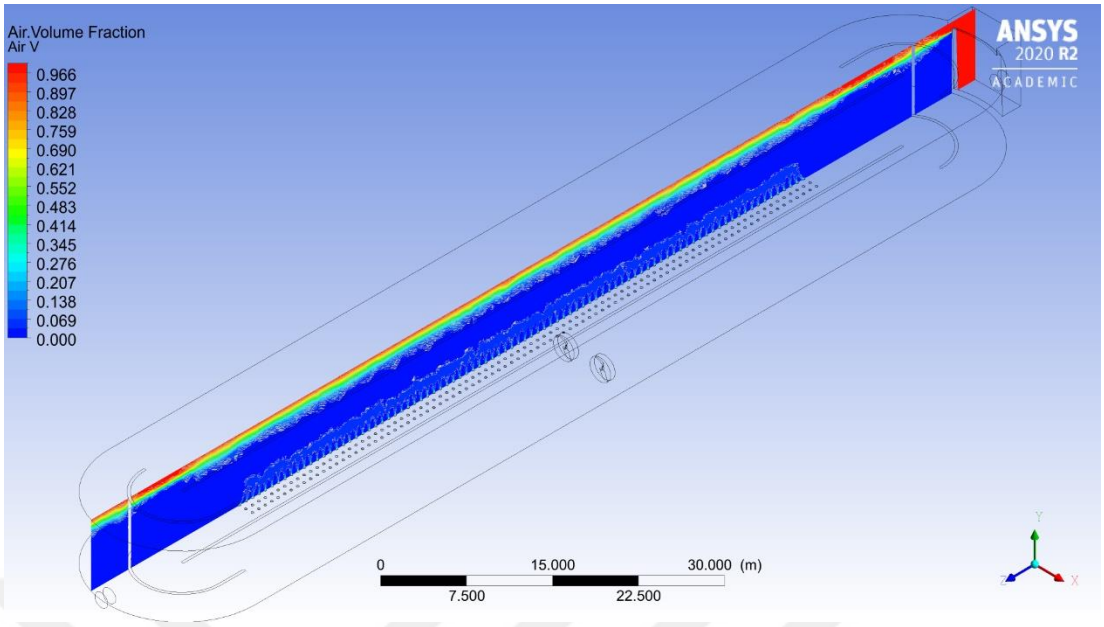


Figure 5.5 Air Volume Fraction right after onset of the operation (t=5sec)

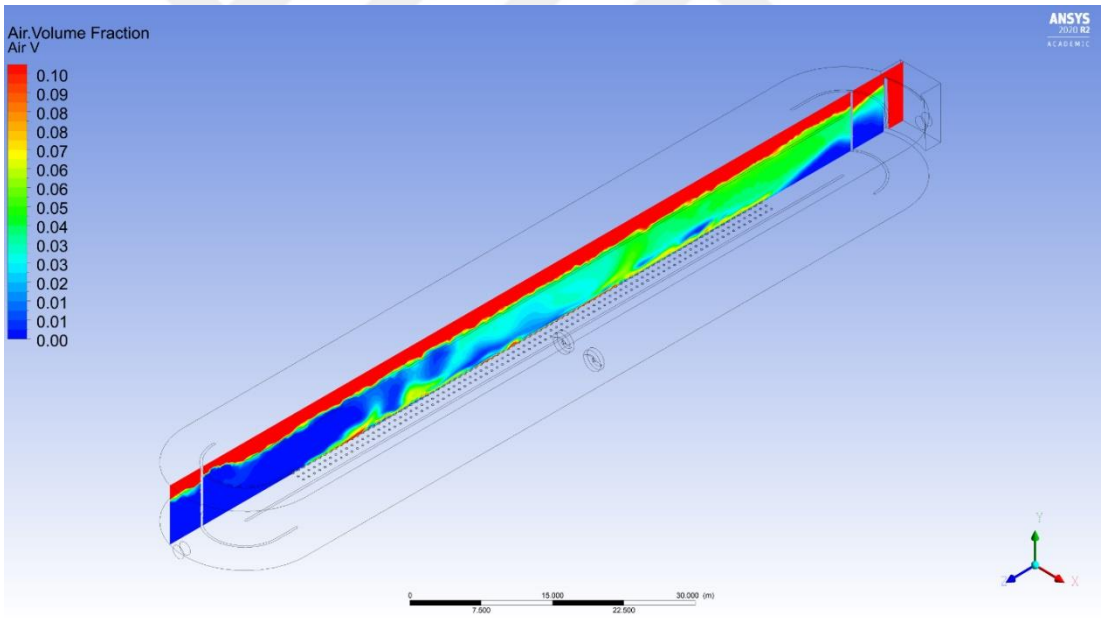


Figure 5.6 Air Volume Fraction after a course of the operation (t=60sec)

The flow velocity also emerges as a parameter to be considered in the design of aeration tanks. The high flow velocity affects the formation of plug-flow reactor conditions and induces the nitrification and denitrification volumes in the reactor to

shift. Moreover, the high flow velocity may not leave any dead volumes but ineffective volumes in the aeration tank.

5.3.4 Comprehension of Investigation Results

The findings indicated that it was possible to idle one of the two aeration tanks. However, the mixers located in the aeration tank -that was supposed to be operated alone must be operated at minimum speed to mitigate high flow velocity. This would decrease the recirculation ratio, maintain better plug-flow conditions, and form better nitrification and denitrification regions in the aeration tank.

The potential of operating the existing treatment plant with half of the available volume allocated for aeration would save almost half of the energy and operational costs of the biological processes since half of the blowers would be suspended.

Consequent to idling one of the two aeration tanks, it was required to split the effluent of the aeration tank into two clarifiers; however, there were no flow splitters placed between the aeration tanks and clarifiers, since each aeration tank was followed by a clarifier. Therefore, instead of building a new flow splitter, it was hypothesized that one of two clarifiers could also be switched to the idle position, and the clarifier was supposed to be operated alone at the ultimate limit.

5.4 Investigation of Hydrodynamics within the Conventional Clarifier

The existing clarifiers have a 27.4 $m^3/m^2/day$ overflow rate and a 6.8 $kg/m^2/h$ sludge loading rate. However, in the case of idling one of the two clarifiers, the clarifier that was supposed to be operated alone would bear a 54.8 $m^3/m^2/day$ overflow rate and a 13.6 $kg/m^2/h$ sludge loading rate once the influent was doubled; these values were 12.5% and 40% above the design criteria for the overflow and sludge loading rates, respectively (Tchobanoglous, Burton, & Stensel, 2003). Therefore, some measures were necessary to operate the clarifier at high overflow and sludge loading rates. In this context, the hydrodynamics in the existing clarifier was investigated first before

investigating which measures would be taken to operate the single clarifier at high overflow and sludge loading rates. The flow and concentration fields were simulated considering the rheological properties of settling sludge and the effect of stratification on the turbulent diffusion was elucidated in the following headings, for the existing conventional secondary clarifier.

5.4.1 Velocity Flow Field

Although the flow velocity was investigated in 3D, cross-sections in 2D were taken for the sake of illustrating the outputs. The cross-sections of the velocity field in the horizontal and vertical directions were elucidated and elaborated in the following headings.

5.4.1.1 Horizontal Cross-Section of the Velocity Flow Field

The velocity field in the original conventional clarifier at the elevation of the orifices (the elevation where the influent was diffused to the clarification zone) was depicted in Figure 5.7. The energy of the influent must be well-dissipated in the influent well and then orifices should distribute the flow evenly to the clarifier.

The outflow velocity at the orifices of the influent well was simulated at around 75 mm/s in the original clarifier. Besides, the original clarifier was known that it had been running efficiently under existing conditions. It was also advised to take the outflow velocity at the orifices at 75-300 mm/s, as a design criterion (Tchobanoglous, Burton, & Stensel, 2003). This simulation confirmed that no problems should be sought in the original clarifier under existing conditions.

Although no flocculation well existed in the original clarifier, the flow velocities were found below 30 cm/s within the clarification zone and no drawbacks have been reported by the operator.

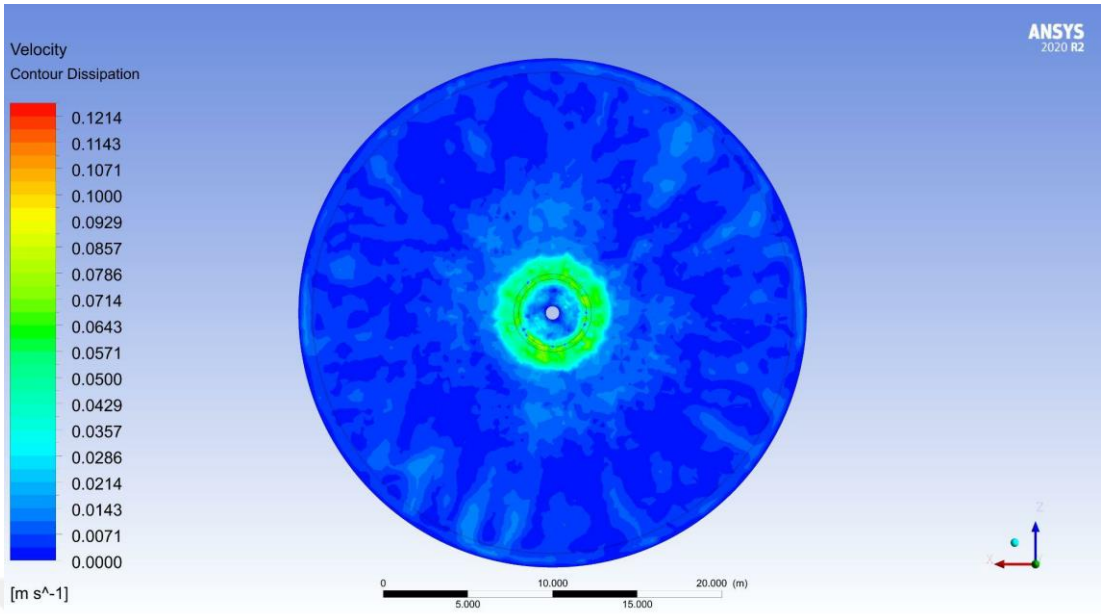


Figure 5.7 The flow velocity contours at the elevation of orifices in the original conventional clarifier and simulated under existing conditions

The flow velocity in the conventional clarifier is variant across the radial direction; while the flow velocity is as high as 0.05 m/s on the periphery of the influent well, it ranges from 0.015 m/s to 0.025 m/s across the clarifier.

5.4.1.2 Vertical Cross-Section of the Velocity Flow Field

Figure 5.8 represents the cross-section of the flow velocity field in the clarifier. As was aforementioned, the influent well in the conventional clarifier performed fair enough to dissipate the influent energy under existing conditions; although the influent velocity was 0.6 m/s, the velocity diminished down to 0.75 mm/s. The flow exited from the influent-well-orifices could not be dissipated more until the flow travelled 2/3rd of the radius of the clarifier, since there were no other measures for energy dissipation at the influent-well-orifices (Figure 5.8).

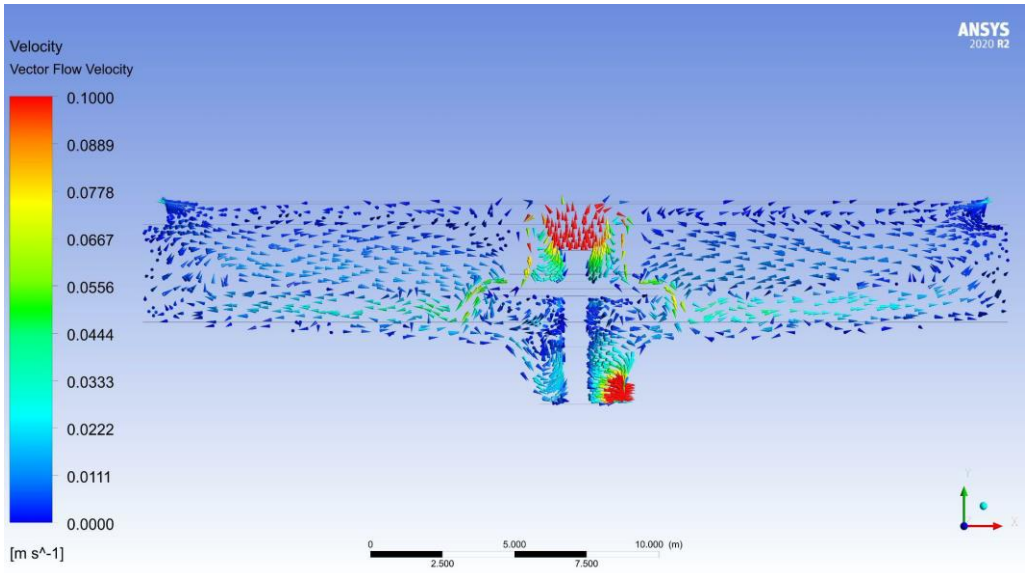


Figure 5.8 Flow velocity vectors in the original conventional clarifier and simulated under existing conditions

5.4.2 Solids Settling Velocity

The solids settling velocity contours, which were modeled using the Takács function (1991), were represented in Figure 5.9.

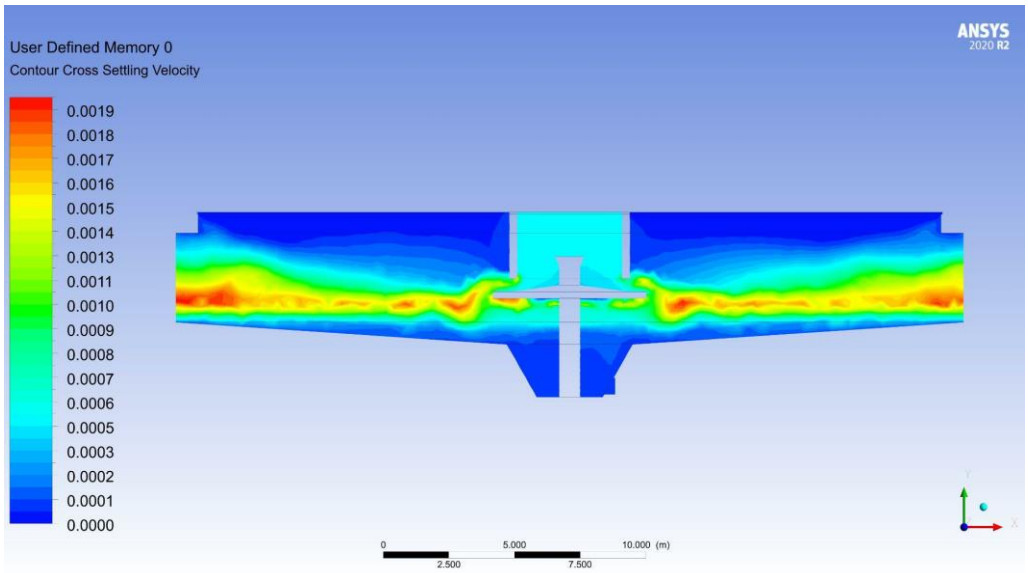


Figure 5.9 Solids settling velocity contours (m/s) in the original conventional clarifier and simulated under existing conditions

The most favorable zone for solids settling in clarifiers is the region between the influent well orifices and the overflow weirs, above the sludge blanket; therefore, the colors that reflect the settling velocity change in Figure 5.9 have a wide range of the spectrum in that region. The settling velocity values were found low at the bottom of the clarifier, as expected, since the sludge blanket was formed and thickened at the bottom, and therefore settling is minimum in this region. The settling velocity values were found maximum at the plume exiting the orifices of the influent well. Moreover, the plume was found dispersed in a conical shape in the horizontal direction.

5.4.3 Solids Concentration

The main objective of having clarifiers in treatment plants is to facilitate the sedimentation of solids. In this regard, the performance of achieving this objective could be best visualized by observing solid concentration in the clarifier.

Figure 5.10 represents the solids concentration in the clarifier. Any reader will first focus on the red region in Figure 5.10, at first sight. This red region represents the most thickened sludge in the clarifier.

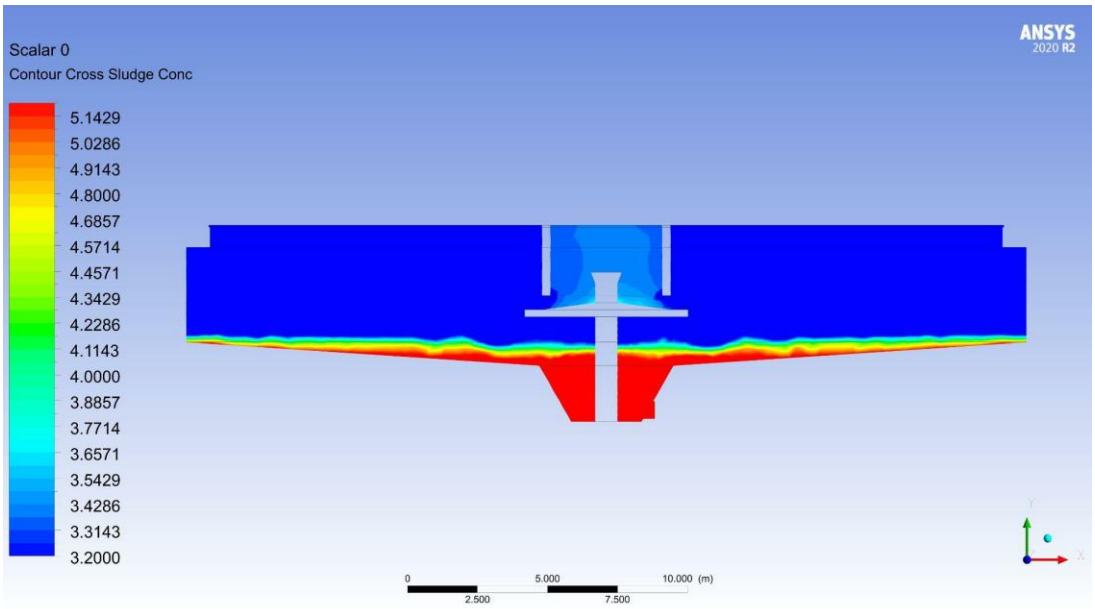


Figure 5.10 Solids concentration contours (kg/m³) in the original conventional clarifier and simulated under existing conditions

The simulations confirmed that the original clarifier that has been operated under existing conditions, which was designed with nominal design parameters, can yield very well-thickened sludge (Figure 5.10). Obviously, the conventional clarifiers enable the best conditions for the thickening of settled sludge compared to the clarifiers with EDIs (Figure 5.17, Figure 5.24).

The change in the solids concentration during the abstraction of sludge from the beginning of the simulation was depicted in Figure 5.11.

The solids concentration abstracted from the conventional clarifier was found to have reached the fourth phase of the sedimentation phase, which is compression. This is the fact why the most thickened sludge was found to be achieved in the conventional clarifier, as depicted in Figure 5.11.

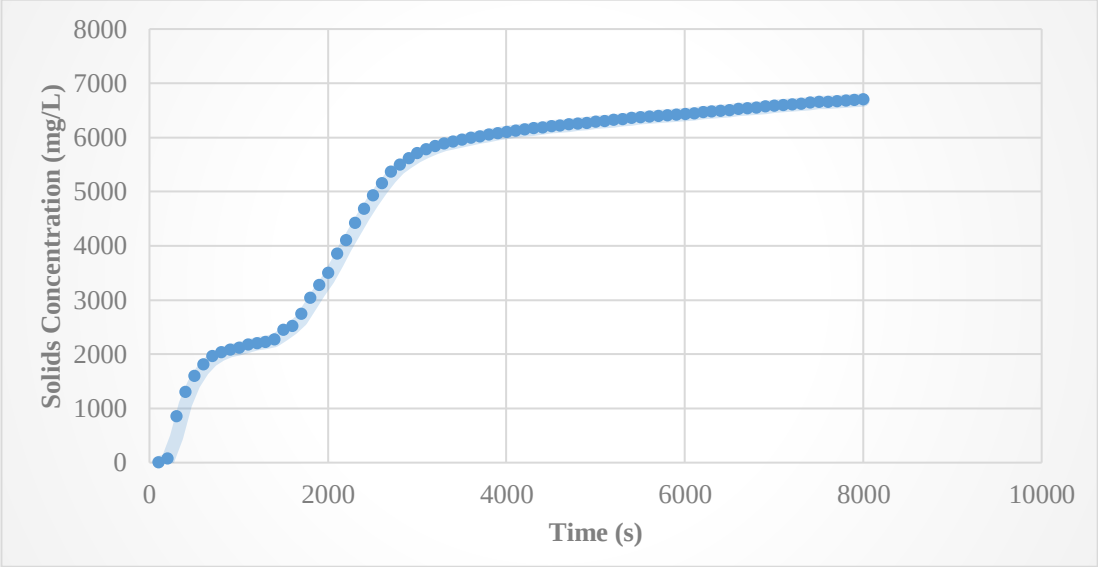


Figure 5.11 The change of solids concentration drawn-off from the original conventional clarifier

5.4.4 Streamlines

Figure 5.12 represents the streamlines that occurred during sludge draw-off. The streamlines in the conventional clarifier have only appeared in the lower half of the sidewall, where the sludge blanket occurs; in other words, the drawn-off sludge was thickened.

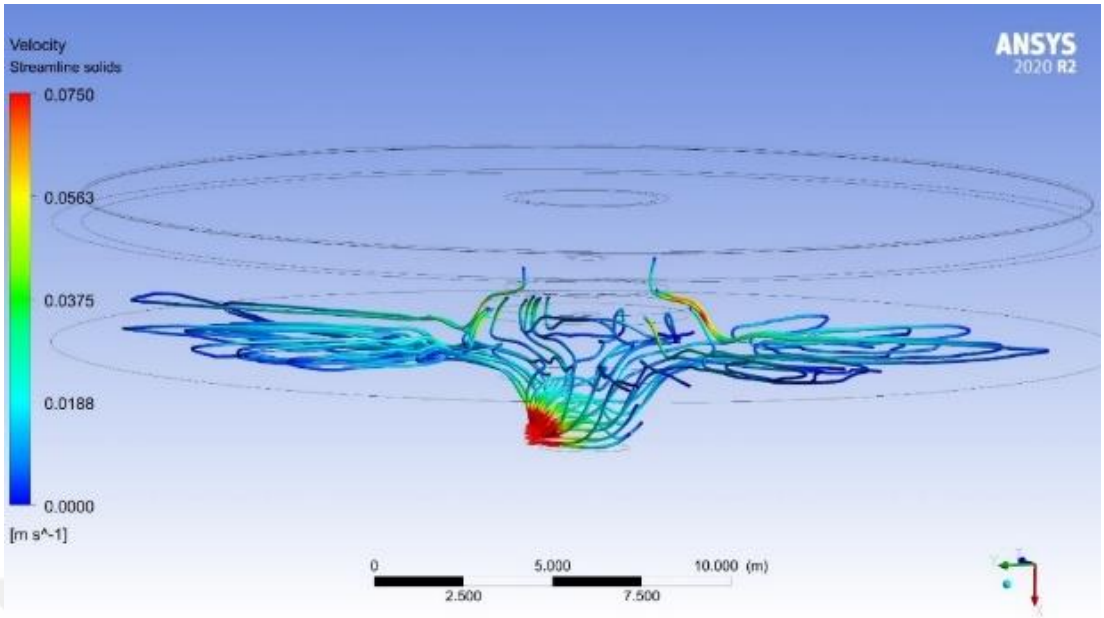


Figure 5.12 Streamlines simulated in the original clarifier during sludge withdrawal under existing inflow conditions

5.4.5 Comprehension of Investigation Results

The findings indicated that the energy of the influent was well-dissipated in the influent well and the orifices distribute the flow evenly to the clarifier. It was also found that the conventional clarifier yielded very well-thickened sludge. The simulations confirmed that no problems should be sought in the conventional clarifier that has been operated under the existing conditions, which were designed with nominal design parameters.

In the case of idling one of the two clarifiers, the first measure that comes to mind would be retrofitting the conventional clarifier that was supposed to be operated alone with an EDI. It is known that installing an EDI to a conventional clarifier could enhance the hydrodynamic conditions in the clarifier, operate the clarifier with higher overflow and sludge loading rates, and also satisfy the discharge limits at the outlet of the WWTP. Therefore, it was considered to equip the clarifier that was supposed to be operated with an EDI since EDIs can well-increase the treatment capacity of the clarifiers.

Plenty of EDIs has been invented in the last few decades, which are either patented or patent-pending. Several comparative studies were published assessing the benefits and drawbacks of retrofitting conventional clarifiers with different types of EDIs. The opposing-jet nozzle type EDIs, particularly the LA-EDI, was reported to be one of the most superior among their alternatives in the literature, due to the fact that the multiple wing-type outlet nozzles that were configured to create flow impingement by opposing jets can effectively dissipate energy and promote flocculation.

It was considered to retrofit the conventional clarifier -that was supposed to be operated alone with an LA-EDI in order to enable it to operate at doubled inflow conditions. Although it was confirmed that the conventional clarifier experiences no hydrodynamic problems under existing conditions, the conventional clarifier would first be retrofitted with an LA-EDI and simulated under existing conditions to compare and contrast what would change when the clarifier was retrofitted with an EDI.

5.5 Retrofitting Conventional Central-Feed Circular Secondary Clarifiers with Opposing-Jet Type EDIs

Conventional clarifiers do not always equip with an EDI. However, EDIs are useful equipment that facilitates the dissipation of energy and promotes flocculation in the clarifiers. Since opposing-jet nozzle-type EDIs were reported to be superior among their alternatives, the benefits and detriments of retrofitting the conventional clarifier -that was supposed to be operated alone of the investigated WWTP with an opposing-jet nozzle-type EDI were investigated. In this context, the conventional influent well was replaced with an LA-EDI, and the flow and concentration fields were simulated under the existing inflowing conditions. The rheological properties of settling sludge and the effect of stratification on turbulent diffusion were already considered in the simulation. The tranquilizing effect in the influent streams, the promotion of flocculation, the mitigation of density currents, the scouring of sludge blanket, and the short-circuiting of overflow and underflow consequent to the enhanced energy dissipation at the inlet diffusers were explored. The most well-known example of the

opposing-jet nozzle type EDI is LA-EDI. Since there are two configurations of the LA-EDI, both configurations were examined separately.

5.5.1 LA-EDI Type-I

The simulated flow and concentration fields, considering the rheological properties of settling sludge and the effect of stratification on the turbulent diffusion were elucidated in the following headings, for the scenario of retrofitting the existing conventional clarifier with an LA-EDI Type-I.

5.5.1.1 Velocity Flow Field

Although the flow velocity was investigated in 3D, cross-sections in 2D were taken for the sake of illustrating the outputs. The cross-sections of the velocity field in the horizontal and vertical directions were elucidated and elaborated in the following headings.

5.5.1.1.1 Horizontal Cross-Section of the Velocity Flow Field. The velocity field of the investigated scenario at the elevation of the orifices (the elevation where the influent was diffused to the clarification zone) was depicted in Figure 5.13. The energy of the influent must be well-dissipated in the influent well and then orifices should distribute the flow evenly to the clarifier. EDIs are usually utilized for this purpose as a supplementary measure if the influent energy could not be mitigated by conventional influent wells (Ghawi & Kris, 2011).

The satisfying energy dissipation in LA-EDI Type-I can easily be caught the eye. The energy dissipation in LA-EDI Type-I is better both conventional clarifier and LA-EDI Type-II. The velocities are simulated below 0.01 m/s in the clarification zone in LA-EDI Type-I. The essential duty of EDIs is to dissipate energy and distribute the flow evenly at the outlet of the influent well. Figure 5.14 depicts how the opposing jets form at the nozzles of the wing-type outlets, and also the performance of flow impingement, and energy dissipation.

While velocity at the inner nozzles was almost 0.15 m/s, it was almost 0.1 m/s at the outer nozzles and the velocity of the influent plume decreased below 0.025 m/s in LA-EDI Type I.

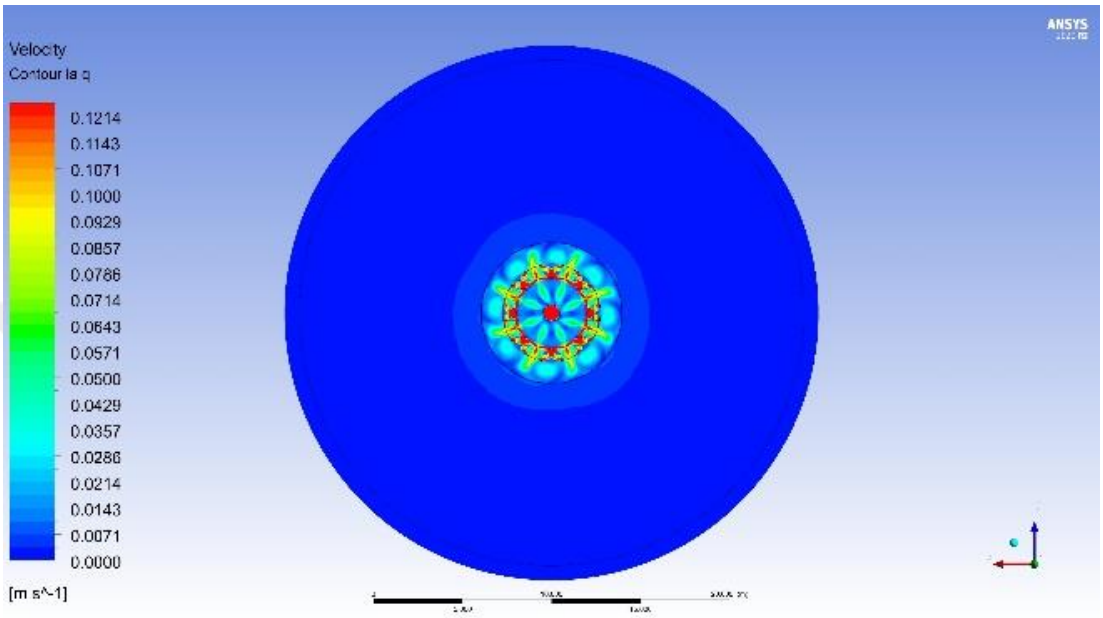


Figure 5.13 The flow velocity contours at the elevation of orifices in the clarifier equipped with only an Standard Type-1 LA-EDI and simulated under existing conditions

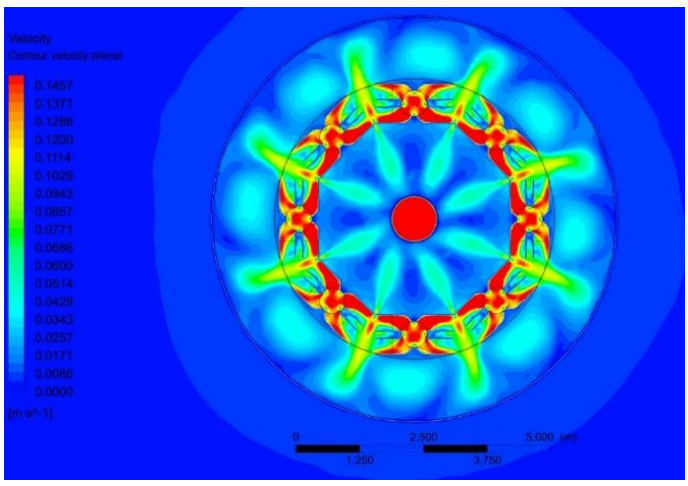


Figure 5.14 The flow velocity contours at the elevation of orifices at which represent the formation of opposing jets in the case where the existing influent well was replaced with an LA-EDI Type-1

The flow field in the clarifier with LA-EDI Type-I was calmer than the conventional clarifier and the clarifier with LA-EDI Type-II. The potential up-flow short-circuiting of sludge in the clarifier with LA-EDI Type-I is expected minimum compared to the conventional clarifier and the clarifier with LA-EDI Type-II.

5.5.1.1.2 *Vertical Cross-Section of the Velocity Flow Field.* Figure 5.15 shows the cross-section of the flow velocity field in the clarifier. It could be observed in Figure 5.15 that sludge abstraction velocity was high, and the velocity profile was not symmetrical as expected in a circular clarifier, since the abstraction was performed from a single point.

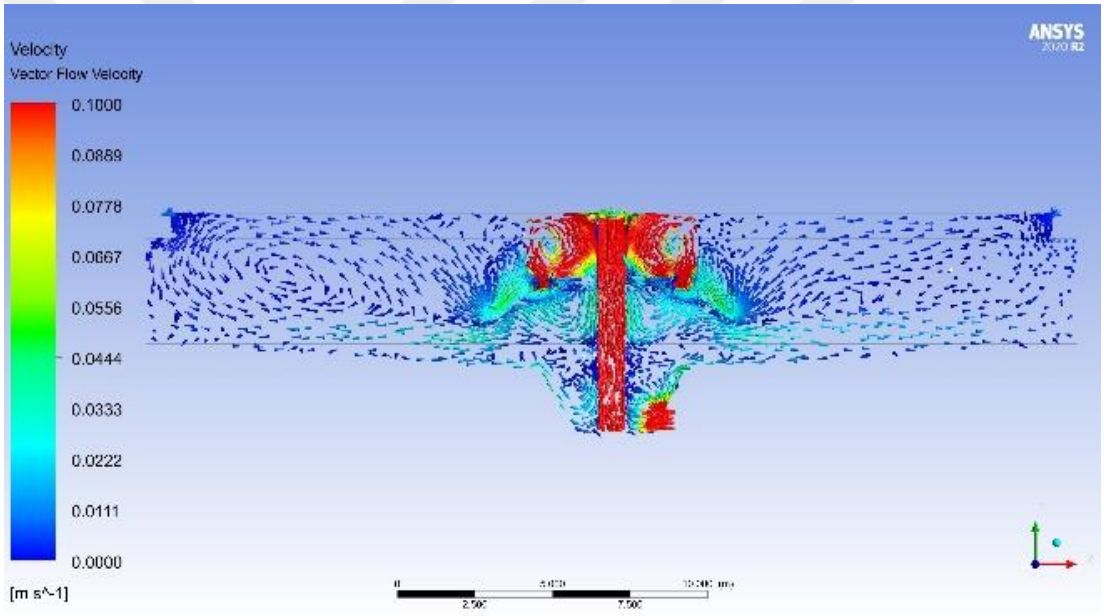


Figure 5.15 Flow velocity vectors in the clarifier equipped with only a Standard Type-1 LA-EDI and simulated under existing conditions

5.5.1.2 Solids Settling Velocity

The solids settling velocity contours, which were modeled using the Takács function (1991), were represented in Figure 5.16.

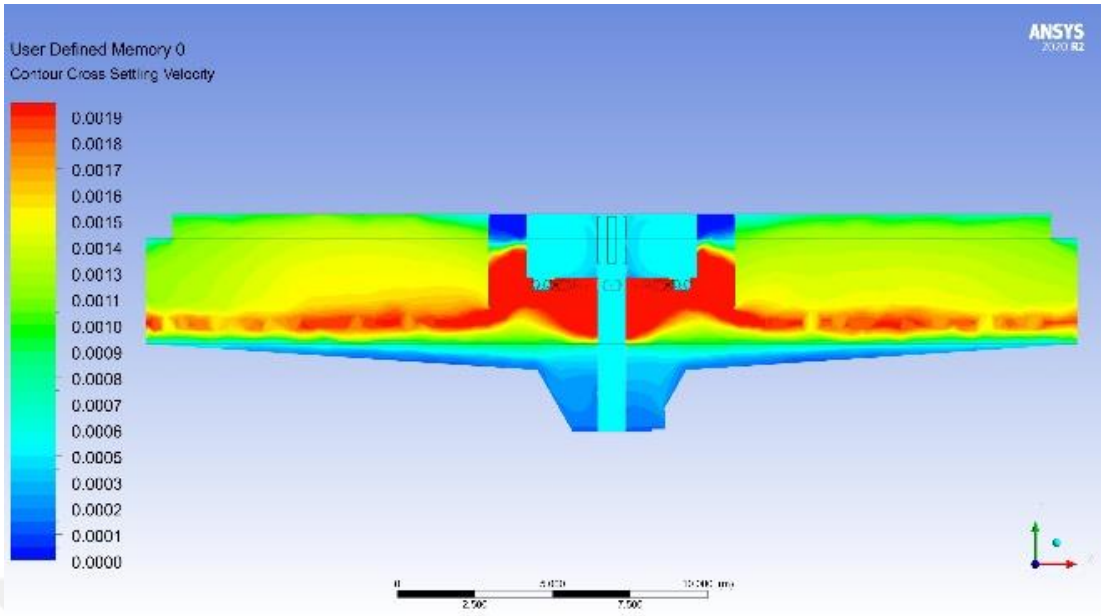


Figure 5.16 Solids settling velocity contours (m/s) in the clarifier equipped with only a Standard Type-1 LA-EDI and simulated under existing conditions

The LA-EDI Type-1 has enabled the most favorable conditions for sedimentation, since the energy was well-dissipated in this clarifier. This finding also supported that flocculation wells facilitate sedimentation conditions in clarifiers.

5.5.1.3 Solids Concentration

Figure 5.17 represents the solids concentration in the clarifier. Although the settling performance of clarifiers with an LA-EDI was regarded as good (Figure 5.16), the sludge thickening performance was found worse than the original clarifier (Figure 5.17).

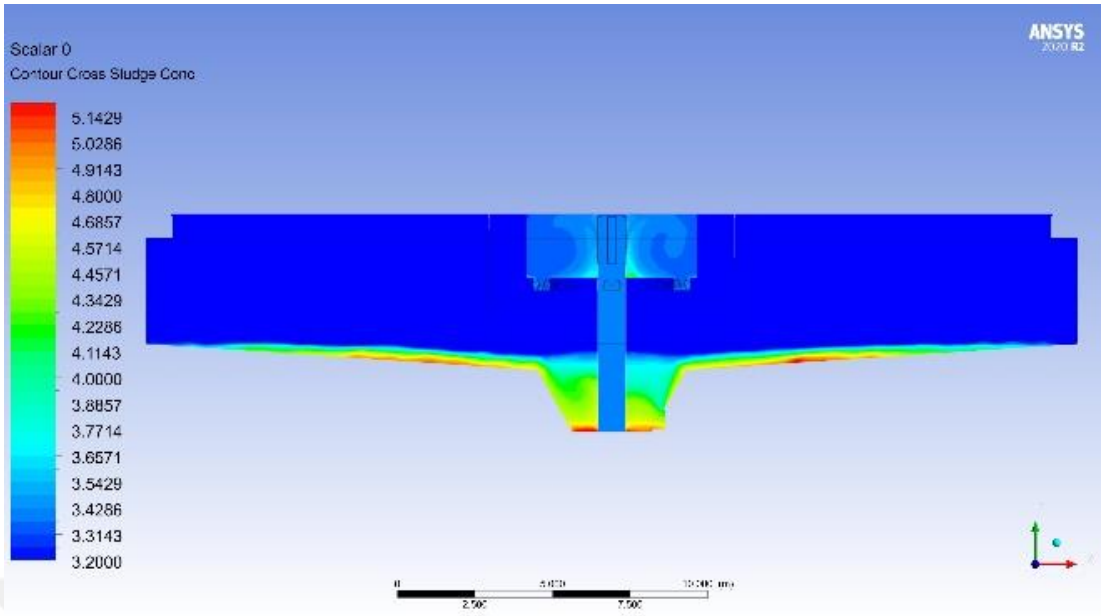


Figure 5.17 Solids concentration contours (kg/m³) in the clarifier equipped with only a Standard Type-1 LA-EDI and simulated under existing conditions

The solids concentration difference across the diameter of the sludge outlet was well-depicted in Figure 5.17. Moreover, while the withdrawn solids concentration was 5.2 kg/m³ in the original clarifier, it was decreased down to 4.6 kg/m³ in the clarifier equipped with only an LA-EDI. This difference could be addressed as deformation of the sludge blanket, not only due to the LA-EDI type inlet structure, but also due to the non-uniform withdrawal of sludge from the clarifier. Due to the fact that the sludge was withdrawn from a single point, either the sludge would be withdrawn from a pipe in larger dimensions, or the discharge velocity would be increased to withdraw the required volume. This also confirmed that sludge withdrawal from a single point promoted turbulence within the clarifier. In order to mitigate this problem, a new outlet pipe must be designed that supports the uniform abstraction of sludge from the sludge hopper.

The change in the solids concentration during the abstraction of sludge from the beginning of the simulation was depicted in Figure 5.18.

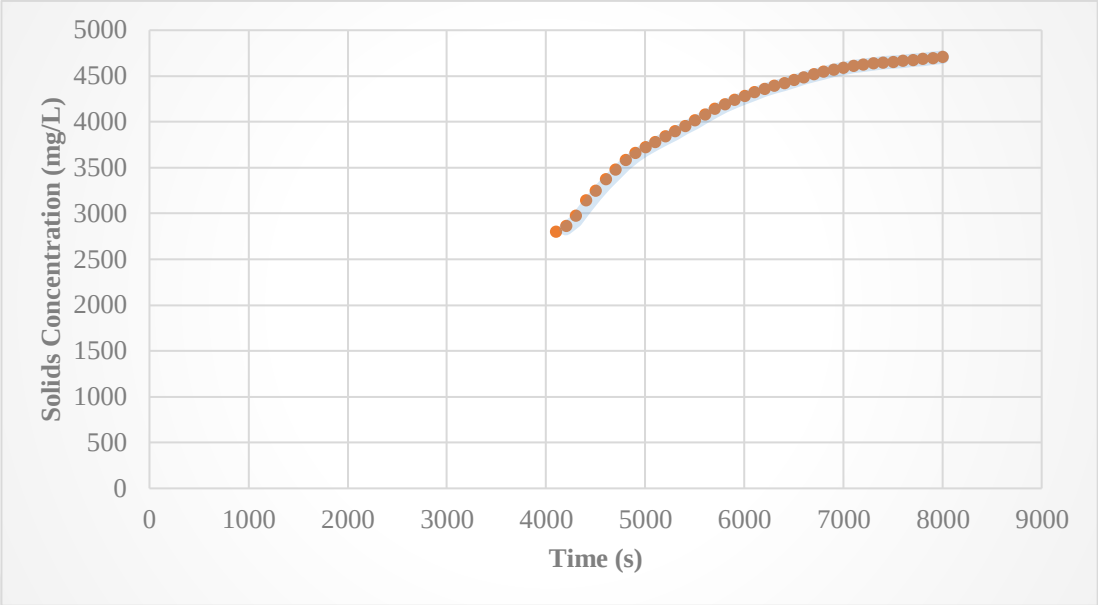


Figure 5.18 The change of solids concentration drawn-off from the clarifier equipped with a Standard Type-1 LA-EDI

While the solids concentration abstracted from the conventional clarifier was found to have reached the fourth phase of the sedimentation phase (Figure 5.11), the abstracted solids concentration from the clarifiers with EDIs were found to have reached the third phase of the sedimentation phase, which is transition. Therefore, the thickened sludge in the clarifiers with EDIs was not as concentrated as in the conventional clarifiers.

5.5.1.4 Streamlines

Figure 5.19 represents the streamlines that occurred during sludge withdrawal.

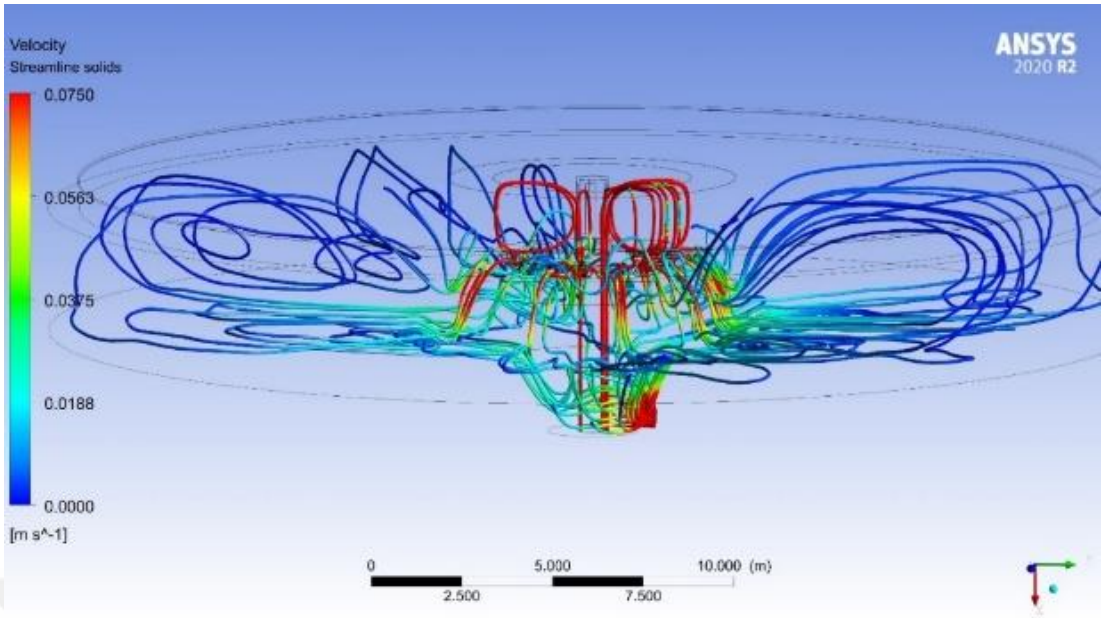


Figure 5.19 Streamlines simulated in the clarifier equipped with only a Standard Type-1 LA-EDI and simulated under existing conditions

The streamlines were displayed arbitrarily scattered within clarifiers with LA-EDI, which means not only settled sludge but also clarified water with low solid content is abstracted from the sludge outlet. Besides, if the reader follows the red noodles in Figure 5.19, they were mostly moved within the influent well, indicating that the influent was not retained in the clarifier sufficiently to thicken, and it discharged right after it was diffused in the clarification zone. This causes low solids concentration in the abstracted sludge. This phenomenon was entitled short-circuiting into the underflow; however, it has not been discussed in detail in the literature (Grau & Aquanova, 2022; Esler J. K., 2022). It was uncovered that, on one hand, the EDIs prevent short-circuiting of overflow, on the other hand, they facilitate short-circuiting of the underflow.

5.5.2 LA-EDI Type-II

The simulated flow and concentration fields, considering the rheological properties of settling sludge and the effect of stratification on the turbulent diffusion were elucidated in the following headings, for the scenario of retrofitting the existing conventional clarifier with an LA-EDI Type-II.

5.5.2.1 Velocity Flow Field

Although the flow velocity was investigated in 3D, cross-sections in 2D were taken for the sake of illustrating the outputs. The cross-sections of the velocity field in the horizontal and vertical directions were elucidated and elaborated in the following headings.

5.5.2.1.1 Horizontal Cross-Section of the Velocity Flow Field. The velocity field of the investigated scenario at the elevation of the orifices (the elevation where the influent was diffused to the clarification zone) was depicted in Figure 5.20. As aforementioned, the energy of the influent must be well-dissipated in the influent well and then orifices should distribute the flow evenly to the clarifier. EDIs are usually utilized for this purpose as a supplementary measure if the influent energy could not be mitigated by conventional influent wells (Ghawi & Kris, 2011).

The energy dissipation in LA-EDI Type-2 is better compared to the conventional clarifier, but worse than in LA-EDI Type-1. There are regions, where flow velocity varies between 0.015 and 0.020 m/s in the clarification zone in LA-EDI Type-2.

The essential duty of EDIs is to dissipate energy and distribute the flow evenly at the outlet of the influent well. Figure 5.21 depicts how the opposing jets form at the nozzles of the wing-type outlets, and also the performance of flow impingement, and energy dissipation. The velocity of the influent plume was around 0.1 m/s in LA-EDI Type-II.

Although the energy dissipated well enough at the opposing-jet nozzles in LA-EDI Type-2, the remaining energy could not be mitigated by the baffle lowered from the periphery of the influent well, and the plume exited from the influent-well-orifices travelled not only in the horizontal direction (as it was in the conventional clarifier), but also climbed in the vertical direction. In such cases, the clarifiers are usually equipped with baffles at the side wall below (such as Crosby-type weirs) the effluent weir to mitigate up-flow short-circuiting of sludge.

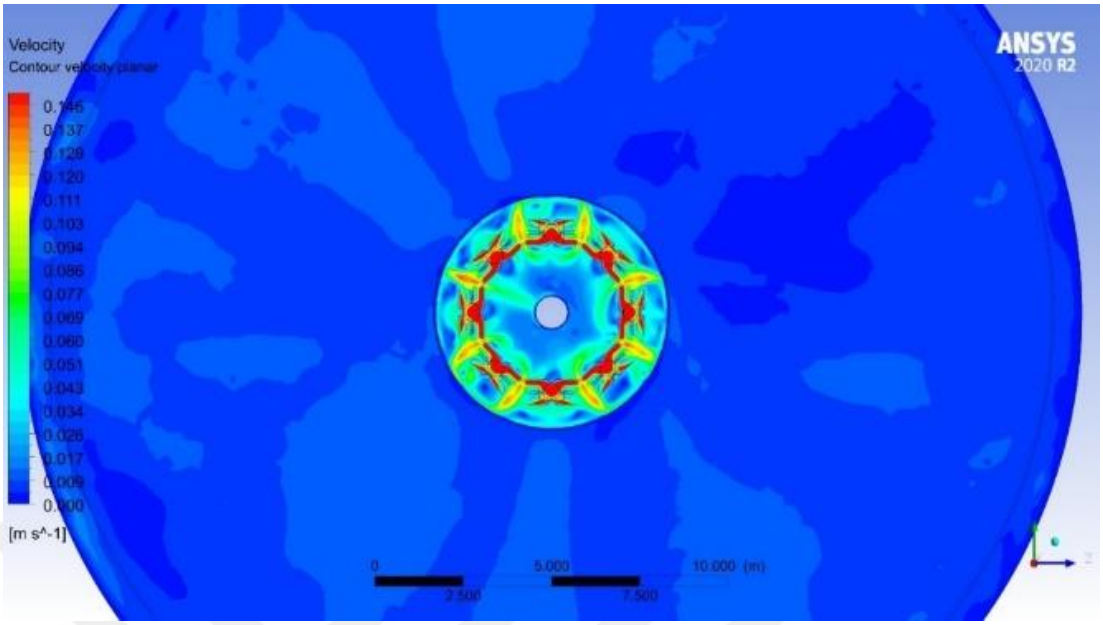


Figure 5.20 The flow velocity contours at the elevation of orifices in the clarifier equipped with only an Standard Type-2 LA-EDI and simulated under existing conditions

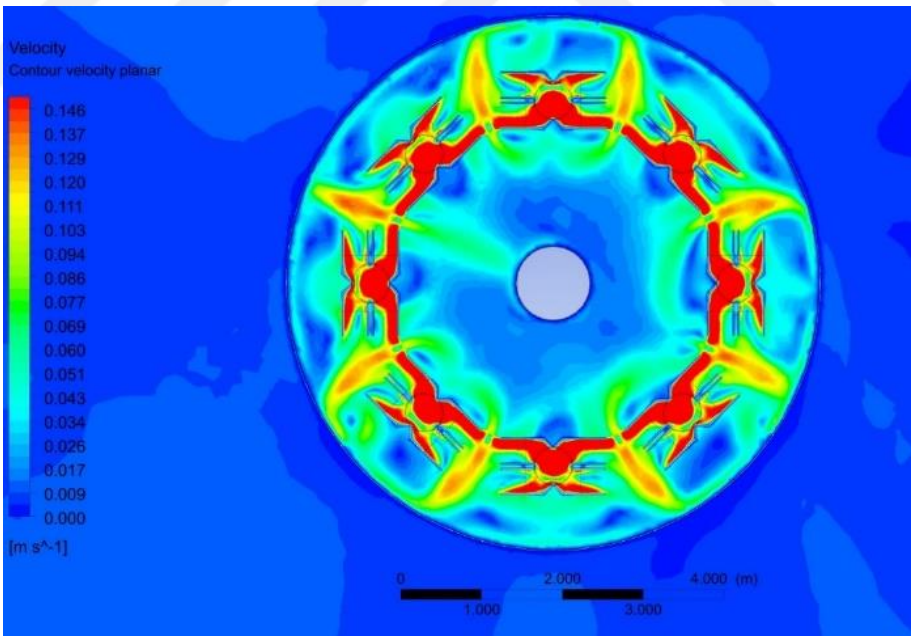


Figure 5.21 The flow velocity contours at the elevation of orifices at which represent the formation of opposing jets in the case where the existing influent well was replaced with an LA-EDI Type-2

5.5.2.1.2 Vertical Cross-Section of the Velocity Flow Field. Figure 5.22 shows the cross-section of the flow velocity field in the clarifier. It could be observed in Figure 5.22 that sludge abstraction velocity was high, and the velocity profile was not symmetrical as expected in a circular clarifier, since the abstraction was performed from a single point.

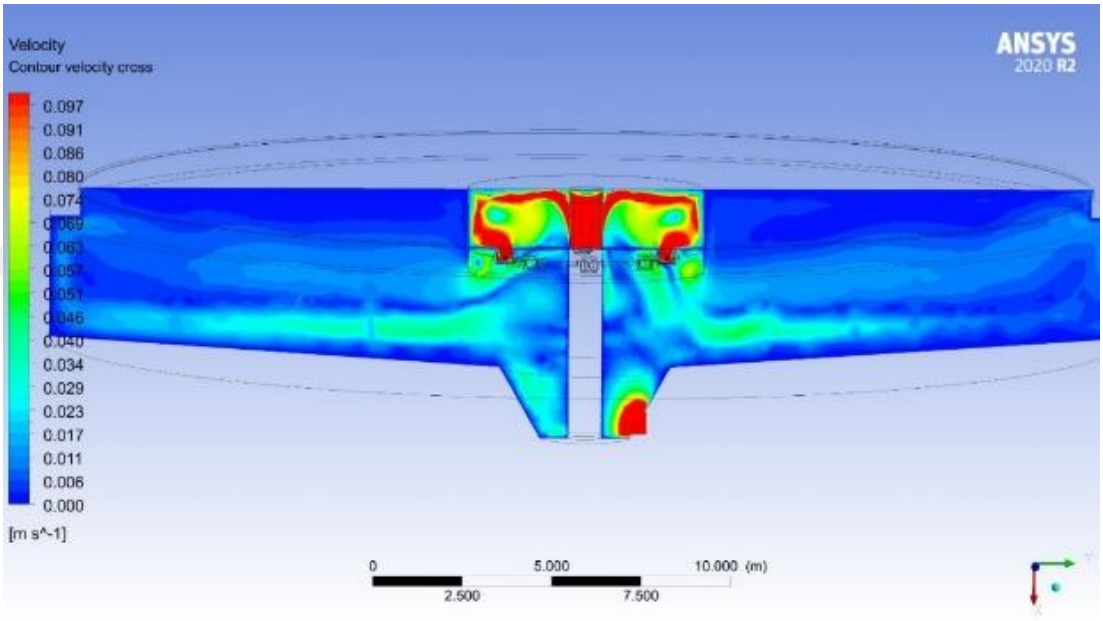


Figure 5.22 Flow velocity contours in the clarifier equipped with only a Standard Type-2 LA-EDI and simulated under existing conditions

5.5.2.2 Solids Settling Velocity

The solids settling velocity contours, which were modeled using the Takács function (1991), were represented in Figure 5.23.

The settling velocity values were found maximum at the plume existing the influent well (or nozzles), as expected. The plume exiting the influent well dispersed in a skirt shape in the vertical direction in the clarifier with LA-EDI Type-2, since the lowered baffle below the periphery of the influent well was short and did not bear a function of a flocculation well. Moreover, the plume was found dispersed in a conical shape in the horizontal direction both in the conventional clarifier and the clarifier with LA-EDI Type-2, due to the fact that the kinetic energy was not sufficiently dissipated.

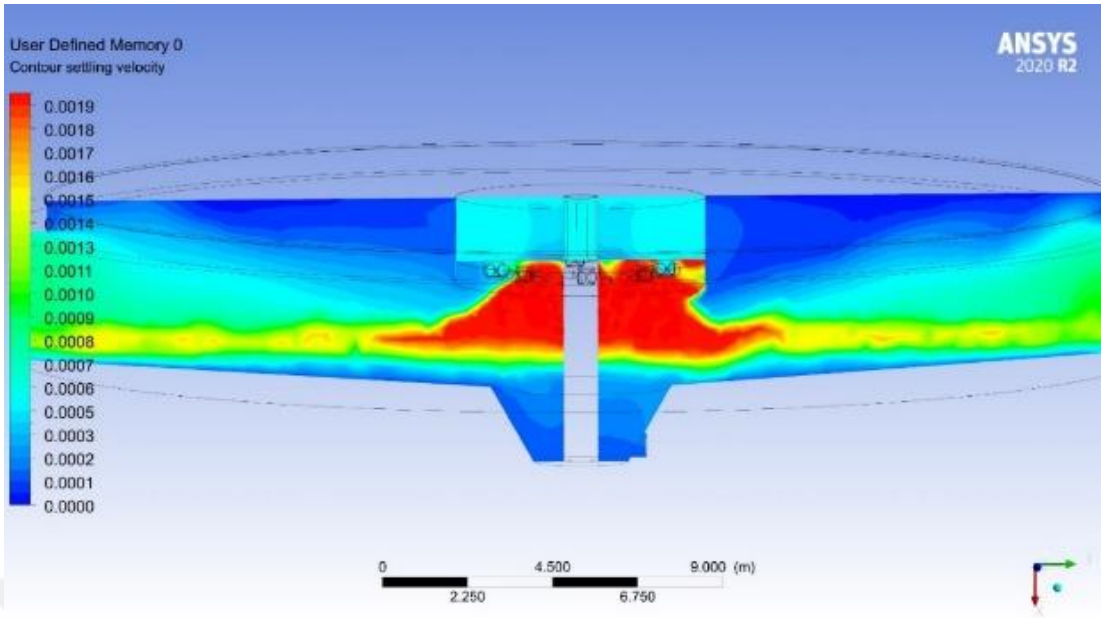


Figure 5.23 Solids settling velocity contours (m/s) in the clarifier equipped with only a Standard Type-2 LA-EDI and simulated under existing conditions

It could be also observed in Figure 5.23 that the plume exiting the influent well dispersed in a skirt shape in the vertical direction in the clarifier with LA-EDI Type-2 was not symmetrical, as expected. The problem was derived due to the turbulence within the clarifier as a consequence of abstracting sludge from a single point.

5.5.2.3 Solids Concentration

Figure 5.24 represents the solids concentration in the clarifier. The solids concentration difference across the diameter of the sludge outlet was well-depicted on the solids concentration profile in Figure 5.24. This difference could be addressed as a sort of deformation of sludge, resulted not exactly due to the LA-EDI type inlet structures, but also from the non-uniform abstraction of sludge from the clarifier. Due to the fact that the sludge is abstracted from a single point, consequently, the sludge is abstracted from a pipe in larger dimensions, and discharge velocity is high to discharge the required volume.

The change in the solids concentration during the abstraction of sludge from the beginning of the simulation was depicted in Figure 5.25.

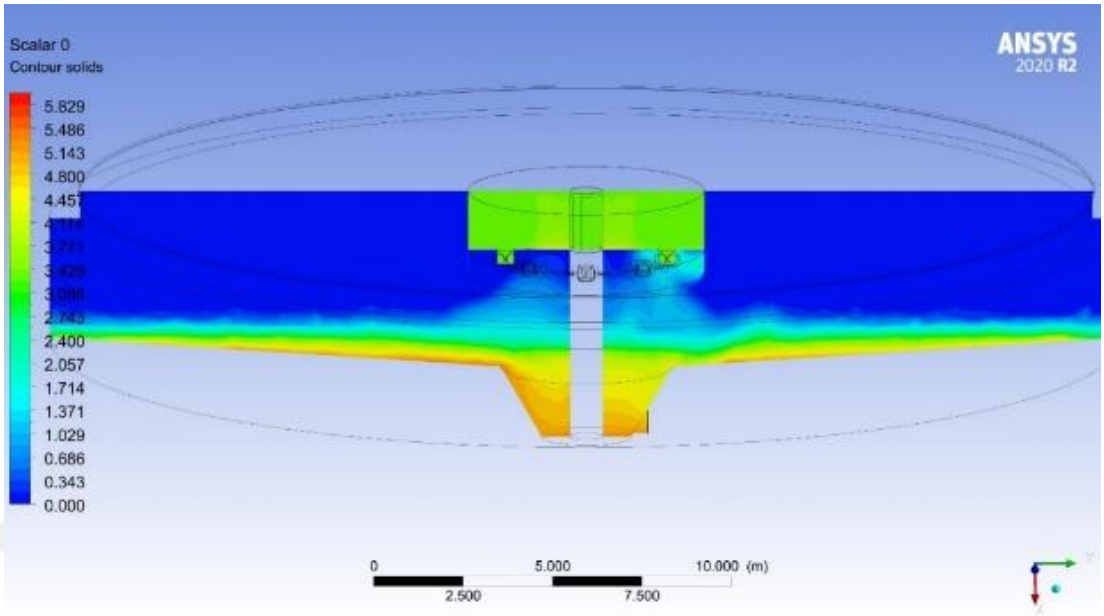


Figure 5.24 Solids concentration contours in the clarifier equipped with only a Standard Type-2 LA-EDI and simulated under existing conditions

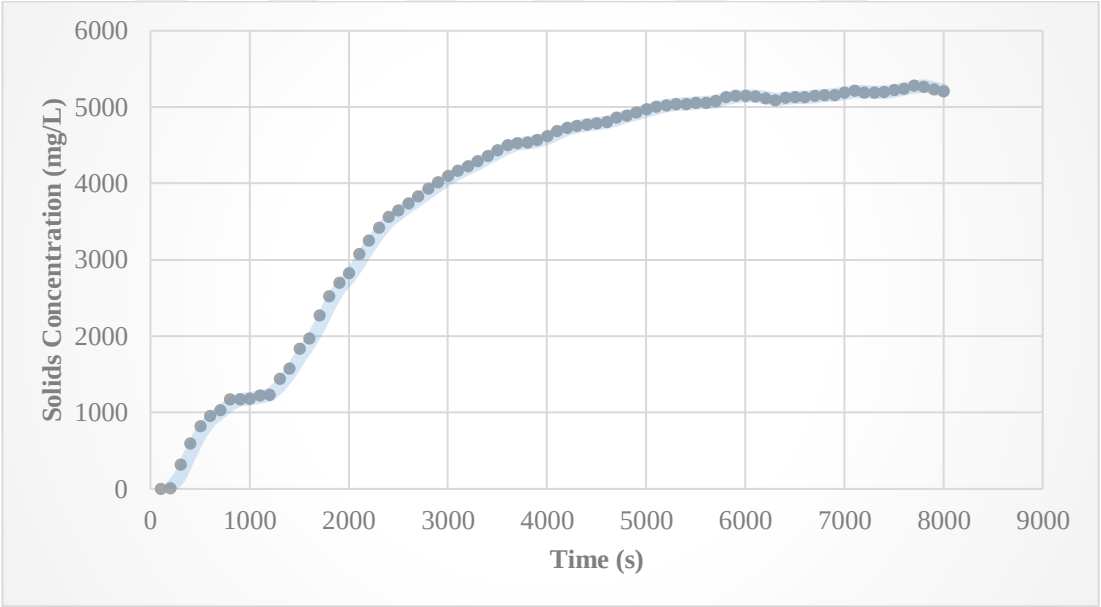


Figure 5.25 The change of solids concentration drawn-off from the clarifier equipped with a Standard Type-2 LA-EDI

While the solids concentration abstracted from the conventional clarifier was found to have reached the fourth phase of the sedimentation phase (Figure 5.11), the

abstracted solids concentration from the clarifiers with EDIs were found to have reached the third phase of the sedimentation phase, which is transition. Therefore, the thickened sludge in the clarifiers with EDIs was not as concentrated as in the conventional clarifiers.

5.5.2.4 Streamlines

Figure 5.26 represents the streamlines that occurred during sludge abstraction. As aforementioned, the streamlines were displayed arbitrarily scattered within clarifiers with LA-EDI, addressing that clarified water with low solid content is abstracted from the sludge outlet along with the settled sludge.

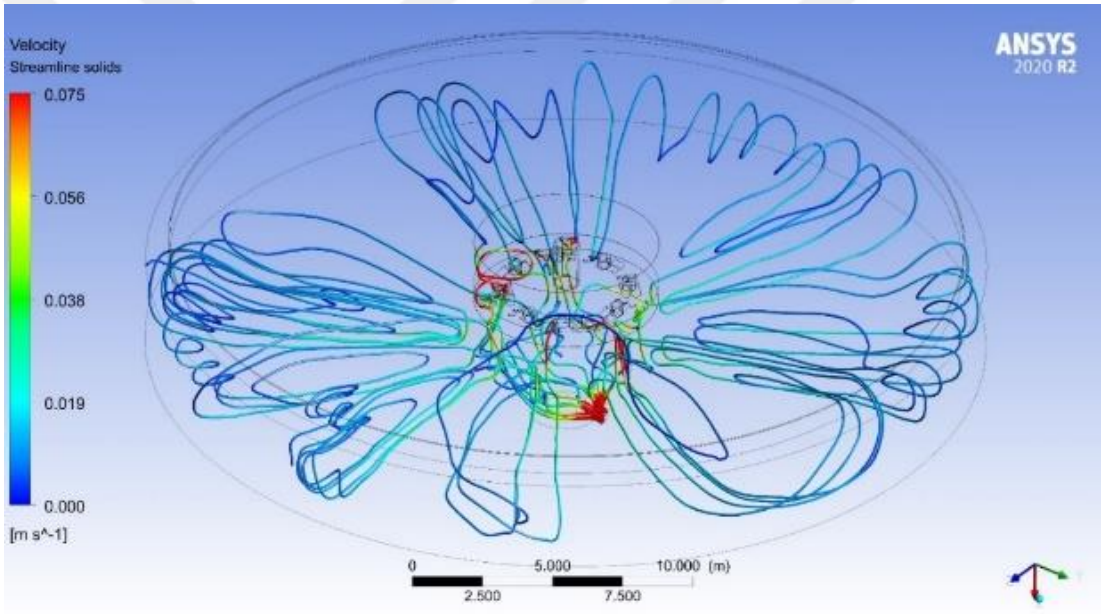


Figure 5.26 Streamlines simulated in the clarifier equipped with only a Standard Type-2 LA-EDI and simulated under existing conditions

5.5.3 Comprehension of Results

This investigation verified that equipping clarifiers with an EDI increases the capacity of the clarifiers and enables operating clarifiers with higher overflow rates. It was uncovered that, on one hand, the EDIs prevent short-circuiting of overflow, on the other hand, they facilitate short-circuiting of the underflow. It was demonstrated that the sludge blankets could be easily deformed in clarifiers that were equipped with

EDIs, particularly if the sludge is drawn off from a single point, although it was not a problem in conventional clarifiers. It was deduced that the observed problems in clarifiers equipped with EDIs might be mitigated if a new design of the draw-off pipe was invented which can withdraw the sludge from multiple points and maintain uniform withdrawal of sludge from the sludge hopper. In this context, simulations would be performed to investigate the impact of the sludge draw-off pipe on the clarification performance and hydrodynamics inside the clarifier; and the design of draw-off pipes would be retrofitted to mitigate the underflow short-circuiting and enhance the treatment performance of clarifiers.

As the benefits and drawbacks of retrofitting conventional clarifiers with EDIs, particularly the effects on the hydrodynamics, were recognized, the EDI-equipped conventional clarifier would now be simulated under doubled inflow conditions in order to assess whether retrofitting the conventional clarifier with an EDI was a competent measure to operate it at high overflow and sludge loading rates.

In the case of idling one of the two clarifiers, the clarifier -that was supposed to be operated alone equipped with an LA-EDI would be operated at doubled inflow conditions. In other words, the required treatment capacity increase was 100%. However, the reported capacity increase so far through equipping a clarifier with an LA-EDI was 50% at maximum (CPE Services Inc., 2022). The other option would be equipping the clarifier with a multilayer-type EDI, particularly the MEDIC, instead of an LA-EDI. In such cases, the reported capacity increase was only 30% at maximum (Hydrosims, 2022). In this regard, the conditions limiting the further capacity increase were investigated for the diagnosis and prognosis of the problem.

5.6 Two Novel Sludge Draw-Off Pipe Designs for Central-Feed Circular Secondary Clarifiers Retrofitted with Different Types of EDIs

Short-circuiting is an essential phenomenon in secondary clarifiers. Although there are two routes of short-circuiting, up-flow (or effluent) short-circuiting comes first to mind, which can be explained shortly as the escape of solids by overflowing the weirs. There is another short-circuiting route at the sludge outlet; however, not considerable attention is given since it is not as visible as the up-flow short-circuiting. The underflow short-circuiting is the discharge of the supernatant along with the thickened sludge from the draw-off pipe. This phenomenon is mainly encountered in clarifiers equipped with EDIs. Since EDIs can well-dissipate the energy of larger influent volumes, clarifiers equipped with EDIs are usually operated at higher treatment capacities than conventional clarifiers. As the influent volume of a clarifier increase, the outflow volume increases accordingly, however, the capacity of a conventional draw-off pipe is limited and cannot convey the thickened sludge at high capacities; consequently, the sludge blanket is deformed and solids are withdrawn from the draw-off pipe below the solicited concentration. Therefore, retrofitting the design of draw-off pipes was hypothesized to mitigate the underflow short-circuiting and enhance the treatment performance of clarifiers. In this context, two novel sludge draw-off pipe (snail- and spiral-shaped) designs were drafted and their underflow short-circuiting mitigation performance was investigated in clarifiers equipped with two different types of EDIs (multilayer- and opposing jet-type).

The flow and concentration fields were simulated using CFD tools under doubled inflow conditions to assess the feasibility of doubling the treatment capacity of the clarifier that was supposed to be operated alone in the case of idling one of the two clarifiers. The rheological properties of settling sludge and the effect of stratification on turbulent diffusion were already considered in the simulation. The tranquilizing effect in the influent streams, the promotion of flocculation, the mitigation of density currents, the scouring of sludge blanket, and the short-circuiting of overflow and underflow, consequent to the enhanced energy dissipation at the inlet diffusers were also explored.

5.6.1 Velocity Flow Field

Although the flow velocity was investigated in 3D, cross-sections in 2D were taken for the sake of illustrating the outputs. The cross-sections of the velocity field in the horizontal and vertical directions were elucidated and elaborated in the following headings.

5.6.1.1 Horizontal Cross-Section of the Velocity Flow Field

The velocity fields for the investigated case at the elevation of the orifices (the elevation where the influent was diffused to the clarification zone) were depicted in Figure 5.27, Figure 5.28, and Figure 5.29.

The influent volume was doubled in the investigated cases compared to the original clarifier. Both MEDIC and LA-EDI satisfyingly dissipated the influent energy of the doubled inflow. The flow through MEDIC was simulated as very calm below 30 mm/s until it reached the flocculation well wall; and, the flow velocity was found at around 50 mm/s as it collided with the flocculation well wall. Figure 5.27 and Figure 5.28 were depicted very well how the opposing jets were formed at the nozzles of the wing-type outlets in LA-EDI, and also the performance of flow impingement, and energy dissipation.

In LA-EDI simulated under doubled inflow conditions (Figure 5.27 and Figure 5.28), while the flow velocity at the inner and outer nozzles was slightly higher than 300 mm/s, and the flow velocity decreased below 300 mm/s after opposing jet impingement. However, in LA-EDI simulated under existing conditions (Figure 5.14), while the flow velocity at the inner and outer nozzles was almost 150 mm/s and 200 mm/s, the resultant flow velocity decreased below 100 mm/s after opposing jet impingement. The outflow velocities were found acceptable considering the design criterion (Tchobanoglous, Burton, & Stensel, 2003).

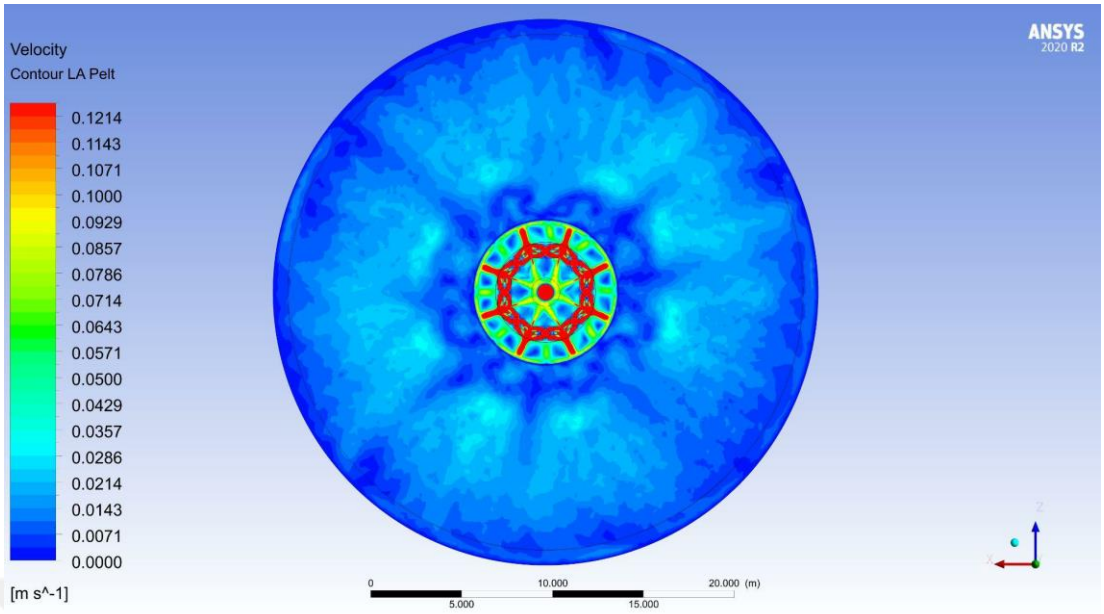


Figure 5.27 The flow velocity contours at the elevation of orifices in the clarifier equipped with an LA-EDI, and a spiral-shaped draw-off pipe and simulated for doubled inflow conditions.

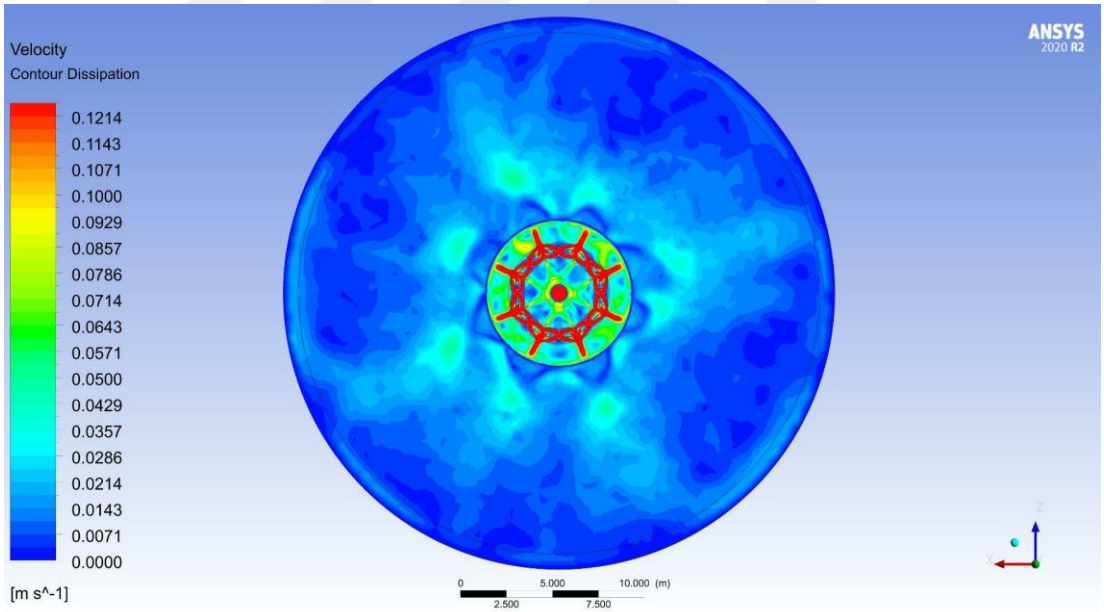


Figure 5.28 The flow velocity contours at the elevation of orifices in the clarifier equipped with an LA-EDI, and a snail-shaped draw-off pipe and simulated under doubled inflow conditions.

Although no flocculation well existed in the original clarifier (Figure 5.7, Figure 5.8), the clarifiers simulated in the investigated cases were equipped with flocculation wells, because flocculation wells are essential elements of EDIs (Tchobanoglous,

Burton, & Stensel, 2003). They well-facilitated the dissipation of the remaining influent energy before entering the clarification zone.

The flow velocities were simulated very calm below 25 cm/s in the clarification zone in the clarifier equipped with a MEDIC (Figure 5.29). While the flow velocity in the clarifier equipped with an LA-EDI, and a spiral-shaped draw-off pipe was found below 25 cm/s, it was found around 35 cm/s in the clarifier equipped with an LA-EDI, and a snail-shaped draw-off pipe. Besides, the flow velocities in the clarification zone were found to be simulated more uniformly dispersed across the perimeter in the clarifier equipped with an LA-EDI, and a spiral-shaped draw-off pipe. This finding pointed out that the draw-off method impacted the flow field in the clarification zone. It could be also said that the energy dissipation of MEDIC was better than the LA-EDI since the flow velocities were found calmer in MEDIC than in LA-EDI.

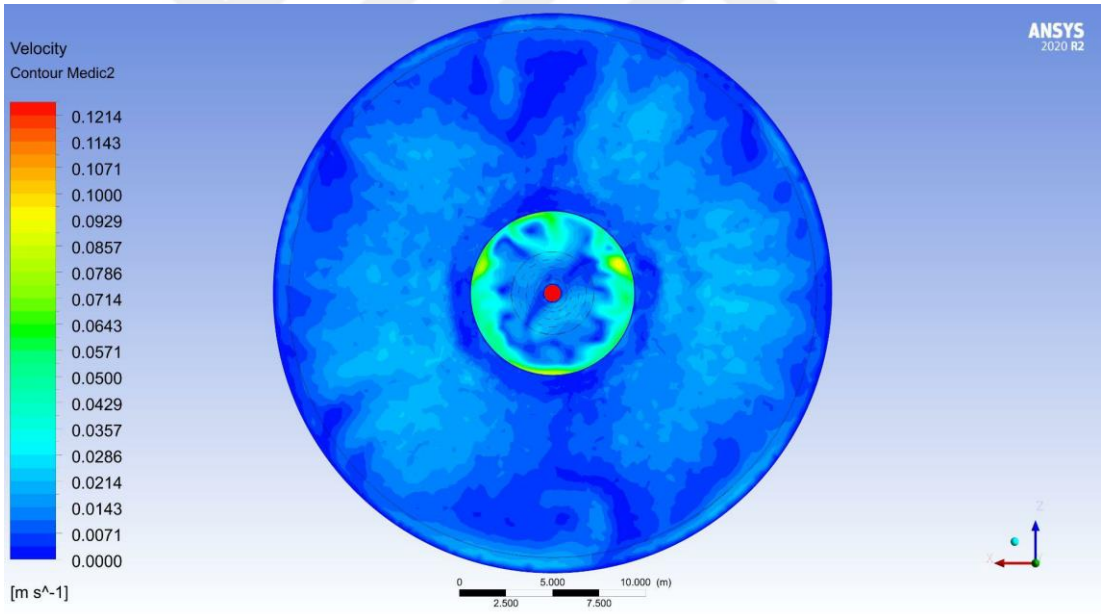


Figure 5.29 The flow velocity contours at the elevation of orifices in the clarifier equipped with a MEDIC, and a snail-shaped draw-off pipe and simulated under doubled inflow conditions.

5.6.1.2 Vertical Cross-Section of the Velocity Flow Field

Figure 5.30, Figure 5.31 and Figure 5.32 represent the cross-section of the flow velocity field in the clarifiers equipped with an EDI, and a novel draw-off pipe and simulated for doubled inflow conditions.

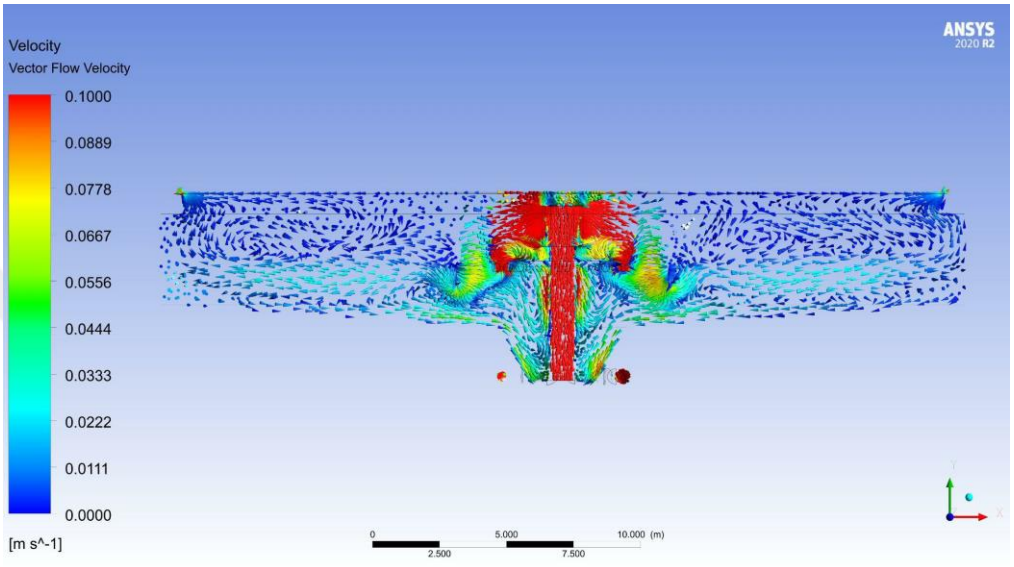


Figure 5.30 Flow velocity vectors in the clarifier equipped with an LA-EDI, and a spiral-shaped draw-off pipe and simulated for doubled inflow conditions

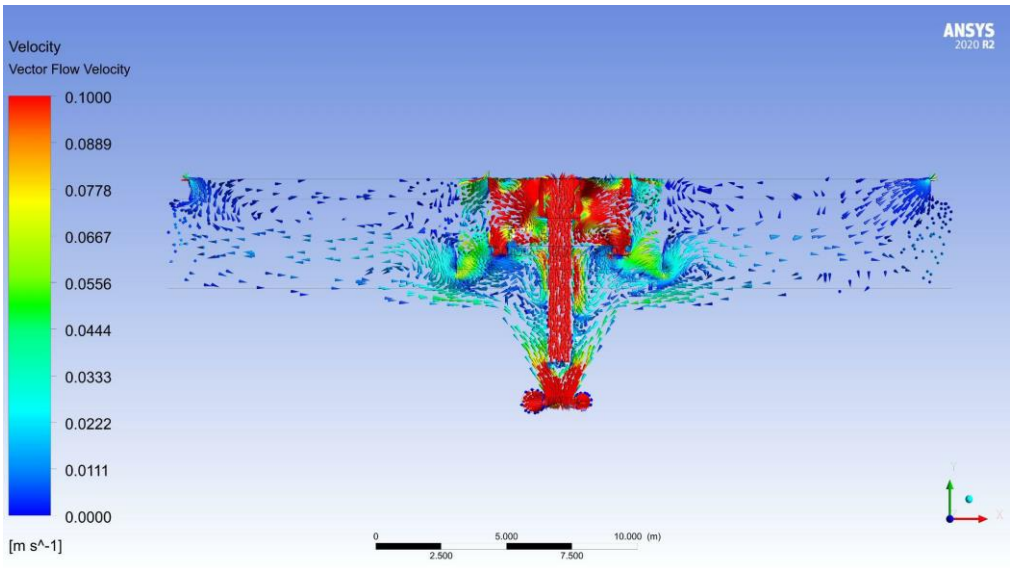


Figure 5.31 Flow velocity vectors in the clarifier equipped with an LA-EDI, and a snail-shaped draw-off pipe and simulated for doubled inflow conditions

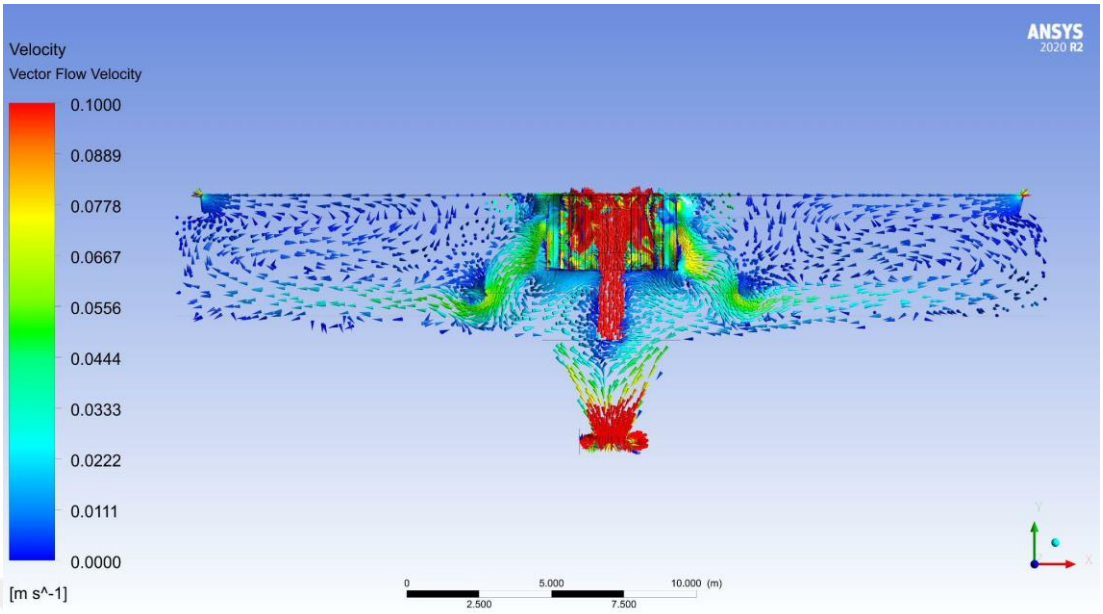


Figure 5.32 Flow velocity vectors in the clarifier equipped with a MEDIC, and a snail-shaped draw-off pipe and simulated under doubled inflow conditions

Although the flow was simulated as turbulent in the flocculation zone, it was found well-dissipated in the clarification zone in the clarifier equipped with a MEDIC, and a spiral-shaped draw-off pipe (Figure 5.32). It could be also noted that the flow field in the clarifier equipped with a MEDIC was simulated as calm as it was in the original clarifier, although the influent volume was doubled (Figure 5.8 and Figure 5.32). This could also be said for the clarifiers equipped with an LA-EDI; their flow field was almost simulated as calm as in the original clarifier (Figure 5.8 and Figure 5.30). This comparison could not be done for the clarifiers simulated with a MEDIC or an LA-EDI, since both yielded enough good conditions for clarification and their difference could not be differentiated (Figure 5.8 and Figure 5.30).

As it was also depicted in Figure 5.30 and Figure 5.31, the opposing jet nozzles were found to be very effective in dissipating energy. Although the flow velocities of the plumes, which were formed after the opposing jet impingement, were found at around 100 mm/s, the flow velocity of the plumes was found to be well-plunged while flowing in the flocculation zone, and the remaining energy was mitigated as the plume collided with the flocculation well wall (Figure 5.30 and Figure 5.31). In the case of clarifier equipped with an LA-EDI, and a spiral-shaped draw-off pipe, the plume

surpassed beneath the flocculation well wall and glided in the horizontal direction and the flow velocity decreased down to 10 mm/s before it reached the side wall and then climbed upward to the weirs (Figure 5.30). However, the plume followed the same path but was calmer in the case of the clarifier equipped with an LA-EDI, and a spiral-shaped draw-off pipe (Figure 5.31). Although the flow velocity in the clarification zone was found calm, the clarifiers could be also equipped with baffles (such as Crosby-type weirs) at the side wall below the effluent weir to divert the climbing plume in the horizontal direction to increase the distance of the flow path as an extra measure for up-flow short-circuiting, since the clarifiers were designed to be operated under high-rate conditions. It was also worth noting that small eddies were developed between the influent well and the sludge hopper, although the nozzles divert the plume to the outbound direction, some of the flow drain inwards direction, because the nozzles were ending with half-cut pipes. This problem was not observed when the clarifier was simulated with the design flow (Figure 5.15).

Although uniformity is being sought during inflow distribution and effluent laundering along the perimeter of the circular central-feed secondary clarifiers, this concept is neglected during sludge draw-off, since the sludge has to be discharged from a single point. Consequently, the flow velocity profile should be not symmetrical in the sludge hopper, as it was well-depicted in Figure 5.8 for the conventional clarifier. However, the discharge from the bottom outlet is usually two-to-three times more than the weirs. This could be one of the facts that facilitate the rotational currents occurring in some clarifiers; however, this problem was not extensively researched in the scope of this article. However, the proposed draw-off pipes have yielded almost uniform flow velocity profiles in the sludge hopper (Figure 5.31, Figure 5.30).

5.6.2 Solids Settling Velocity

Figure 5.33, Figure 5.34, and Figure 5.35 represent the solids settling velocity contours in the clarifiers equipped with an EDI, and a novel draw-off pipe, which are simulated under doubled inflow conditions.

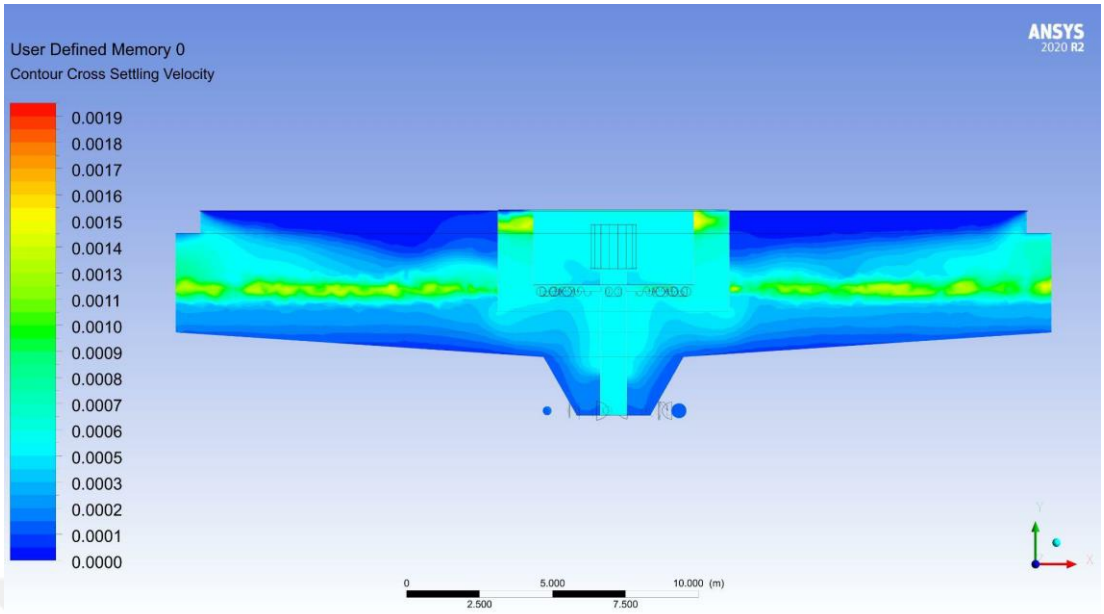


Figure 5.33 Solids settling velocity contours (m/s) in the clarifier equipped with an LA-EDI, and a spiral-shaped draw-off pipe and simulated for doubled inflow conditions.

The solids settling velocities in the clarifiers simulated for the doubled inflow volume were found lower than the original clarifier, as expected, however, the clarifiers still perform well enough, due to the fact that flocculation wells facilitate sedimentation conditions in clarifiers. The small eddies occurred between the influent well and the sludge hopper in the clarifiers equipped with an LA-EDI. The eddies prohibited the solids to be settled in this region (Figure 5.33, Figure 5.34), due to the fact that the kinetic energy was not sufficiently dissipated; this was not observed in the clarifier equipped with MEDIC (Figure 5.35). Among the three modifications, the clarifier with MEDIC has enabled the most favorable conditions for sedimentation, since the energy was well-dissipated in this clarifier.

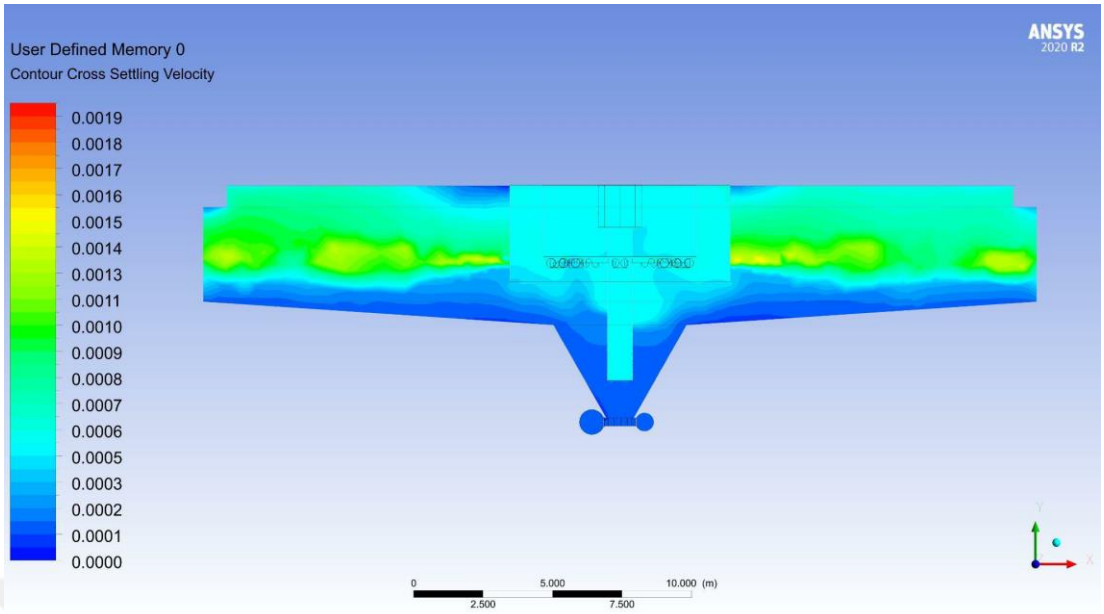


Figure 5.34 Solids settling velocity contours (m/s) in the clarifier equipped with an LA-EDI, and a snail-shaped draw-off pipe and simulated for doubled inflow conditions.

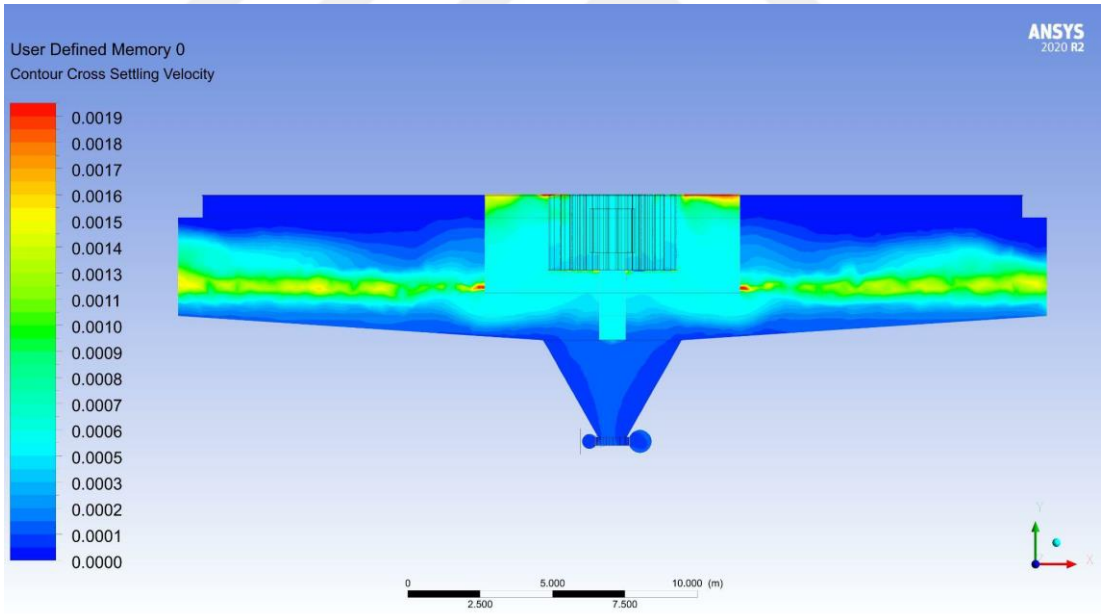


Figure 5.35 Solids settling velocity contours (m/s) in the clarifier equipped with a MEDIC, and a snail-shaped draw-off pipe, and simulated under doubled inflow conditions.

5.6.3 Solids Concentration

Figure 5.36, Figure 5.37, and Figure 5.38 represent the solids concentration in the clarifiers equipped with an EDI, and a novel draw-off pipe, which are simulated under doubled inflow conditions.

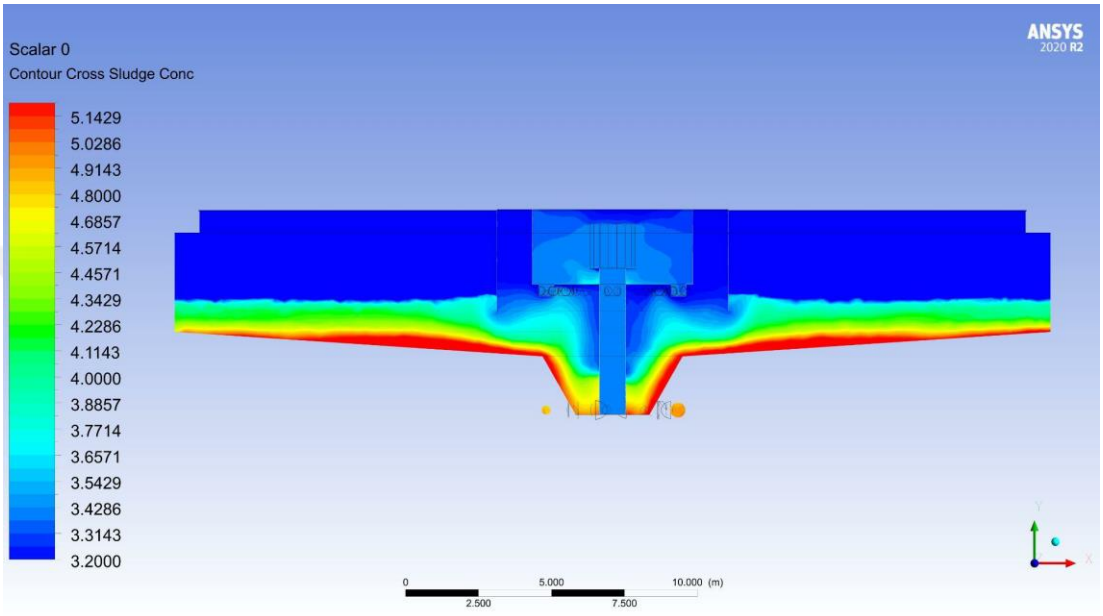


Figure 5.36 Solids concentration contours in the clarifier equipped with an LA-EDI, and a spiral-shaped draw-off pipe and simulated for doubled inflow conditions.

The clarifiers that were demanded to be operated at doubled inflow volume, particularly the clarifier equipped with an LA-EDI, could not yield well-thickened sludge (Figure 5.36, Figure 5.37). This was due to the small eddies occurring between the influent well and the sludge hopper which facilitated scouring of the sludge blanket in the clarifiers equipped with an LA-EDI. Since the eddies were closer to the draw-off pipes in the clarifier equipped with spiral-shaped draw-off pipe than in the clarifier equipped with snail-shaped draw-off pipe, the withdrawn solids concentration was lower in the clarifier equipped with spiral-shaped draw-off pipe than in the clarifier equipped with snail-shaped draw-off pipe. While the withdrawn solids concentration was 4.6 kg/m³ in the clarifier equipped with spiral-shaped draw-off pipe, it was increased up to 5.2 kg/m³ in the clarifier equipped with a snail-shaped draw-off pipe.

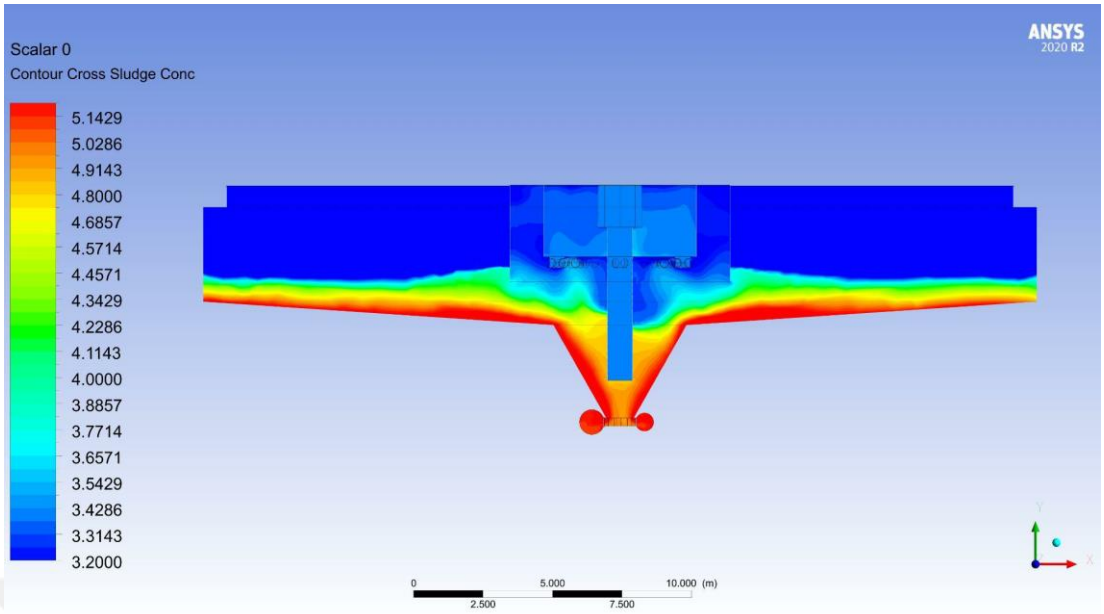


Figure 5.37 Solids concentration contours in the clarifier equipped with an LA-EDI, and a snail-shaped draw-off pipe and simulated for doubled inflow conditions.

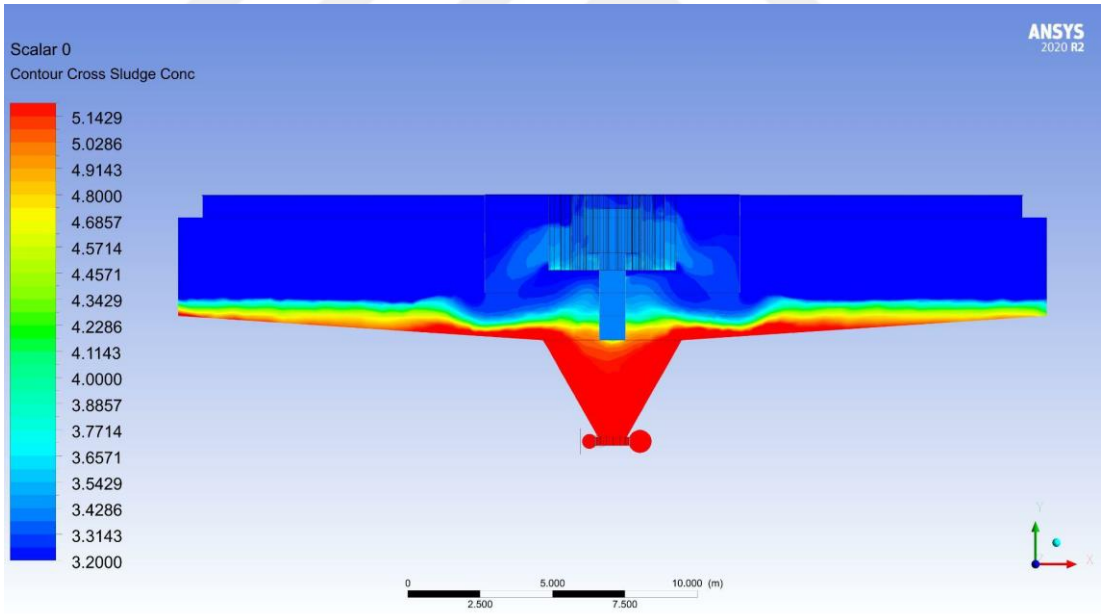


Figure 5.38 Solids concentration contours in the clarifier equipped with a MEDIC, and a snail-shaped draw-off pipe and simulated under doubled inflow conditions.

The sludge blanket was well-formed particularly in the clarifier equipped with a MEDIC, and a snail-shaped draw-off pipe (Figure 5.38), although it was simulated considering doubled inflow volume.

5.6.4 Streamlines

Figure 5.39 and Figure 5.40 represent the streamlines that occurred during sludge withdrawal in the clarifiers equipped with an EDI, and a novel draw-off pipe, which are simulated under doubled inflow conditions.

Figure 5.39 represents the full picture of the downstream short-circuiting that occurred in the clarifier in which the conventional influent well was replaced with a Standard Type-1 LA-EDI. Besides, if the reader follows the red noodles in Figure 5.39, they were mostly moved within the influent well, indicating that the influent was not retained in the clarifier sufficiently to thicken, and it discharged right after it was diffused in the clarification zone. Contrary to Figure 5.39, Figure 5.40 demonstrated that the streamlines in the clarifier equipped with a MEDIC only appeared in the lower half of the sidewall, where the sludge blanket occurs; in other words, the drawn-off sludge was thickened since better hydraulic conditions exist in the clarifier.

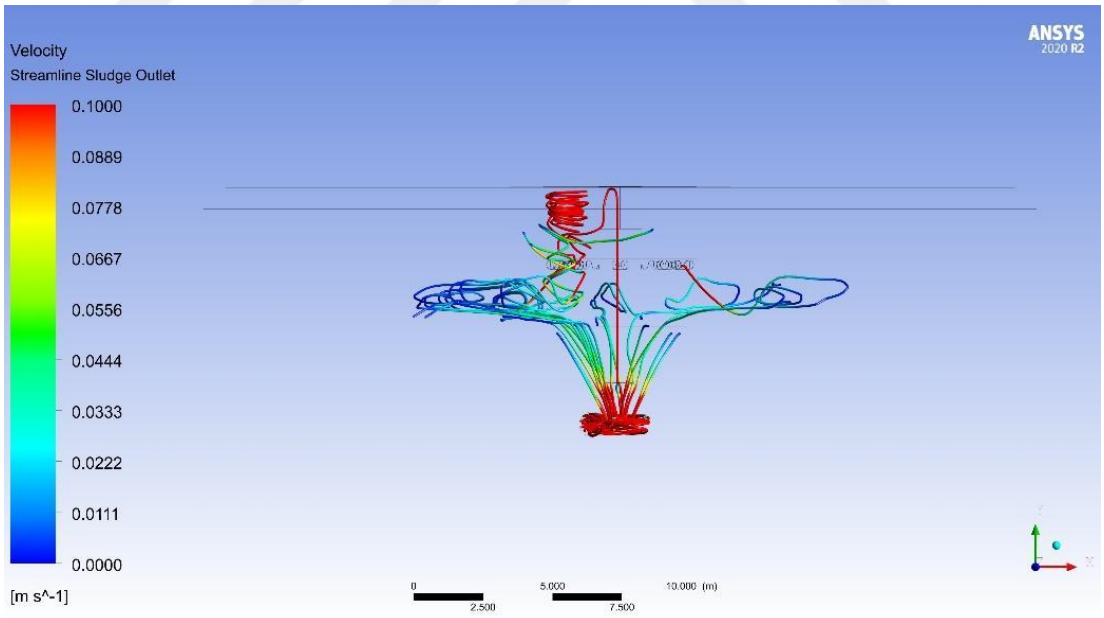


Figure 5.39 Streamlines simulated during sludge withdrawal in the clarifier equipped with an LA-EDI, and a spiral-shaped draw-off pipe and simulated for doubled inflow conditions.

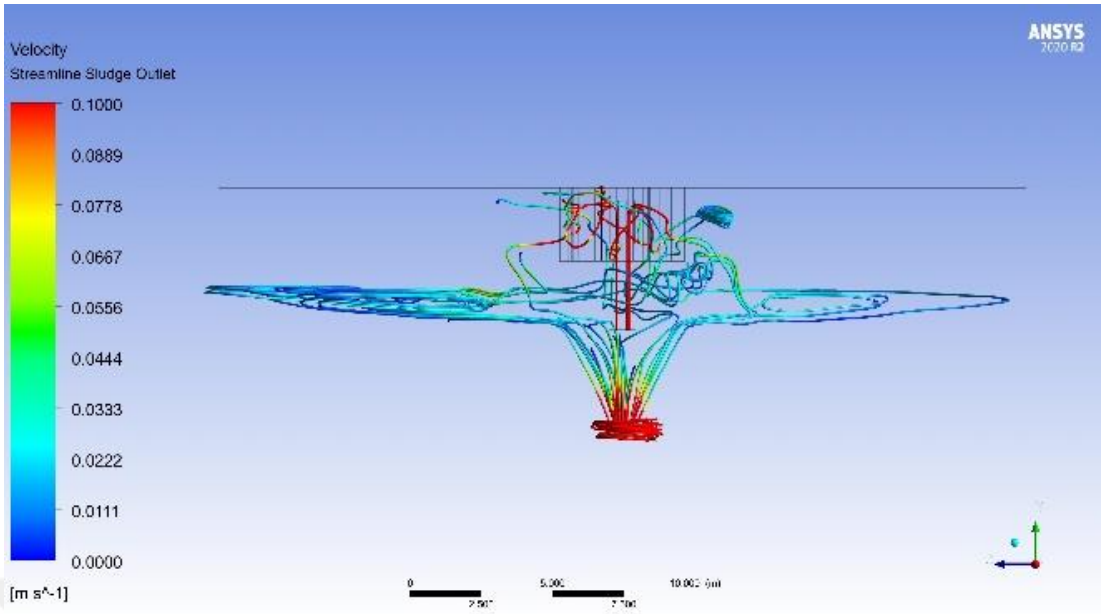


Figure 5.40 Streamlines simulated during sludge withdrawal in the clarifier equipped with a MEDIC, and a spiral-shaped draw-off pipe and simulated for doubled inflow conditions.

5.6.5 Comprehension of Results

It was found that the withdrawn solids concentration in the clarifier equipped with an LA-EDI, and a new-design draw-off pipe was increased by a magnitude of 20% although the influent volume was doubled. Moreover, it was found that by retrofitting the researched clarifier with a MEDIC and a snail-shaped draw-off pipe, the solids concentration was found to be close to the original clarifier simulated under existing conditions, although the influent volume was doubled. This research demonstrated that equipping clarifiers with either a snail-shaped sludge draw-off pipe or a spiral-shaped sludge draw-off pipe increases the sludge discharge capacity and mitigates the underflow short-circuiting potential in clarifiers equipped with EDIs.

The best retrofit option for the researched urban wastewater treatment plant was determined as equipping the clarifier with a MEDIC and a snail-shaped draw-off pipe. This option enabled idling one of the aeration tanks, and its clarifier. Accordingly, half of the blowers and sludge pumps would be suspended, and almost half of the energy and other operational costs of the biological processes would be saved while meeting the discharge limits.

While the reported treatment capacity was 50% for clarifiers equipped with LA-EDI (CPE Services Inc., 2022), it was only 30% for clarifiers equipped with MEDIC (Hydrosims, 2022); however, the findings demonstrated that the clarifier equipped with MEDIC was found to be more suitable to double the treatment capacity than LA-EDI. The problem in the clarifier equipped with an LA-EDI was suspected to be due to the small eddies occurring between the influent well and the sludge hopper which facilitated the scouring of the sludge blanket. Therefore, a measure would be investigated to eliminate the eddies formed in the clarifier equipped with an LA-EDI.

5.7 A Novel Deflector Design in Central-Feed Circular Secondary Clarifiers Equipped with Opposing-Jet Type EDIs

The opposing-jet nozzle type EDIs, particularly the LA-EDI, was reported to be one of the most superior among their alternatives in the literature, due to the fact that the multiple wing-type outlet nozzles that were configured to create flow impingement by opposing jets can effectively dissipate energy and promote flocculation. However, performed simulations demonstrated that the sludge blanket in the clarifier equipped with LA-EDI was found to be scoured due to the small eddies occurring between the influent well and the sludge hopper. Therefore, a deflector was designed to mitigate the scouring of the sludge blanket and the settled sludge in the sludge hopper.

The design of the deflector is comprised of multiple layers and each layer has multiple orifices that do not coincide vertically. The inflows entering from neighboring orifices on the top layer impinge with each other within the deflector, and the inflowing flows left the deflector with dissipated energy from either the orifices on the bottom layer or the orifices on the surrounding shell of the deflector.

The flow and concentration fields were simulated using CFD tools under doubled inflow conditions to assess the feasibility of doubling the treatment capacity of the clarifier that was equipped with an LA-EDI, a snail-shaped draw-off pipe, and a deflector between the LA-EDI and the sludge hopper. The rheological properties of settling sludge and the effect of stratification on turbulent diffusion were already

considered in the simulation. The tranquilizing effect in the influent streams, the promotion of flocculation, the mitigation of density currents, the scouring of sludge blanket, and the short-circuiting of overflow and underflow, consequent to the enhanced energy dissipation at the inlet diffusers were also explored.

5.7.1 Velocity Flow Field

Although the flow velocity was investigated in 3D, cross-sections in 2D were taken for the sake of illustrating the outputs. The cross-sections of the velocity field in the horizontal and vertical directions were elucidated and elaborated in the following headings.

5.7.1.1 Horizontal Cross-Section of the Velocity Flow Field

The velocity fields for the investigated case at the elevation of the orifices (the elevation where the influent was diffused to the clarification zone) were depicted in Figure 5.41.

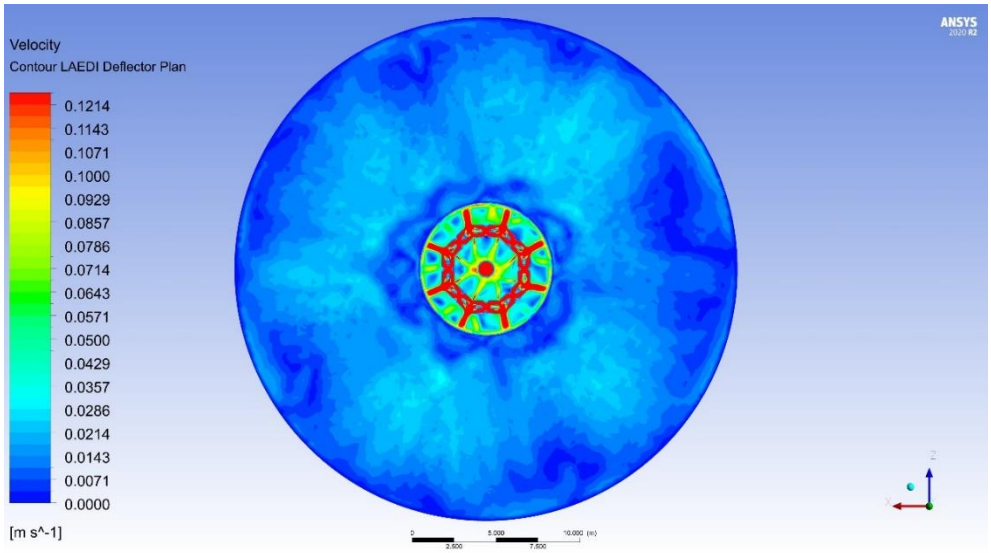


Figure 5.41 The flow velocity contours at the elevation of orifices in the clarifier equipped with an LA-EDI, a spiral-shaped draw-off pipe, and a novel deflector and simulated for doubled inflow conditions.

5.7.1.2 Vertical Cross-Section of the Velocity Flow Field

Figure 5.42 represents the cross-section of the flow velocity field in the clarifiers equipped with an EDI, a spiral-shaped draw-off pipe, and a novel deflector, and simulated for doubled inflow conditions.

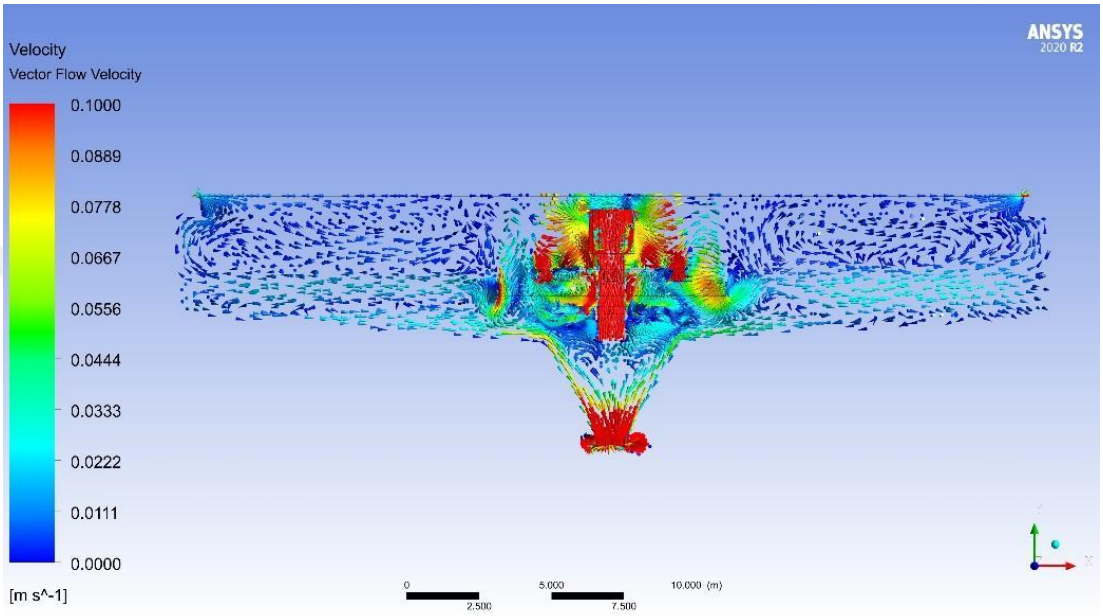


Figure 5.42 Flow velocity vectors in the clarifier equipped with an LA-EDI, a spiral-shaped draw-off pipe, and a deflector and simulated for doubled inflow conditions

As it was depicted in Figure 5.31 and Figure 5.42, the opposing jet nozzles were found to be very effective in dissipating energy. The flow velocity of the plumes, which were formed after the opposing jet impingement, was found to be well-plunged while flowing in the flocculation zone, and the remaining energy was mitigated as the plume collided with the flocculation well wall (Figure 5.31 and Figure 5.42). However, due to the shapes and positioning of the nozzles, while the majority of the flow draining out of the nozzles flows toward the baffle of the flocculation well, the remaining flow flows toward the center of the clarifier and facilitates the formation of eddies in the core of the clarifier. Therefore, the flow regime in the flocculation zone is turbulent.

It was determined that the eddies formed in the core of the clarifier, between the LA-EDI and sludge hopper, hindered solids settling in this region since there was no measure to mitigate the eddies in the Standard Type-1 LA-EDI. As it was depicted in Figure 5.42, the eddies formed in the core of the clarifier were confined in the flocculation zone and the impacts of eddies were mitigated in the sludge hopper, by taking the advantage of the novel deflector which was mounted to an optimum depth between the LA-EDI and the sludge hopper. The deflector takes in part of the turbulent flow that drains out of the nozzles but whose energy is not decently dissipated into its chambers from the orifices on the top plate. The flow entering from neighboring orifices impinges with each other within the deflector as they pass through the staggered chambers between the layers, and their energy dissipates. The flow comparably calmly exits the deflector from the orifices either on the side surfaces in the horizontal direction or on the bottom plate in the vertical direction. The flow colliding on the upper surface of the deflector dissipates some of its energy on the deflector and the remainder by impinging with other flows in the flocculation zone. In addition, the conical side surface of the deflector directs the flows exiting from the flocculation zone to the horizontal direction. To this extent, the eddies formed in the core of the clarifier, and scouring of the sludge blanket are mitigated. Besides, a uniform radial distribution of the incoming flow horizontally over the entire clarifier is provided.

The flow vectors in the sedimentation zone of the clarifier (Figure 5.31) whose influent well was replaced with a Standard Type-1 LA-EDI are low in number. This finding points out that underflow short-circuiting occurs, the LA-EDI is not very sufficient to distribute the incoming flow uniformly across the surface of the clarifier, the eddies in the core of the clarifier mitigate the formation of the sludge blanket, and consequently, the activated sludge exits the clarifier from the bottom outlet without effective sedimentation.

However, the flow vectors in the clarifier whose influent well was replaced with a Standard Type-1 LA-EDI and retrofitted with the novel deflector (Figure 5.42) are found more in number in the sedimentation zone than in the clarifier whose influent

well was replaced only with a Standard Type-1 LA-EDI (Figure 5.31). Besides, although the flow is doubled, the flow velocity vectors in the clarifier whose influent well was replaced with a Standard Type-1 LA-EDI and retrofitted with the novel deflector (Figure 5.42) have a similar distribution as in the conventional clarifier (Figure 5.8). Although the flow velocity as it passes from the flocculation zone to the sedimentation zone is around 40 mm/sec, it decreases to 5 mm/sec as it approaches the side wall, and then it floats upwards to the weirs. Although the flow rates in the sedimentation zone are calm, the clarifier can be equipped with Crosby-type weirs on the side walls as an extra measure. Crosby-type weirs redirect the vertical climbing flow to the horizontal direction and increase the distance of the flow path.

Central-feed circular clarifiers are usually preferred in the secondary treatment of wastewater since hydrodynamic conditions directly impact the sedimentation process. Wastewater is introduced into the clarifier from the center of the clarifier, and the wastewater is assumed to be radially and homogeneously distributed across the diameter of the clarifier. The weirs are formed along the perimeter of the clarifier to discharge the supernatant. Although uniform conditions are maintained at the inflow and outflow of the wastewater, it is not being sought in the sludge withdrawal, and sludge draw-off is always done from a single point. Therefore, the flow velocity profile in the sludge hopper is asymmetrical (Figure 5.8). However, sludge withdrawal from the bottom outlet is usually two to three times more than the supernatant outflow from the weirs. This could be one of the facts of the formation of helix currents reported in some clarifiers; however, this issue has not been investigated in the scope of this thesis. The novel snail-shaped draw-off pipe invented in the scope of this thesis, and mounted at the bottom of the existing conventional clarifier, which enables doubling the sludge withdrawal since the inlet flow has been doubled, mitigates the formation of underflow short-circuiting. Therefore, the flow velocity profiles in the sludge hopper are simulated as almost uniform (Figure 5.31 and Figure 5.42).

5.7.2 Solids Settling Velocity

Figure 5.43 represents the solids settling velocity contours in the clarifier equipped LA-EDI, a spiral-shaped draw-off pipe, and a novel deflector, which is simulated under doubled inflow conditions.

The small eddies occurred between the influent well and the sludge hopper in the clarifier equipped with an LA-EDI, and a snail-shaped draw-off pipe (Figure 5.34) are mitigated by means of the novel deflector (Figure 5.43).

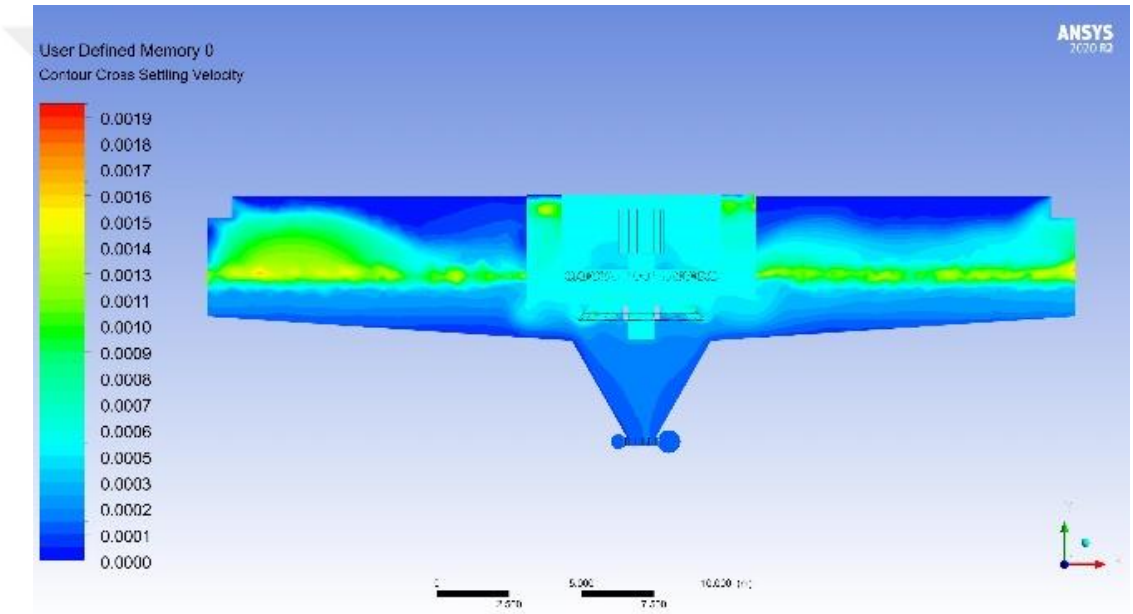


Figure 5.43 Solids settling velocity contours (m/s) in the clarifier equipped LA-EDI, a spiral-shaped draw-off pipe, and a deflector and simulated for doubled inflow conditions.

The settling velocity values were found low at the bottom of the clarifier, as expected, since the sludge blanket was formed and thickened at the bottom, and therefore settling is minimum in this region. The settling velocity values were found maximum at the level of orifices of the influent well. Moreover, the plume was found dispersed in a conical shape in the horizontal direction.

5.7.3 Solids Concentration

Figure 5.44 represents the solids concentration in the clarifier equipped with an EDI, a spiral-shaped draw-off pipe and a novel deflector, which is simulated under doubled inflow conditions.

The clarifiers that were demanded to be operated at doubled inflow volume, particularly the clarifier equipped with an LA-EDI, could not yield well-thickened sludge (Figure 5.37). However, the deflector mitigated the small eddies occurring between the influent well and the sludge hopper and scouring of the sludge blanket (Figure 5.44).

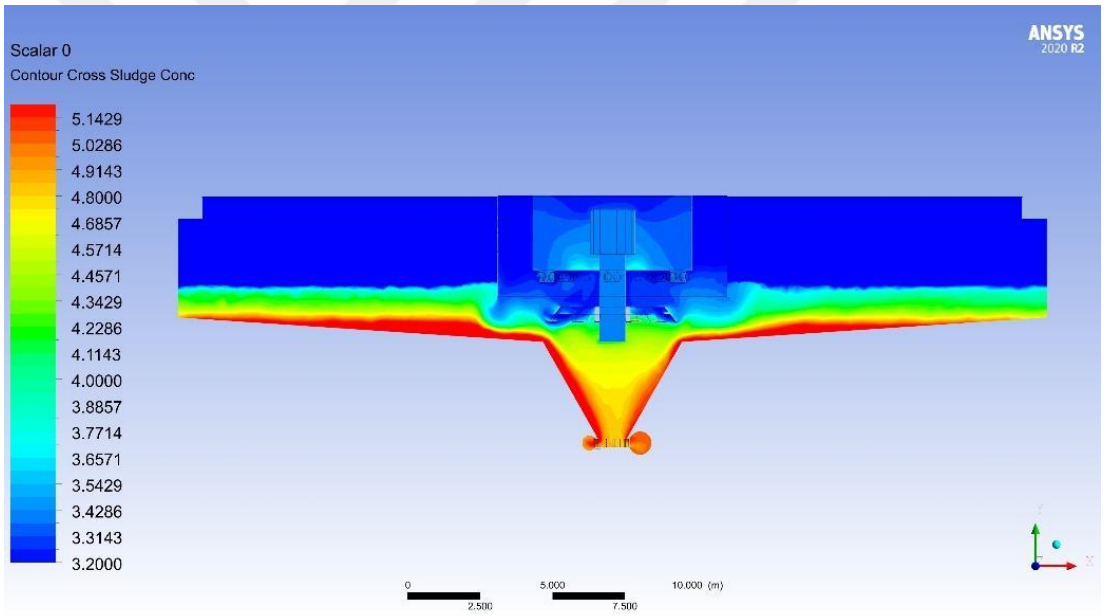


Figure 5.44 Solids concentration contours in the clarifier equipped with an LA-EDI, a spiral-shaped draw-off pipe, and a novel deflector and simulated for doubled inflow conditions.

5.7.4 Streamlines

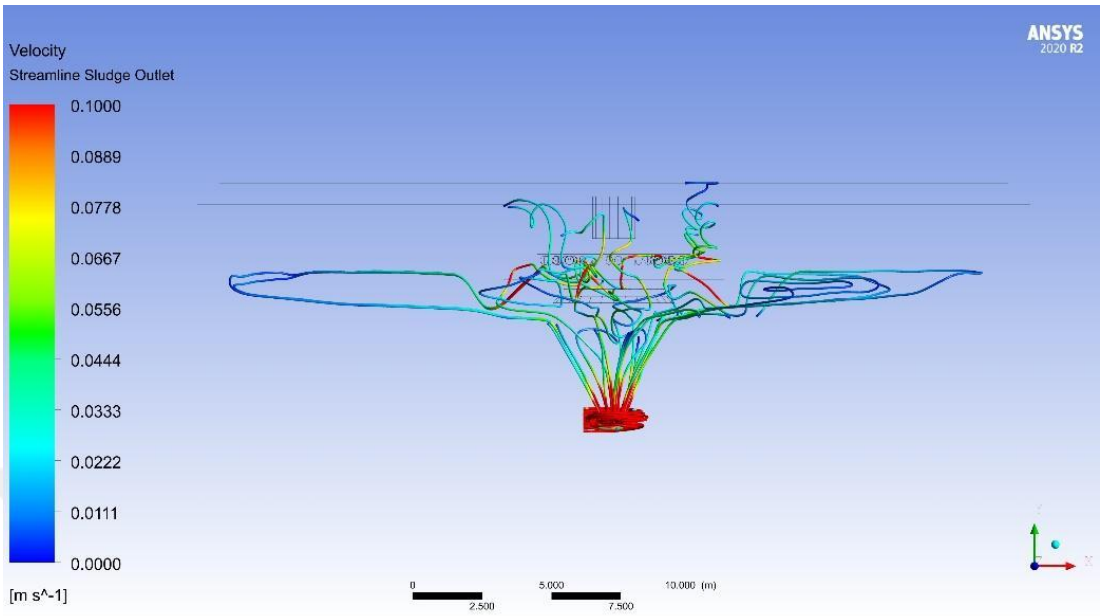


Figure 5.45 Streamlines simulated during sludge withdrawal in the clarifier equipped with an LA-EDI, a spiral-shaped draw-off pipe, and a novel deflector and simulated for doubled inflow conditions.

Figure 5.45 represent streamlines that occurred during sludge draw-off for the investigated case. The streamlines in the conventional clarifier (Figure 5.12) have only appeared in the lower half of the sidewall, where the sludge blanket occurs; in other words, the drawn-off sludge was thickened.

Contrary to Figure 5.39, Figure 5.45 demonstrated that the streamlines in the clarifier equipped with a Standard Type-1 LA-EDI, and a novel deflector only appeared in the lower half of the sidewall, where the sludge blanket occurs; in other words, the drawn-off sludge was thickened since better hydraulic conditions exist in the clarifier.

5.7.5 Comprehension of Results

The reported treatment capacity was 50% for clarifiers equipped with LA-EDI (CPE Services Inc., 2022). The conditions limiting the further capacity increase were found to be due to the small eddies occurring between the influent well and the sludge

hopper. Therefore, a deflector between the LA-EDI and the sludge hopper was mounted to mitigate the scouring of the sludge blanket and the settled sludge in the sludge hopper.

It was demonstrated that the novel deflector enhanced the hydrodynamic conditions in the clarifier, mitigated the underflow short-circuiting, mitigated eddies that scour the sludge blanket, and supported uniform radial distribution of the influent across the diameter of the clarifier.

Consequently, it was demonstrated that the conventional clarifier could be operated at doubled inflow conditions if the influent well was replaced with an LA-EDI that is retrofitted with the novel deflector. This solution would enable the operation of the existing treatment plant with half of the available volume allocated for biological processes. Therefore, it was decided to idle one of the aeration tanks and its clarifier, accordingly half of the blowers and sludge pumps would be suspended, and almost half of the energy and other operational costs of the biological processes would be saved while meeting the discharge limits.

CHAPTER 6
CONCLUSIONS AND RECOMMENDATIONS

The aim of this dissertation was to investigate the benefits of utilizing Computational Fluid Dynamics (CFD) tools to examine hydrodynamic conditions in wastewater treatment facilities. Specifically, the study focused on the activated sludge system used in biological wastewater treatment and conducted in-depth modeling of the secondary clarifiers. Hydrodynamic optimization studies were carried out using CFD to consider the design and operational data of the treatment units in the wastewater treatment plant being investigated.

At first, the design review of the wastewater treatment plant, based on 465 days of operational records, revealed that the total volume of the aeration tanks was twice the required volume. As a result, one of the aeration tanks could be deactivated, allowing the plant to continue operating with only one aeration tank.

In order to investigate ways to improve process efficiency and reduce energy consumption, the configuration of mixers in the aeration tanks was modified and simulated in a CFD environment. The submerged mixers were found to create a very high flow velocity inside the aeration tank, which affected the formation of plug-flow reactor conditions and caused the nitrification and denitrification volumes in the reactor to shift. The study revealed that operating the mixers at minimum speed would decrease the recirculation ratio, maintain better plug-flow conditions, and form better nitrification and denitrification regions in the aeration tank.

CFD tools were used to visualize the sedimentation process in its entirety. The conventional clarifier was found to operate well under existing conditions, designed with nominal design parameters. The energy of the influent was well-dissipated, and the orifices distributed the flow evenly to the clarifier, yielding well-thickened sludge.

Although it was confirmed that the conventional clarifier experienced no hydrodynamic problems under existing conditions, it was examined to deactivate one

of the clarifiers as it was feasible to operate the plant with only one aeration tank. Subsequently, the conventional clarifier was retrofitted with a LA-EDI to increase its capacity without increasing the volume. CFD simulations verified that equipping conventional clarifiers with an EDI increases their capacity and enables them to operate with higher overflow rates. The study also revealed that while EDIs prevent short-circuiting of overflow, they facilitate short-circuiting of the underflow.

CFD simulations were used to diagnose the conditions limiting the further capacity increase in clarifiers equipped with EDIs. It was found that the sludge blankets could be easily deformed in clarifiers equipped with EDIs since the sludge is drawn off from a single point.

It was conceptualized that having multiple draw-off pipes would decrease the underflow capacity, however, the multiple draw-off pipes must be combined with a collector and conveyed to the sump pit. To that end, inspired by the spiral-casing in reaction-type turbines and distribution pipes in impulse-type turbines, which are customized penstocks that maintain even flow distribution in hydropower, snail- and spiral-shaped sludge draw-off pipes were drafted; however, the penstocks were operated in the opposite direction for the flow collection purpose. The underflow short-circuiting mitigation performance of the draw-off pipe designs was examined using CFD tools.

It was demonstrated that equipping clarifiers with either a snail- or a spiral-shaped sludge draw-off pipe increases the sludge discharge capacity and mitigates the underflow short-circuiting potential in clarifiers equipped with EDIs. The proposed draw-off pipes yielded almost uniform flow velocity profiles in the sludge hopper. The withdrawn solids concentration in the clarifier equipped with an LA-EDI and a new-design draw-off pipe was increased by 20% even though the influent volume was doubled.

Simulations also showed that the sludge blanket in the clarifier equipped with an LA-EDI was scoured by small eddies between the influent well and the sludge hopper.

To mitigate this, a novel deflector was designed that enhanced the hydrodynamic conditions in the clarifier, mitigated the underflow short-circuiting, and prevented eddies from scouring the sludge blanket. The deflector also facilitated uniform radial distribution of the influent across the diameter of the clarifier. Consequently, it was shown that the conventional clarifier could be operated at double the inflow conditions if the influent well was replaced with an LA-EDI retrofitted with the novel deflector.

It was found that the best retrofit option of equipping the clarifier with a MEDIC and a snail-shaped draw-off pipe would make it feasible to operate the existing treatment plant with only half of the available volume allocated for biological processes. As a result, it was decided to idle one of the aeration tanks and its clarifier. Half of the blowers and sludge pumps would be suspended, resulting in significant energy and operational cost savings, while still meeting the discharge limits.

In conclusion, this dissertation demonstrated that CFD is a tried-and-true tool to optimize hydrodynamics, which is the final step in the design process. Besides, this dissertation also demonstrated that by optimizing hydrodynamics, it is possible to minimize energy input, reduce operating costs, and improve treatment performance.

6.1 Future Works

The focus of this dissertation was to demonstrate that snail- and spiral-shaped draw-off pipe designs can mitigate underflow short-circuiting performance and assist in enhancing further capacity increase in clarifiers equipped with EDIs, benefiting from the CFD models. Further studies are necessary to refine the novel draw-off pipe designs. Lab-scale experiments on snail- and spiral-shaped draw-off pipe designs should be conducted. The experimental measurements of these two physical models are proposed to be utilized in the calibration of CFD models since the calibration and validation are not complete. The results of these two simulations will then be compared to determine which of the two designs might be the most efficient.

REFERENCES

Ahmed, F. H., Kamel, A., & Jawad, S. A. (1996). Experimental determination of the optimal location and contraction of sedimentation tank baffles. *Water, Air, and Soil Pollution, 92*(3), 251–271.

Al-Mafraji, E. A., & Al-Mussawy, H. A. (2021). Using lower and upper baffle arrangements to enhance sedimentation tank performance using lower and upper baffle arrangements to enhance sedimentation tank performance. *4th International Conference on Engineering Sciences (ICES 2020).* doi:10.1088/1757-899X/1067/1/012009

Alonso, G., & Alex, M. J. (2006). Optimum design of your center well: Use of a CFD model to understand the balance between flocculation and improved hydrodynamics. *Proceedings of the Water Environment Federation, 2006*(13), 263–280. doi:10.2175/19386470678371058

Al-Sammarraee, M., & Chan, A. (2009). Large-eddy simulations of particle sedimentation in a longitudinal sedimentation basin of a water treatment plant. Part 2: The effects of baffles. *Chemical Engineering Journal, 152*(2-3), 315–321. doi:10.1016/j.cej.2009.01.052

ANSYS, Inc. (2019). *ANSYS Fluent Theory Guide, Release 2019 R2.*

Asgharzadeh, H., Firoozabadi, B., & Afshin, H. (2011). Experimental investigation of effects of baffle configurations on the performance of a secondary sedimentation tank. *Scientia Iranica, 18*(4B), 938–949. doi:10.1016/j.scient.2011.07.005

Bajcar, T., Gosar, L., Širok, B., Steinman, F., & Rak, G. (2010). Influence of low field on sedimentation efficiency in a circular settling tank with peripheral inflow and central effluent. *Chemical Engineering and Processing: Process Intensification, 49*(5).

Bajcar, T., Steinman, F., Širok, B., & Prešeren, T. (2011). Sedimentation efficiency of two continuously operating circular settling tanks with different inlet- and outlet arrangements. *Chemical Engineering Journal, 178*, 217–224. doi:10.1016/j.cej.2011.10.054

Bokil, S. D., & Bewtra, J. K. (1972). Influence of Mechanical Blending on Aerobic Digestion of Actiated Sludge. *Advances in Water Pollution Research, 6*.

Bradley, B. D., & Coombs, S. G. (1994). *US Patent No. 5,340,485.*

Brouckaert, C. J., & Buckley, C. A. (1999). The use of computational fluid dynamics for improving the design and operation of water and wastewater treatment plants. *Water Science and Technology, 40*(4-5), 81–89. doi:10.1016/S0273-1223(99)00488-6

Burt, D. J. (2010). *Improved design of settling tanks using an extended drift flux model.* Bristol: University of Bristol.

Burt, D., & Ganeshalingam, J. (2005). Design and optimisation of final clarifier performance with CFD modelling. *CIWEM/Aqua Enviro joint conference, Design and Operation of Activated Sludge Plants.*

CPE Services Inc. (2022, 09 26). *The LA-EDI (Types I and II)*. Retrieved from https://www.clarifiers.com/la-edi.cfm

Crosby, R. M. (1984). *Hydraulic characteristics of activated sludge secondary clarifiers.* U.S. Environmental Protection Agency.

Dadvand, A., & Motlagh, S. Y. (2022). Chapter 1 - Introduction on principle of computational fluid dynamics. In A. Basile, & K. Ghasemzadeh, *Current Trends and Future Developments on (Bio-) Membranes* (pp. 1-26). Elsevier. doi:10.1016/B978-0-12-822294-2.00006-0

Das, S., Bai, H., Wu, C., Kao, J. H., Barney, B., Kidd, M., & Kuettel, M. (2016). Improving the performance of industrial clarifiers using three-dimensional computational fluid dynamics. *Engineering Applications of Computational Fluid Mechanics, 10*(1), 130-144. doi:10.1080/19942060.2015.1121518

De Clercq, B. (2003). *Computational fluid dynamics of settling tanks.* Gent: Universiteit Gent. doi:1854/242

De Clercq, B., & Vanrollelghem, P. A. (2002). Computational fluid dynamics in wastewater treatment. *Mededelingen Faculteit Landbouwkundige En Toegepaste Biologische Wetenschappen, 67*(4), 15–18.

Deininger, A. (1994). Inluence of combined sewage influent on secondary clarifiers of activated sludge plants. *Water Science and Technology, 30*(4).

Deininger, A., Holthausen, E., & Wilderer, P. A. (1998). Velocity and solids distribution in circular secondary clarifiers: Full scale measurements and numerical modelling. *Water Research, 32*(10), 2951–2958. doi:10.1016/S0043-1354(98)00072-4

DeVantier, B. A., & Larock, B. E. (1987). Modeling sediment induced density currents in sedimentation basins. *Journal of Hydraulic Engineering, 113*(1), 80-94. doi:10.1061/(asce)0733-9429(1987)113:1(80)

Ekama, G. A., & Marais, P. (2004). Assessing the applicability of the 1D flux theory to full-scale secondary settling tank design with a 2D hydrodynamic model. *Water Research, 38*(3), 495–506. doi:10.1016/j.watres.2003.10.026

Ekama, G., Barnard, J., Gunthert, F., Krebs, P., McCorquodale, J., Parker, D., & Wahlberg, E. (1997). *Secondary Settling Tank: Theory, Modelling, Design and Operation.* London: IAWQ Scientific and Technical Report No. 6.

Esler, J. K. (2022, 06 19). *An Evaluation of Energy-Dissipating Inlets.* Retrieved from CPE Services Inc.: https://www.clarifiers.com/pdfs/EDIs%20Available.pdf

Esler, K., Hartnett, W. J., & Haug, R. A. (2001, August 21). *US Patent No. 6,276,537 B1.*

Fan, L., Xu, N., Ke, X., & Shi, H. (2007). Numerical simulation of secondary sedimentation tank for urban wastewater. *Journal of the Chinese Institute of Chemical Engineers, 38*(5-6), 425–433.

Frost, R. C., Halliday, J., & Dee, A. S. (1993). Continuous consolidation of sludge in large scale gravity thickeners. *Water Science and Technology, 28*(1), 77-86.

Gao, H., & Stenstorm, M. K. (2017). Computational fluid dynamics applied to secondary clarifier analysis. *World Environmental and Water Resources Congress,* (pp. 301–315).

Gao, H., & Stenstrom, M. K. (2018). Evaluation of three turbulence models in predicting the steady state hydrodynamics of a secondary sedimentation tank. *Water Research, 143*, 445–456. doi:10.1016/j.watres.2018.06.067

Gao, H., & Stenstrom, M. K. (2019a). The influence of wind in secondary settling tanks for wastewater treatment — A computational fluid dynamics study.

Part I: Circular secondary settling tanks. *Water Environment Research, 92*(4), 541–550. doi:10.1002/wer.1241

Gao, H., & Stenstrom, M. K. (2019b). The influence of wind in secondary settling tanks for wastewater treatment — A computational fluid dynamics study. Part II: Rectangular secondary settling tanks. *Water Environment Research*, 1–11. doi:10.1002/wer.1244

Gao, H., & Stenstrom, M. K. (2020). Development and applications in computational fluid dynamics modeling for secondary settling tanks over the last three decades: A review. *Water Environment Research, 92,* 796-820. doi:10.1002/wer.1279

German Water, Wastewater and Solid Waste Organization. (2000, May). Dimensioning of Single Stage Activated Sludge Process. *ATV-DVWK-A 131E*.

Ghawi, A. H., & Kriš, J. (2008). Design and optimisation of settling tanks performances in Slovakia. *XX-TH Jubilee-National, VIII-TH International Scientific and Technical Conference Water Supply and Water Quality.*

Ghawi, A. H., & Kriš, J. (2012). A computational fluid dynamics model of low and settling in sedimentation tanks. In H. W. Oh, *Applied Computational Fluid Dynamics* (pp. 19–34). InTech.

Ghawi, A., & Kris, J. (2011). Improvement performance of secondary clarifiers by a computational fluid dynamics model. *Slovak Journal of Civil Engineering, 19*(1).

Gkesouli, A., & & Stamou, A. (2018). A CFD modeling procedure to assess the effect of wind in settling tanks. *Journal of Hydroinformatics, 21*. doi:10.2166/hydro.2018.048

Goodarzi, D., Lari, K. S., & Alighardashi, A. (2018). A large eddy simulation study to assess low-speed wind and baffle orientation effects in a water treatment sedimentation basin. *Water Science and Technology, 2018*(2), 412–421. doi:10.2166/wst.2018.171

Goula, A. M., Kostoglou, M., Karapantsios, T. D., & Zouboulis, A. I. (2008). The effect of influent temperature variations in a sedimentation tank for potable

water treatment — A computational fluid dynamics study. *Water Research, 42*(13), 3405–3414. doi:10.1016/j.watres.2008.05.002

Goula, A., Kostoglou, M., Karapantsios, T., & Zouboulis, A. (2007). A CFD methodology for the design of sedimentation tanks in potable water treatment. Case Study: The Influence of A Feed Flow Control Baffle. *Chemical Engineering Journal, 140*, 110-121.

Grau, P., & Aquanova. (2022, 06 22). *Short-circuiting*. Retrieved from Final Clarifiers in Activated Sludge Process: http://www.aquanova.cz/short.htm

Gun, S., Chatterjee, S., & Hens, A. (2022). CFD based analysis of chlorination contact tank design. *Materials Today: Proceedings, 57*(4), 1813-1818. doi:10.1016/j.matpr.2021.12.533

Hadi, G. A., & Kriš, J. (2009). A CFD methodology for the design of rectangular sedimentation tanks in potable water treatment plants. *Journal of Water Supply: Research and Technology - AQUA, 58*(3), 212–220. doi:10.2166/aqua.2009.027

Hazen, A. (1904). On sedimentation. *Transactions of the American Society of Civil Engineers, 53*, 45-71. doi:10.1061/TACEAT.0001655

Hirom, K., & Devi, T. T. (2022). Application of Computational Fluid Dynamics in Sedimentation Tank Design and Its Recent Developments: A Review. *Water Air Soil Pollut, 233*(22). doi:10.1007/s11270-021-05458-9

Hydrosims. (2022, 09 21). *Hydrosims.* Retrieved from Why An Energy Dissipating Inlet (EDI) in a Center-feed Clarifier: https://www.hydrosims.com/MEDICPAGES.html

Karpinska Portela, A. (2013). *New design tools for Activated Sludge process.* Porto: FEUP, University of Porto.

Karpinska, A., & Bridgeman, J. (2015). CFD-Aided Modelling of Activated Sludge Systems – A Critical Review. *Water Research*. doi:10.1016/j.watres.2015.11.008

Kawamura, S., & Lang, J. (1986). Re-evaluation of launders in rectangular sedimentation basins. *Water Pollution Control Federation*, 1124–1128.

Kleine, D., & Reddy, B. D. (2005). Finite element analysis of flows in secondary settling tanks. *International Journal for Numerical Methods in Engineering, 64*(7), 849-876. doi:10.1002/nme.1373

Köken, E., & Büyükkamacı, N. (2022). The Influence of Different Energy Dissipating Inlets on the Hydrodynamics within the Clarifiers. *8th International Conference on Environmental Science and Technology (ICOEST 2022)*, (pp. 29-38). İstanbul.

Kovalev, N. N. (1965). *Hydroturbines, Design and Construction (Vol. 64, No. 11087)*. Israel Program for Scientific Translations.

Krebs, P. (1991). The hydraulics of final settling tanks. *Water Science and Technology, 23*(4-6), 1037–1046. doi:10.2166/wst.1991.0555

Krebs, P. (1995). Success and shortcomings of clarifier modelling. *Water Science and Technology, 31*(2), 181-191. doi:10.1016/0273-1223(95)00191-O

Kriš, J., & Hadi, G. A. (2007). Design and optimization of sedimentation tank in Slovakia with CFD modeling. *International Symposium on Water Management and Hydraulic Engineering*, (pp. 1–13).

Lakehal, D., Krebs, P., Krijgsman, J., & Rodi, W. (1999). Computing shear flow and sludge blanket in secondary clarifiers. *Journal of Hydraulic Engineering, 125*(3), 253-262.

Larsen, P. (1977). *On the Hydraulics of Rectangular Settling Basins, Experimental and Theoretical Studies.* Lund Institute of Technology, Department of Water Resources Engineering, Lund, Sweden.

Le Moullec, Y., Gentric, C., Potier, O., & Leclerc, J. P. (2010). CFD simulation of the hydrodynamics and reactions in an activated sludge channel reactor of wastewater treatment. *Chemical Engineering Science, 65*, 492-498.

Le Moullec, Y., Potier, O., Gentric, C., & Leclerc, J. P. (2008). Flow field and residence time distribution simulation of a cross-flow gas–liquid wastewater treatment reactor using CFD. *Chemical Engineering Science, 63*, 2436–2449.

Lengricht, J., Graw, K.-U., & Schulz, A. (2000). A new concept for circular sedimentation basins. *Proceedings of the 4th Int Conf Hydroscience Eng-ICHE 2000.* Seoul.

Liu, Y. (2003). Chemically reduced excess sludge production in activated sludge process. *Chemosphere, 50*, 1-7.

McCorquodale, J. A., & Zhou, S. (1993). Effects of hydraulic and solids loading on clarifier performance. *Journal of Hydraulic Research, 31*(4), 461–478. doi:10.1080/00221689309498870

McCorquodale, J. A., La Motta, E. J., Griborio, A., Homes, J., & Georgiou, I. (2004). *Development of software for modeling activated sludge clarifier systems. A Technology Transfer Report.* Department of Civil and Environmental Engineering, University of New Orleans, LA.

Mendis, J. B., & Benedek, A. (1980). Tube Settlers in Secondary Clarification of Domestic Wastewaters. *Journal (Water Pollution Control Federation), 52*(7), 1893–1897. Retrieved from http://www.jstor.org/stable/25027651

Mostafa, H., Emad, S. E., & Usama, F. M. (2005). Modeling the effect of inlet baffle longitudinal and vertical positions on the settling tank performance with computational fluid dynamics. *Al-Azhar University Civil Engineering Research Magazine (CERM), 10*(2), 113-140.

NASA Glenn Research Center. (2022, 09 22). *Navier-Stokes Equations*. Retrieved from http://www.grc.nasa.gov/WWW/k-12/airplane/nseqs.html

Park, N. S., Kim, S. S., Lee, Y. J., & Wang, C. K. (2014). Effects of longitudinal baffles on particles settling in a sedimentation basin. *Water Science and Technology, 69*(6), 1212–1218. doi:10.2166/wst.2013.818

Park, N. S., Lim, J. L., Lee, S. J., Lee, K. H., & Kwon, S. B. (2006). Examining the effect of transverse troughs on hydrodynamic behavior in a sedimentation basin with CFD simulation and ADV technique. *Journal of Water Supply: Research and Technology - AQUA, 55*(4), 247-256. doi:10.2166/aqua.2006.010

Patziger, M. (2016). Computational fluid dynamics investigation of shallow circular secondary settling tanks: Inlet geometry and performance indicators. *Chemical Engineering Research and Design, 112*, 122-131.

Patziger, M. (2021). Improving wastewater treatment plant performance by applying CFD models for design and operation: Selected case studies. *Water Science and Technology, 84*. doi:10.2166/wst.2021.019

Patziger, M., Kainz, H., Hunze, M., & Józsa, J. (2012). Influence of secondary settling tank performance on suspended solids mass balance in activated sludge systems. *Water Research, 46*(7), 2415–2424. doi:10.1016/j.watres.2012.02.007

Phiri, Z., Saito, Y., Ishak, B. B., Harada, H., & Nakajima, S. (1996). Optimization of the performance of hoppered peripheral-feed clarifiers. *Water Science and Technology, 33*(8), 125–133. doi:10.1016/0273-1223(96)00268-5

Raeesh, M., Devi, T. T., & Hirom, K. (2023). Recent Developments on Application of Different Turbulence and Multiphase Models in Sedimentation Tank Modeling—a Review. *Water, Air, & Soil Pollution, 234*. doi:10.1007/s11270-022-06007-8

Ratkovich, N. (2010). *Understanding hydrodynamics in Membrane Bioreactor systems for wastewater treatment: Two-phase empirical and numerical modelling and experimental validation.* Ghent: Faculty of Bioscience Engineering, Ghent University.

Rehman, U., Maere, T., Amerlinck, A., Arnaldos, M., & Nopens, I. (2014). Hydrodynamic–biokinetic model integration applied to a full-scale WWTP. *Proceedings of the IWA World Water Congress & Exhibition.* Lisbon, Portugal.

Şahin, N., & Şibil, R. (2023). Hydrodynamic Performance Evaluation of Screening on the Physical Unit Operations in Wastewater Treatment Based on Experimentally Validated CFD Computations. *Process Safety and Environmental Protection, 171*, 136-151. doi:10.1016/j.psep.2022.12.095

Saini, A. K., Paritosh, K., Singh, A. K., & Vivekanand, V. (2021). CFD approach for pumped-recirculation mixing strategy in wastewater treatment: minimizing power consumption, enhancing resource recovery in commercial anaerobic digester. *Journal of Water Process Engineering, 40*. doi:10.1016/j.jwpe.2020.101777

Samstag, R. W., Dittmar, D. F., Vitasovic, Z., Mccorquodale, J. A., Randal, W., Dittmar, F., & McCorquodale, J. A. (1992). Underflow Secondary Geometry Sedimentation. *Water Environment Research, 64*(3), 204–212. doi:10.2175/WER.64.3.3

Samstag, R. W., Wicklein, E. W., Reardon, R. D., Leetch, R. J., Parks, R. M., & Groff, C. D. (2012). Field and CFD Analysis of Jet Aeration and Mixing. *Proceedings of the 84th Annual Water Environment Federation Technical Conference & Exposition.* New Orleans, LA, USA.

Samstag, R., Ducoste, J., Griborio, A., Nopens, I., Batstone, D., Wicks, J., . . . Laurent, J. (2016). CFD for wastewater treatment: an overview. *Water Science and Technology, 74*.

Samstag, R., Wicklein, E., Reardon, R., Leetch, R., Parks, M., & Groff, C. (2012). Field and CFD Analysis of Jet Aeration and Mixing. *Proceedings of the Water Environment Federation.* doi:10.2175/193864712811708301

Sivakumar, M., & Lowe, S. A. (1990). Simulation of the effect of wind on rectangular sedimentation tanks. *Conference on Hydraulics in Civil Engineering*, (pp. 74–78).

Sobremisana, A. P., Ducoste, J. J., & de los Reyes III, F. L. (2011). Combining CFD, Floc Dynamics and Biological Reaction Kinetics to Model Carbon and Nitrogen Removal in Activated Sludge System. *Proceedings of the 83rd Annual Water Environment Federation Technical Conference and Exposition.* Los Angeles, CA, USA.

Stypka, A. (1998). *Advanced Wastewater Treatment Report No. 4 : Factors Influencing Sludge Settling Parameters And Solid Flux In The Activated Sludge Process, A Literature Review.* Stockholm: Royal Institute of Technology.

Takács, I., Patry, G. G., & Nolasco, D. (1991). A dynamic model of the clarification-thickening process. *Water Research, 25*(10), 1263-1271.

Takács, I., Patry, G. G., & Nolasco, D. (1991). A dynamic model of the clarification-thickening process. *Water Research, 25*(10), 1263-1271.

Tamayol, A., Firoozabadi, B., & Ahmadi, G. (2008). Effects of inlet position and baffle configuration on hydraulic performance of primary settling tanks. *Journal of Hydraulic Engineering*, *134*(7), 1004–1009. doi:10.1061/(asce)0733-9429(2008)134:7(1004)

Tamayol, A., Firoozabadi, B., & Ashjari, M. A. (2010). Hydrodynamics of secondary settling tanks and increasing their performance using baffles. *Journal of*

Environmental Engineering, 136(1), 32–39. doi:10.1061/(asce)ee.1943-7870.0000126

Tchobanoglous, G., Burton, F. L., & Stensel, H. D. (2003). *Wastewater Engineering: Treatment and Reuse.* Boston: McGraw-Hill.

Vlaev, S. D., Dzhonova-Atanasova, D., & Tsibranska, I. (2020). CFD evaluation of mass transfer distribution heterogeneity along the membrane-liquid interface in stirred submerged membrane bioreactors. *Chemical Engineering and Processing-Process Intensification, 147*. doi:10.1016/j.cep.2019.107738

Vorwaller, J., & Heimdal, T. (2016). *US Patent No. 9,339,743 B2.*

Wicklein, E., & Samstag, R. (2009). Comparing Commercial and Transport CFD Models for Secondary Sedimentation. *Proceedings of the Water Environment Federation*, (pp. 6066-6081). doi:10.2175/193864709793952765

Wicklein, E., Batstone, D., Ducoste, J., Laurent, J., Griborio, A., Wicks, J., . . . Nopens, I. (2016). Good modelling practice in applying computational fluid dynamics for WWTP modelling. *Water Science & Technology, 73*(5), 969-982.

Wicklein, E., Rauch-Williams, T., Luna, B., Samstag, R., & Michalski, J. (2018). 3D CFD modeling helped develop geometric improvements that increased an existing plant's secondary clarifier capacity. *WEFTEC 2018*, (pp. 4729-4738).

Wright, R. C. (2004). Reducing Sludge Blanket Depth in Circular Scraper Secondary Clarifiers Using a Sludge Collection Ring. *WEFTEC 2004* (pp. 209-227). Water Environment Federation.

Xanthos, S., Gong, M., Ramalingam, K., Fillos, J., Deur, A., Beckmann, K., & McCorquodale, J. A. (2011). Performance assessment of secondary settling tanks using CFD modeling. *Water Resources Management, 25*(4), 1169-1182.

Xanthos, S., Gong, M., Ramalingam, K., Fillos, J., Deur, A., Beckmann, K., & McCorquodale, J. A. (2012). Investigating the effect of baffles on the performance of rectangular (Gould II Type) settling tanks using a 3-D CFD

Model. *Proceedings of the Water Environment Federation, 2008*(13), 3297-307. doi:10.2175/193864708788733549

Yang, M., del Pozo, D. F., Torfs, E., Rehman, U., Yu, D., & Nopens, I. (2021). Numerical simulation on the effects of bubble size and internal structure on flow behavior in a DAF tank: A comparative study of CFD and CFD-PBM approach. *Chemical Engineering Journal Advances, 7*.

Yang, N., & Wen, Y. (2019). Numerical simulation of secondary sedimentation tank based on population balance model. *IOP Conference Series: Earth and Environmental Science, 358*(3). doi:10.1088/1755-1315/358/3/032052

Zhang, D. (2014). *Optimize Sedimentation Tank and Lab Flocculation Unit by CFD.* Norwegian University of Life Sciences.

Zhou, S., McCorquodale, J. A., & Vitasovic, Z. (1992). Influences of density on circular clarifiers with baffles. *Journal of Environmental Engineering, 118*(6), 829–847. doi:10.1061/(asce)0733-9372(1992)118:6(829)